Aus der Klinik für Allgemeine, Unfall- und Wiederherstellungschirurgie
Klinikum der Ludwig-Maximilians-Universität München
Vorstand: Prof. Dr. Wolfgang Böcker

Unravelling the roles of tenomodulin at the nexus of early tendon healing and intervertebral disc homeostasis

Dissertation
zum Erwerb des Doktorgrades der Humanbiologie
an der Medizinischen Fakultät der
Ludwig-Maximilians-Universität zu München

vorgelegt von
Dasheng Lin

aus Fujian, China

May
2020

Mit Genehmigung der Medizinischen Fakultät

der Universität München

Berichterstatter:	Prof. Dr. Denitsa Docheva
Mitberichterstatter:	Prof. Dr. Susanne Mayer
	Priv. Doz. Dr. Andreas Ficklscherer
	Priv. Doz. Dr. Thomas R. Niethammer
Mitbetreuung durch den promovierten Mitarbeiter:	Prof. Matthias Schieker
Dekan:	Prof. Dr. med. dent. Reinhard Hickel
Tag der mündlichen Prüfung:	12. Nov 2020

Affidavit

Lin, Dasheng

Surname, first name

I hereby declare, that the submitted thesis entitled

Unravelling the roles of tenomodulin at the nexus of early tendon healing and intervertebral disc homeostasis

is my own work. I have only used the sources indicated and have not made unauthorised use of services of a third party. Where the work of others has been quoted or reproduced, the source is always given.

I further declare that the submitted thesis or parts thereof have not been presented as part of an examination degree to any other university.

Munich, 08.05.2020

Place, Date

Dasheng Lin

Signature doctoral candidate

Table of contents

Abbreviations

Acan	aggrecan
ADAMTS	a disintegrin and metalloproteinase with thrombospondin motifs
ADSCs	adipose-derived stem cells
AF	annulus fibrosus
AFM	atomic force microscopy
BDNF	brain-derived neurotrophic factor
Bgn	biglycan
BMSCs	bone marrow stem cells
CEPs	cartilaginous endplates
Chm1	chondromodulin I
Col	collagen
COMP	cartilage oligomeric matrix protein
CTGF	connective tissue growth factor
ECM	extracellular matrix
EGF	epidermal growth factor
Egr 1	early growth response 1
ESCs	embryonic stem cells
FGF	fibroblast growth factor
Fn	fibronectin
GDF-5	growth/differentiation factor-5
HIF-1α	hypoxia-inducible factor-1α
IFN-γ	interferon-γ
IGF-1	insulin-like growth factor-1
ILs	interleukins
iPSCs	induced pluripotent stem cells
IVD	intervertebral disc
Lpl	lipoprotein lipase
Mkx	mohawk
MMPs	matrix metalloproteinases
MSC	mesenchymal stem cell
NO	nitric oxide
NP	nucleus pulposus
PDGF	platelet-derived growth factor
Pparγ	peroxisome proliferator-activated receptor gamma

qRT-PCR	quantitative real-time PCR
Scx	scleraxis
SNP	single nucleotide polymorphism
TGF-β	transforming growth factor beta
Tnc	tenascin C
TNF	tumor necrosis factor
Tnmd	tenomodulin
TSPC	tendon stem/progenitor cell
VEGF	vascular endothelial growth factor
WT	wild type
β-NGF	β-nerve growth factor

Publication list

Publication I

Tenomodulin is essential for prevention of adipocyte accumulation and fibrovascular scar formation during early tendon healing

Dasheng Lin, Paolo Alberton, Manuel Delgado Caceres, Elias Volkmer, Matthias Schieker and Denitsa Docheva✉

Cell Death Dis. 2017;8(10):e3116. doi: 10.1038/cddis.2017.510.

Publication II

Loss of tenomodulin expression is a risk factor for age-related intervertebral disc degeneration

Dasheng Lin, Paolo Alberton, Manuel Delgado Caceres, Carina Prein, Hauke Clausen-Schaumann, Jian Dong, Attila Aszodi, Chisa Shukunami, James C Iatridis and Denitsa Docheva✉

Aging Cell. 2020;19(3):e13091. doi: 10.1111/acel.13091.

1. Introduction

1.1 Tenomodulin: gene, protein and known functions

Tenomodulin (Tnmd) was independently identified by both Brandau *et al.* (2001) and Shukunami *et al.* (2001), and was found to be highly homologous to chondromodulin I (Chm1), a cartilage-derived growth regulator and angiogenesis inhibitor (Hiraki *et al.*, 1991). Tnmd represents a member of a novel type II transmembrane glycoprotein family, and has C- and N-terminal extracellular and cytoplasmic domains, respectively. Extracellular Tnmd regions consist of a C-terminal cysteine-rich proteolytically cleaved anti-angiogenic domain and a BRICHOS domain that is thought to serve an intramolecular chaperone function (Brandau *et al.*, 2001; Shukunami *et al.*, 2001). *Tnmd*, located on the X chromosome, encodes a 1.4 kb transcript that is in turn predicted to encode a 317 amino acid protein (Brandau *et al.*, 2001) (**Figure 1**).

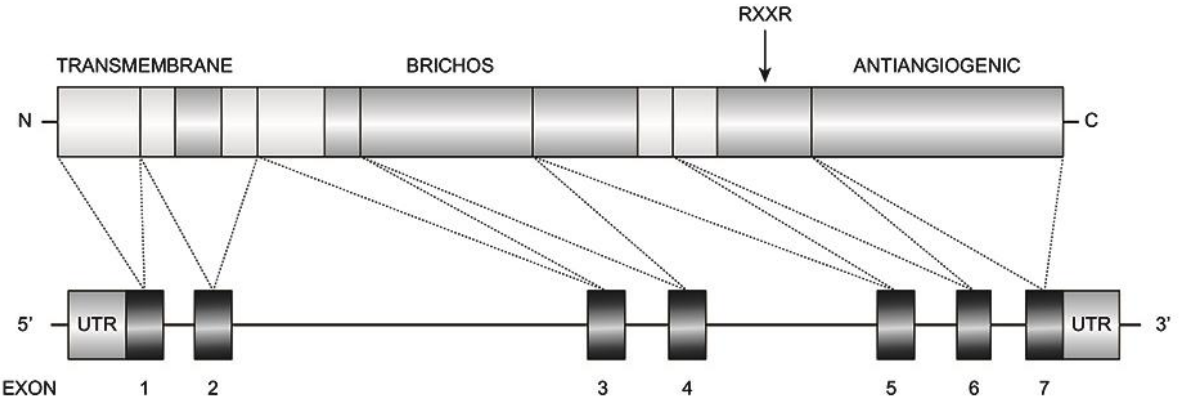

Figure 1. Human tenomodulin (TNMD) organization and the mRNA and protein levels. Grey is used to designate transmembrane, BRICHOS, and the antiangiogenic regions, with an arrow being used to mark the functional RXXR cleavage site. Exons are indicated by black boxes, with the lines between these boxes corresponding to introns. Abbreviation: UTR, untranslated region. This figure is adapted and modified from Tolppanen *et al.* (2010).

Tnmd lacks the furin cleavage site present within the Chm1 precursor, but it contains a protease recognition sequence at positions 233-236 (Shukunami *et al.*, 2005). Near this putative cleavage site is an extracellular domain BRICHOS, which is composed of a conserved 100 amino acid sequence that was first associated with proteins linked to dementia, respiratory distress, and cancer (Sánchez-Pulido *et al.*, 2002). However, its function in Tnmd and Chm1 is not clear. Northern blotting studies of newborn murine tissues revealed the highest Tnmd expression levels in skeletal muscle, diaphragm, and eyes, although a weak signal was observed in most screened tissues (Brandau *et al.*, 2001; Shukunami *et al.*, 2001). Tnmd expression in muscular tissue is exclusive to ligaments and tendons, as demonstrated through in situ hybridization studies (Docheva *et al.*, 2005). It is important to note that the homologous gene, *Chm1*, is predominantly expressed in cartilage tissue, but both *Tnmd* and *Chm1* have an overlapping expression in the eye (Docheva *et al.*, 2005; Hiraki *et al.*, 1991). These expression patterns suggest that Tnmd and Chm1 may not have compensatory roles in their primary expression sites.

During development and in traumatic or inflammatory contexts, a balanced control of angiogenesis is

necessary in cartilage and tendons in order for these tissues to maintain their hypovascularity. Therefore, it has been proposed that the primary function of Tnmd and Chm1 may be to control blood vessel ingrowth. However, developmental studies of *Chm1*- and *Tnmd*- deficient mice have revealed no profound abnormalities in cartilage or tendon vascularisation, respectively (Docheva *et al.*, 2005). Despite the lack of developmental phenotypes, it is important to further examine and challenge these knockout models by subjecting the mice to different disease-like conditions that allow the study of gene function during tissue healing or disease pathogenesis. For example, using a mouse tumor model, Oshima *et al.* (2004) found the Tnmd C-terminal domain to suppress the formation of vascular tubes *in vitro* and to suppress the *in vivo* growth of tumors.

The signalling pathway in which Tnmd participates is still unknown, mostly because of its novel protein domain structure and also because its potential binding partners have not been identified. Two studies by Brent *et al.* (2005) and Shukunami *et al.* (2006) revealed that there is overlap between the expression domains of Tnmd and scleraxis (Scx), the main transcription factor known to be indispensible for tendon formation. Furthermore, over-expression of Scx in cultured chicken tenocytes activated the up-regulation of Tnmd (Shukunami *et al.*, 2006), while in *Scx*-knockout mice, Tnmd expression is markedly diminished (Murchison *et al.*, 2007; Shukunami *et al.*, 2018). Mohawk (Mkx) is another transcription factor that is expressed almost exclusively within ligaments and tendons. When mice do not express Mkx, they exhibit reduction in Tnmd but not Scx expression, highlighting the role of Mkx as the Tnmd regulator (Ito *et al.*, 2010; Liu *et al.*, 2010). Taken together, the above studies suggest that Scx and Mkx are upstream of Tnmd. However, the protein-protein interactions in which Tnmd may be involved remain elusive.

Despite its unknown molecular pathway, Tnmd has been widely utilized as a marker gene for tendon lineage (Delgado *et al.*, 2018; Dex *et al.*, 2016; Jo *et al.*, 2019; Li *et al.*, 2019). Tnmd expression analysis, mainly at the mRNA level, has been used to confirm the presence of tendon-derived cells or to demonstrate the tenogenic differentiation of uncommitted cells. Tnmd loss has recently been shown not to affect *Tnmd*-knockout-derived tendon stem/progenitor cell (TSPC) multipotency, instead resulting in impairment of the ability of these cells to self-renew while increasing their susceptibility to entering a state senescence (Alberton *et al.*, 2015). Additionally, *Tnmd* overexpression in murine mesenchymal stem cell (MSC) improves their commitment to tenogenic differentiation, while inhibiting osteogenesis, chondrogenesis, and adipogenesis (Jiang *et al.*, 2017). Therefore, Tnmd is currently considered as the most specific differentiation marker of ligaments and tendons.

Tnmd expression is largely detected in the ligaments, tendons, and eyes, all of which are hypovascular tissues. Tenocyte proliferation is impaired in mice in which *Tnmd* expression is disrupted, resulting in pathologic collagen fiber thickening, decreased tenocyte density, and significantly inferior running performance (Dex *et al.*, 2017; Docheva *et al.*, 2005). Tnmd is also universally expressed in a concentric

pattern in the normal chordae tendineae cordis, and the local absence of Tnmd, angiogenesis, and activation of matrix metalloproteinases (MMPs) are linked with chordae tendineae cordis rupture (Kimura et al., 2008). In humans, relatively high *TNMD* mRNA expression can also be detected in the intervertebral disc (IVD), as well as in the tongue, brain regions including the globus pallidus and the temporal lobe, and in the cardiac myocytes (Minogue *et al.*, 2010; Su *et al.*, 2002). A recent study found high levels of *TNMD* expression within the adipose tissues of humans, where it acts as a protective factor that drives the proliferation of preadipocytes, adipogenesis, and responsiveness to insulin (Senol-Cosar *et al.*, 2016).

Finally, single nucleotide polymorphism (SNP) studies have demonstrated associations between *TNMD* and diseases such as obesity (Ruiz-Ojeda *et al.*, 2019; Saiki *et al.*, 2009; Tolppanen *et al.*, 2008), type 2 diabetes (Tolppanen *et al.*, 2007), metabolic syndrome (González-Muniesa *et al.*, 2013; Tolppanen *et al.*, 2008), age-related macular degeneration (Tolppanen *et al.*, 2009), apoliprotein E levels, and Alzheimer's disease (Tolppanen *et al.*, 2011). At present, these links remain vague, since the studies have only correlated the presence of *TNMD* gene SNPs to the existence or severity of the diseases, and it remains unclear if changes in Tnmd expression or function are involved. Thus, further studies are required to determine whether Tnmd is important for the development of these conditions.

There is increasing evidence to suggest that Tnmd may have diverse roles in various tissues and pathological conditions. Hence, identifying the specific functions of Tnmd will be helpful not only to the field of tendon biology, but also to other research and clinical fields. Therefore, further analysis of *Tnmd*-knockout mice in combination with different experimental models of pathological conditions is required. This will be a straightforward approach to determine if Tnmd exerts positive or negative effects on the progression of certain diseases.

1.2 Insights from tendon biology to tendon healing

Tendons are composed of dense connective tissue and help transmit force from muscles to bones during mechanical loading. Structurally speaking, ligaments are similar to tendons, but they instead function by stabilizing joints, linking bones together, and typically have lower tensile strength than tendons (Nourissat *et al.*, 2015). The core portion of the tendon which is responsible for load-bearing consists of collagen-rich fascicles that are highly aligned and that exhibit tendon-specific cell interspersion. Type I collagen is the primary component of the tendon extracellular matrix (ECM), with elastin, type III collagen, glycoproteins, and proteoglycans also contributing to this structural network. Tendon fibroblasts, or tenocytes, are the main cells within tendons, wherein they drive ECM synthesis, organization, and maintenance. Tendon tissue degeneration, which can be induced by mechanical overuse, neo-vascularization and/or tendon cell and tissue aging, is a leading cause of tendon rupture (Schneider *et al.*, 2018; Steinmann *et al.*, 2020). Once a tendon is ruptured, this typically resulting in the formation of a scar-like disordered collagen fiber section of tissue that fails to develop normal structural, mechanical, or functional properties (Lee *et al.*, 2015). Due to societal aging and a rise in overuse activities or extreme sports by young people, tendon diseases are among the most prevalent orthopedic problems and they present major clinical challenges. However, as there is insufficient data pertaining the mechanisms governing tendon development, mechano-transduction, pathogenesis, or healing at present, developing therapeutic interventions to remediate tendon diseases remains challenging (Ackerman *et al.*, 2019; Andarawis-Puri *et al.*, 2015).

Following tendon injury, healing is slow relative to muscle and bone healing processes, with tendon tissue repair taking longer than 1 year in humans (No *et al.*, 2019). Precisely how tendon healing remains to be fully studied, as there have not been sufficient in-depth analyses of the histopathological changes, biomechanics, and biochemical processes associated with such healing. Following surgical tendon repair, a short inflammatory phase typically first occurs, followed by a proliferative phase and a remodeling phase (Docheva *et al.*, 2015; Schneider *et al.*, 2018). These phases overlap, and are associated with specific cellular activities and cytokine secretion profiles that vary in a time- and space-dependent manner. Inflammatory cytokines are generally prevalent early during these responses, whereas anti-inflammatory cytokines and other factors associated with tissue healing are expressed at higher levels at later time points (Leong *et al.*, 2020). During the inflammatory phase, which lasts approximately 1 week, there are increases in vascular permeability leading to an increase in the infiltration of inflammatory cells into the site of damage (**Figure 2A**). These cells release growth factors and cytokines, including connective tissue growth factor (CTGF), epidermal growth factor (EGF), fibroblast growth factor (FGF), insulin-like growth factor-1 (IGF-1), interleukins (ILs), platelet-derived growth factor (PDGF), transforming growth factor beta (TGF-β), tumor necrosis factor (TNF), and vascular endothelial growth factor (VEGF), which result in the proliferation and recruitment of macrophages and tendon cells (Chazaud *et al.*, 2014; Evrova

et al., 2017; Manning *et al.*, 2014) (**Figure 2A**). Tendon injuries are also associated with the upregulation of a range of genes that encode various collagens (*Col1a1, Col1a2, Col3a1, Col12a1* and *Col14a1*) and other tendon-associated genes such as *Scx, Mkx, Tnmd*, early growth response 1 (*Egr1*), and tenascin C *(Tnc)*. The secondary proliferative phase extends for a few weeks, and is characterized by macrophage-mediated production of growth factors and chemokines (Docheva *et al.*, 2015; Schneider *et al.*, 2018). This leads tendon fibroblasts to be recruited from the synovial sheath and the epitenon while also recruiting proximal tenocytes to the injured site, wherein they produce type III collagen, fibronectin (Fn) and other constituents of the ECM to generate a disorganized ECM. Initial type III collagen production is eventually replaced by stronger type I collagen production. This proliferative phase is typically associated with high amounts of water absorption and cellularity. Following a 6-8 weeks period, a remodeling phase then initiates and lasts for 6-12 or more months depending on patient age and overall condition (Docheva *et al.*, 2015; Schneider *et al.*, 2018) (**Figure 2B**). The remodeling phase in turn consists of both consolidation and maturation stages, with the former being 10 weeks long and being characterized by changes in the tissue from a more cellular to a more fibrous state. During this period, tenocytes remain highly active, and collagen fiber alignment with stress directionality begins to occur. This in turn facilitates improvements in tendon strength and stiffness, with type III collagen synthesis being exchanged for type I collagen production. Tendon fibroblasts undergo myofibroblastic transformation, leading to granulation tissue contraction into a permanent scar. The maturation stage, in turn, can extend for 1-2 years, and during this period the tendon tissue switches from a fibrous to a more scar-like state, with concomitant reductions in tendon vascularity and in tenocyte metabolic activity (Schneider *et al.*, 2018).

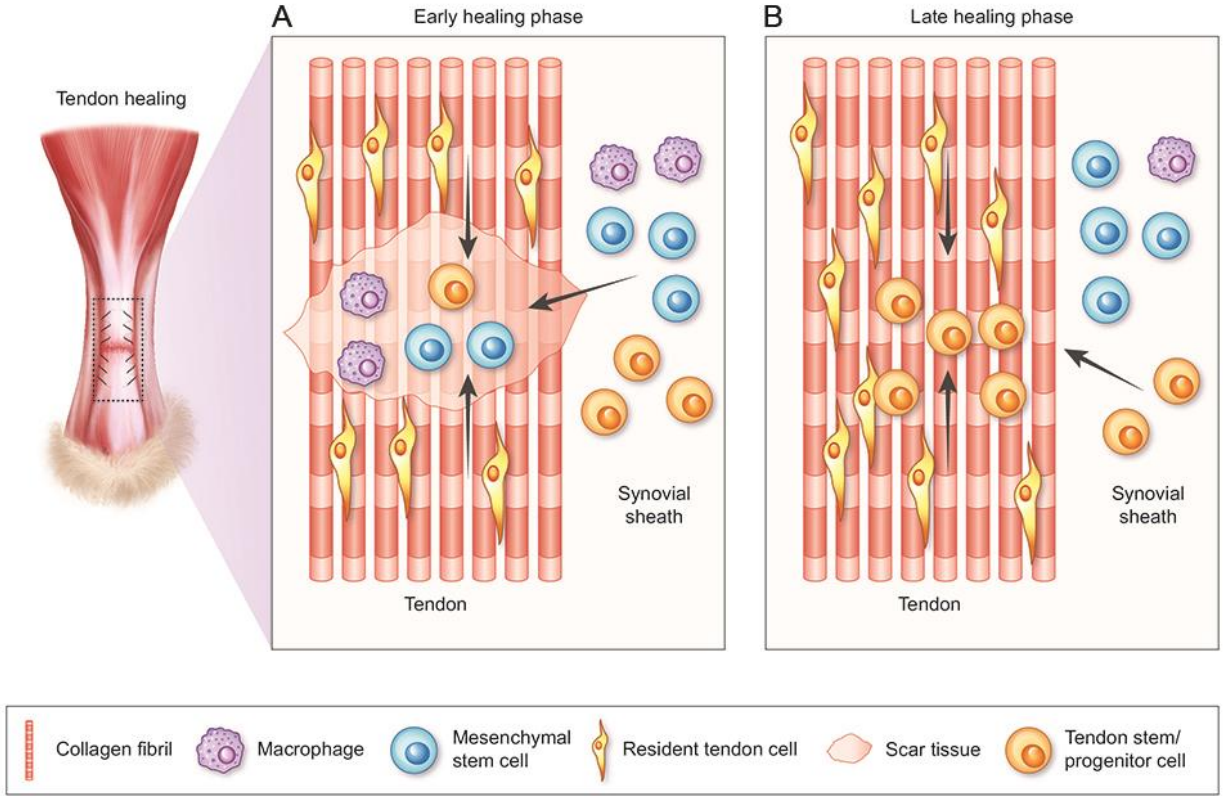

Figure 2. A simplified schematic of the tendon healing. (**A**) Early healing phase characterized with the entry of extrinsic cells to the site of injury (macrophages, mesenchymal stem cells, etc.) and (**B**) Late healing phase characterized with maturation of intrinsic cells and matrix.

Two related mechanisms have been proposed to mediate tendon healing, with the mechanism being engaged being dependent upon the types of cells involved therein. Tendon cells mediate intrinsic healing, whereas cells that migrate to the tendon from surrounding tissues mediate extrinsic healing. Due to the relatively small number and limited reparative abilities of resident tendon cells, the tendon has very little intrinsic regenerative capacity (Glenn *et al.*, 2019). Both intrinsic and extrinsic mechanisms are thought to govern tendon healing, with injury- and site-specific factors determining which process predominates in a given patient (Lomas *et al.*, 2015). Extrinsic healing can result in the deposition of significant quantities of disordered collagen, leading to large quantities of scar tissue and adhesion formation (Stauber *et al.*, 2019). As mentioned above, scar tissue reduces the mechanical properties of tendons, leaving them more susceptible to subsequent rupture (Lomas *et al.*, 2015).

Experimental strategies for improving tendon healing primarily consist of growth factor and cytokine application, either alone or as a combination therapy (Disser *et al.*, 2019; Docheva *et al.*, 2015; Schneider *et al.*, 2018), stem cells in native or genetically modified form (Bi *et al.*, 2007; Chong *et al.*, 2007; Deng *et al.*, 2014; Harvey *et al.*, 2019; Okamoto *et al.*, 2010); and biomaterials, alone or cell-loaded (Liu *et al.*, 2006; No *et al.*, 2019; Wang *et al.*, 2008; Wang *et al.*, 2018), at the site of tendon injury. Targeted blockade of inflammatory mechanisms after tendon repair can reduce scar formation but can also lead to marked impairment of the tendon's mechanical properties (Abraham *et al.*, 2019; Ackerman *et al.*, 2019). Additionally, poor vascularity may prevent adequate tissue repair, but hypervascularity can also have a detrimental effect on tendon healing (Leong *et al.*, 2020). To accelerate healing, inflammatory and angiogenic responses must, therefore, be balanced and followed by quick regression to prevent functional compromise (Titan *et al.*, 2019). Several studies have sought to understand how cytokines and growth factors impact tendon biology and healing, with some of these studies having evaluated the impact of these factors on stem cells (Schneider *et al.*, 2018). However, the majority of these factors that are produced in the context of tendon healing are associated with angiogenic and inflammatory processes, and as such it can be challenging to determine the pathways involved in the proteinogenic effect. Based on the results of genetic loss-of-function studies, only a few factors, including *Egr1*, growth/differentiation factor-5 (*Gdf-5*), and *Smad3*, have been shown to be essential for full tendon-healing responses (Chhabra *et al.*, 2003; Delgado *et al.*, 2018; Guerquin *et al.*, 2013; Katzel *et al.*, 2011).

Despite promising research, studies thus far have failed to facilitate the complete restoration of normal tendon functionality after rupture, or have been hampered by poor cell source availability (Kraus *et al.*, 2014; Nourissat *et al.*, 2015). Indeed, few functional tenocytes are generally available, while muscle cells and dermal fibroblasts generally exhibit uncertain specificity. Tendon aging is associated with a loss of

division in tendon cells, preventing full tendon healing following injury (Kohler *et al.*, 2013). However, even in adults a subset of tendon cells are capable of undergoing division, and this activity may be vital for healing responses (Grinstein *et al.*, 2019). Adult bone marrow stem cells (BMSCs), adipose-derived stem cells (ADSCs), TSPCs, and embryonic stem cells (ESCs) can differentiate into tendon-like cells. However, their corresponding abilities *in vivo* are not fully understood. Reprogrammed/engineered cells, such as induced pluripotent stem cells (iPSCs) have been linked to many concerns pertaining to efficacy and safety following the respective use of polymeric and viral vectors, and when they differentiate towards specific cell lineages, developmental stage mismatch processes may occur (Gaspar *et al.*, 2015; No *et al.*, 2019).

Effective approaches to expediting tendon healing have yet to be developed, as we do not currently understand tendon biology as well as we understand that of other components of the musculoskeletal system. Moreover, the molecular mechanisms controlling tendon cell migration, proliferation, and fate in the context of such tendon repair remain to be fully elucidated (Dex *et al.*, 2016; Nourissat *et al.*, 2015). Therefore, it is very important to dissect the cellular and molecular processes of tendon healing after surgical repair, in order to develop therapies that promote timely and complete repair of injured tendons.

1.3 Insights into the pathogenesis of IVD degeneration

IVD degeneration is a primary driver of chronic low back pain (Nguyen *et al.*, 2015). IVD degeneration is a complex and multifactorial process. It is mainly caused by aging, genetic predisposition, abnormal biomechanical loading, and environmental components (Pye *et al.*, 2007; Risbud *et al.*, 2014; Sakai *et al.*, 2015; Silagi *et al.*, 2019; Williams *et al.*, 2011). Numerous factors are believed to be capable of initiating the dysregulation of the anabolic/catabolic balance and a decline in the cell density of the nucleus pulposus (NP). Despite low back pain being a major medical and socioeconomic burden in modern society, the initiation and progression of IVD degeneration is not well understood. Therefore, it is important to understand the molecular basis of the pathogenesis of IVD degeneration translate this into the development of clinical treatments.

There are three primary compartments that compose the avascular IVD: an outer fibrocartilaginous annulus fibrosus (AF), an inner proteoglycan-rich NP, and cartilaginous endplates (CEPs) present at junctions with vertebral bodies. NP cells lack access to any significant blood supply, and thus adapt to the metabolic constraints of growing in a nutrient-poor, hypoxic, acidic setting. If their normal homeostatic capabilities are disrupted, however, this can lead to the onset of a pathological condition, during IVD degeneration. The initiating event that induces IVD degeneration is believed to arise from complex interactions between predisposing genetic factors and lifestyle or environmental factors including illness, obesity, poor posture, or poor nutrition. When normal metabolic activity is disrupted, imbalanced catabolism and anabolism can often occur along with inflammation, leading to a destructive feedback cycle wherein the breakdown of the matrix can lead to the generation of other inflammatory mediators, in turn driving MMPs upregulation and expression of a disintegrin and metalloproteinase with thrombospondin motifs (ADAMTS), leading to further matrix breakdown (Patil *et al.*, 2019).

IVD serves as the main intervertebral junction, and possesses fibrocartilaginous properties that enable it to resist mechanical stress. Gelatinous NP tissue redistribution is one key regulator of this process. Resident NP cells serve as key regulators of metabolic activity within NP tissues, wherein they produce proteoglycans and type II collagen that lead these tissues their gelatinous properties. Increased apoptotic death of NP cells as a result of metabolic disease can result in ECM metabolism disorders that accompany IVD degeneration (Kadow *et al.*, 2015; Song *et al.*, 2018). The loss of proteoglycan in the NP is accompanied by increased fibrosis, and the transition of cells from a vacuolated notochordal phenotype to one that resembles hypertrophic chondrocytes (Gorth *et al.*, 2019). Cumulatively, NP cells switching from producing anabolic to catabolic factors is a hallmark of IVD degeneration (Tessier *et al.*, 2019). Characteristically, the loss of the disc matrix proteoglycan aggrecan (Acan) leads to a reduction in compressive force resistance, with this being one well-characterized hallmark of degenerative disc disease (Patil *et al.*, 2019). There is also evidence of increases in matrix fragments production by the proteolytic actions of MMPs and ADAMTS.

The health and integrity of the AF are pivotal to IVD health. A longitudinal analysis of the relationships between AF tears and IVD degeneration in adults determined that annular tears are likely to arise early during disc disease, whereupon the result in accelerated degeneration of the NP (Sharma *et al.*, 2009). Disorganized concentric lamellae and fissures have the potential to arise in the AF, leading to an overall structural weakening that increases the susceptibility of the NP to bulging, herniation, or rupturing, that results in back or leg pain as a result of the irritation of compression of adjacent nerve roots. Vascular ingrowth is considered pathological, since normal IVDs are primarily avascular structures (Freemont *et al.*, 1997). Moreover, neovascularization of degenerated IVD occurs most frequently in the AF tissue, underscoring the importance of studying the interaction between resident AF cells and invading vascular cells (Pohl *et al.*, 2016). When AF fissures initiate in the outer AF prior to progressing inwards, this leads to the induction of a reparative response such that AF innervation, growth factor secretion, and vascularized granulation tissue development are all evident upon observation. In a healthy AF, neuronal fibers are only detectable in the outermost lamellae, whereas annular damage can lead to *de novo* innervation as undamaged NP cells generally suppress the outgrowth of neurites, while degenerative NP cells and infiltrating immune cells release neurogenic proteins including β-nerve growth factor (β-NGF) and brain-derived neurotrophic factor (BDNF) to stimulate innervation (Risbud *et al.*, 2014). Remarkably, nerve ingrowth is frequently accompanied by vascularization. Inflammation can further enhance innervation-related nociceptive triggers. Therefore, vascular, nerve ingrowth, and inflammatory mediator secretion are essential components of direct IVD pain (**Figure 3**). Nevertheless, the pathomechanism of this process remains unclear.

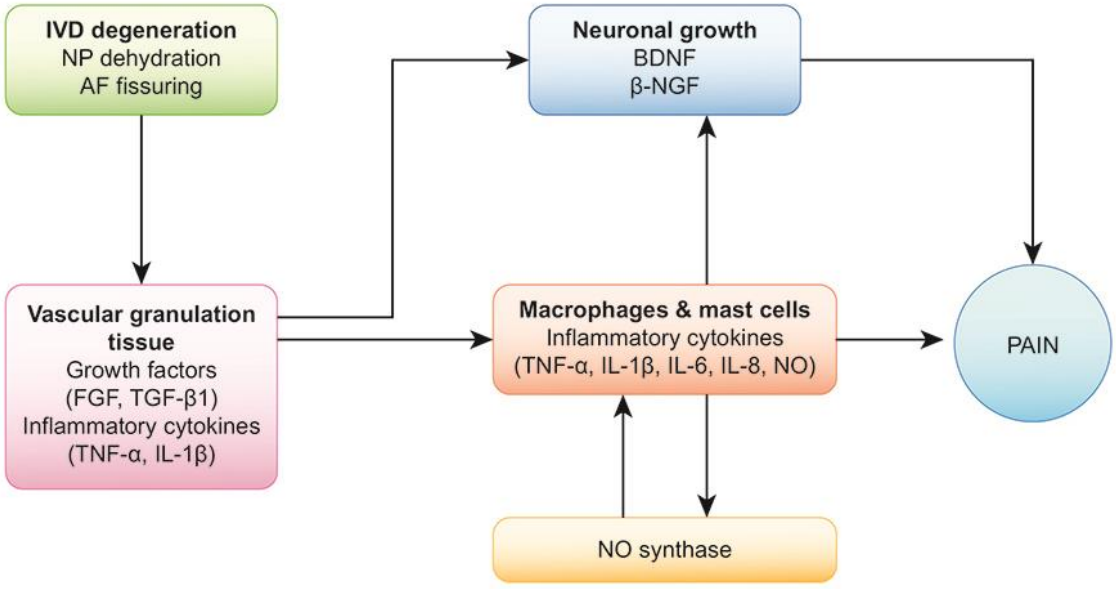

Figure 3. A series of events occur during IVD degeneration that are proposed to cause low back pain. AF, annulus fibrosus; BDNF, brain-derived neurotrophic factor; FGF, fibroblast growth factor; IL, interleukin; IVD, intervertebral disc; NO, nitric oxide; NP, nucleus pulposus; TGF-β1, transforming growth factor beta 1; TNF-α, tumor necrosis factor alpha; β-NGF, β-nerve growth factor. This figure is adapted and modified from Kadow *et al.* (2015).

Under healthy conditions, the CEP acts as a physical barrier to the NP, facilitating the distribution of intradiscal pressure while preventing NP tissue protrusion into the adjacent vertebral centrum. In disease contexts, the resulting damage can lead to focal weakening in the CEP, increasing its susceptibility to failure. Calcification of CEPs has been observed, with chondrocyte hypertrophy, the occlusion of marrow spaces, and sclerosis, thus altering the energy supply/demand balance and reducing the rate of nutrient and metabolite diffusion. With the recruitment of immune cells, the nutrient supply decreases, whereas the demand increases. This imbalance between demand and supply decreases the availability of nutrients to disc cells, thereby leading to adverse effects on cellular activity and viability. In addition, a reduction in metabolite excretion and acidification of the IVD microenvironment occurs with the calcification of CEPs, resulting in cellular stress that stimulates the apoptosis and senescence of NP cells. The accumulation of metabolites in the NP boosts the production of MMPs and ADAMTS, which further increases the degradation of ECM components (Huang *et al.*, 2014). For example, hypoxia can promote apoptotic cell death and inhibit proliferative activity, whereas it can also drive IVD progenitor cells to differentiate in a chondrogenic manner. Under hypoxic settings of following hypoxia-inducible factor-1α (HIF-1α) induction CEP-derived cells from degenerative IVD tissues exhibit disrupted osteogenesis, whereas under normoxic conditions their osteogenic potential was increased (Lyu *et al.*, 2019).

Various studies have found associations between IVD degeneration risk and mutations in genes associated with metabolism or the ECM. *Col I*, *Col IX*, *Col XI*, *Acan*, and asporin gene polymorphisms, as well as mutations in genes encoding IL-1 signaling-related proteins, have been shown to contribute to IVD degeneration susceptibility (Williams *et al.*, 2011). The deletion of IL-1α/β alters systemic inflammation and the morphology of vertebral bones, but does not impact IVD health in expected manners, instead resulting in the amplification of degeneration following IL-1α/β deletion (Gorth *et al.*, 2019). The actin-related protein 2/3 (Arp2/3) complex serves as a key mediator of cell-matrix interactions and matrix homeostasis. Conditional loss of Arp2/3 leads to IVD defects evident both at early postnatal time points and during adulthood (Tessier *et al.*, 2020). The Mkx transcription factor serves as a key regulator of AF development and maintenance. Mkx deficiency results in more rapid IVD degeneration (Nakamichi *et al.*, 2016). p16 is an important regulator of IVD degeneration, and its deletion attenuates IVD degeneration by promoting cell cycle progression and inhibiting the senescence-associated secretory phenotype, cell senescence, and oxidative stress (Che *et al.*, 2020). Taken together, these results suggest that a genetic predisposition plays a significant role in IVD degeneration. Thus, it is essential to understand how polymorphisms in matrix proteins or metabolic mediators impact the resulting molecular mechanisms involved in IVD degeneration.

IVD cells are primary producers of pro-inflammatory cytokines such as IL-1α/β, IL-2, IL-4, IL-6, IL-8, IL-12, IL-17, TNF-α, and interferon-γ (IFN-γ), all of which can drive the production of downstream factors including prostaglandins and nitric oxide (NO). Of these, IL-1 and TNF-α have been studied

extensively in the context of disc degeneration, wherein they are believed to drive degeneration by activating MMPs and ADAMTS (Gorth *et al.,* 2019; Patil *et al.,* 2019; Risbud *et al.,* 2014). Mechanical loading additionally influences progenitor cell fate, with persistent cyclic stress leading to disc cell osteogenic gene induction and apoptotic death. Similarly, the apoptosis of these disc cells can be promoted by nutrient deficiencies such as those observed when serum is removed from cultured cells (Lyu *et al.,* 2019). Furthermore, degeneration is closely linked to the overall aging process, suggesting that gradual matrix breakdown occurs naturally over time. The acceleration of this natural process, however, can arise for the reasons described above. It is thus essential that the source of pain be accurately located in order to facilitate efficacious therapeutic treatment.

In summary, the IVD represents the largest avascular tissue, and its potential for self-renewal is very limited in humans. The process of IVD degeneration is complex and multifactorial, involving the dysregulation of multiple processes, including the overexpression of degradative enzymes, the up-regulation of pro-inflammatory cytokines, the loss of healthy cells, and a decrease in matrix synthesis. Understanding the molecular basis of vascular control in the IVD as well as the exact pathogenesis of IVD degeneration will be important for facilitating the development of clinical treatments.

1.4 Aims of the thesis

1.4.1 Study I

We hypothesized that *Tnmd*-knockout mice will display delayed and inferior tendon healing when challenged with surgically induced Achilles tendon rupture. Our hypothesis is based on previous findings that Tnmd plays a regulatory role in the proliferation of tendon cells and the maturation of collagen fibrils, processes that are crucial during tendon healing. It is well known that the treatment of tendon injuries is currently limited to the use of painkillers, anti-inflammatory drugs, and glucocorticoids and there is a profound lack of treatment options that specifically and efficiently influence the performance of tendon cells. Since the loss of Tnmd may be associated with poor tendon healing, we propose that this research will provide new insights into Tnmd as a novel target for development of tendon-specific therapeutic agents.

In study I, we focused on the following three main objectives:

i) to apply surgically induced Achilles tendon rupture in Tnmd-deficient and wild type (WT) mice

ii) to carry out profound histomorphometry analysis at the early stage of tendon healing (via histology, immunohistology staining and quantification, cell proliferation and apoptosis analysis, and quantitative real-time PCR (qRT-PCR) of tendon tissues)

iii) to perform in vitro analysis of TSPCs derived from Tnmd-deficient tendons and control (via migration, proliferation, adipogenic differentiation assays, ELISA and qRT-PCR of TSPCs)

1.4.2 Study II

We hypothesized that the expression of Tnmd may suppress vascular ingrowth in the typically avascular IVD tissue, thus contributing to the IVD homeostasis. Conversely, the absence of Tnmd will lead to IVD degeneration.

In study II, we focused on the following three main objectives:

i) to investigate the phenotypic changes of Tnmd-deficient versus WT IVD tissues (via histology, immunohistology, histomorphometry, atomic force microscopy (AFM), western blotting, and qRT-PCR of IVD tissues)

ii) to investigate the phenotypic changes of Tnmd- and Chm1-deficient IVD tissues (double knockout mice) (via histology, immunohistology, and western blotting)

iii) to perform in vitro analysis of IVD-derived cells from Tnmd-deficient and WT mice (via co-culture with vascular cells, immunohistology, migration, proliferation, apoptosis, and qRT-PCR analyses).

1.5 Own contributions

1.5.1 Publication I

I designed, performed, and analyzed the experiments and wrote the manuscript.

Paolo Alberton assisted with the operations and performed tissue dissections and analyses.

Manuel Delgado Caceres performed ELISA and qRT-PCR experiments.

Elias Volkmer performed tendon surgery.

Matthias Schieker reviewed and approved the manuscript.

Denitsa Docheva conceived the study, designed the experiments, analyzed the data, and wrote the manuscript.

1.5.2 Publication II

I designed, performed, and analyzed the experiments and wrote the manuscript.

Paolo Alberton performed the co-culture experiments.

Manuel Delgado Caceres performed western blotting and qRT-PCR experiments.

Carina Prein performed AFM analyses.

Hauke Clausen-Schaumann performed AFM analyses.

Jian Dong reviewed and approved the manuscript.

Attila Aszodi reviewed and approved the manuscript.

Chisa Shukunami reviewed and approved the manuscript.

James C Iatridis reviewed and approved the manuscript.

Denitsa Docheva conceived the study, designed the experiments, analyzed the data, and wrote the manuscript.

2. Summary

Tenomodulin (Tnmd) is a tendon/ligament-specific marker that also serves as an anti-angiogenic protein. It is a novel type II transmembrane glycoprotein class member, and exhibits a cysteine-rich C-terminal domain that can readily be cleaved. Chondromodulin I (Chm1) is the only other characterized protein with homology to Tnmd. *Tnmd* expression is mainly observed in hypovascular tissues, including ligaments, tendons, and eyes. There is increasing evidence that Tnmd may have diverse roles in various tissues and pathological conditions. Therefore, it was of great importance to further examine *Tnmd*-knockout (*Tnmd*$^{-/-}$) model by subjecting it to disease-like conditions, namely tendon rupture, as well as to investigate its potential role in the intervertebral disc (IVD) being also avascular tissue.

First, we carried out an Achilles tendon injury in 6-month-old *Tnmd*$^{-/-}$ mice and investigated the early tendon repair at day 8, at which time it is possible to observe clear evidence of the development of scar tissue, infiltration by inflammatory and vascular cells, increased cell migration, proliferation and extracellular matrix (ECM) deposition. When comparing wild type (WT) and *Tnmd*$^{-/-}$ tendons, we observed clear reductions in the expression of tendon-associated transcription factors and ECM genes, impaired cellular proliferation, altered scar organization, and enhanced apoptosis and blood vessel/adipocyte accumulation in *Tnmd*$^{-/-}$ tendons. We further found that the scars in *Tnmd*$^{-/-}$ tendons exhibited increased biglycan (Bgn), cartilage oligomeric matrix protein (COMP), and fibronectin (Fn) deposition within the ECM; an altered macrophage profile, with predominantly M1 macrophages; and reduced CD146-positive cell numbers, which may be tendon stem/progenitor cells (TSPCs). *In vitro*, *Tnmd*$^{-/-}$ TSPCs were found to be markedly less proliferative and migratory than were WT TSPCs. The supernatant protein levels of Bgn and Fn were also markedly elevated in media collected from *Tnmd*$^{-/-}$ TSPCs, and these cells were found to more rapidly undergo adipogenic differentiation and to exhibit higher mRNA-level expression of peroxisome proliferator-activated receptor gamma (*Pparγ*) and lipoprotein lipase (*Lpl*). We therefore concluded that Tnmd is capable of inhibiting the accumulation of adipocytes and the formation of a fibrovascular scar in the context of tendon healing.

Second, to investigate whether loss of Tnmd expression may lead to IVD degeneration, we performed immunolocalization and western blotting analyses of WT IVD tissues revealing that Tnmd was age-dependent and was detectable primarily in the outer annulus fibrosus (AF), with its expression being reduced at 6 months of age (the time at which mice begin to exhibit early signs of IVD degeneration). We also confirmed that TNMD was predominantly expressed within the ECM of the outer AF of human lumbar discs. IVD phenotypic analyses demonstrated more rapid progression of age-related IVD degeneration in *Tnmd*$^{-/-}$ IVD. This included reductions in the diameters of collagen fibrils, decreases in compressive stiffness, reductions in the expression of genes associated with tendons/ligaments and with IVD, increases in macrophage infiltration and angiogenic activity in the outer AF, and a greater number of hypertrophic-like chondrocytes within the nucleus pulposus (NP). Furthermore, *Tnmd* and *Chm1* double

knockout mice displayed an ectopic bone formation in the IVD. *In vitro* studies demonstrated reduced proliferation and migration but increased apoptosis when comparing *Tnmd*$^{-/-}$ *versus* WT outer AF-derived cells. Furthermore, these cells showed p65 and matrix metalloproteinases (MMPs) upregulation and promoted the migration of human umbilical vein endothelial cells. Hence, we concluded that Tnmd can inhibit angiogenesis in the context of homeostatic IVD maintenance while protecting against IVD degeneration that occurs as a result of aging.

In summary, we reported that reduced Tnmd expression results in inferior tendon healing and increasing the risk of age-related IVD degeneration. These novel findings provided new information pertaining to the important role of Tnmd in tendon and IVD tissues, which can facilitate the development of novel therapeutic interventions that can prevent or treat tendon and IVD diseases.

3. Zusammenfassung

Tenomodulin (Tnmd), ein Sehnen-/Ligamentspezifischer Marker und antiangiogenetisches Molekül, gehört zu den novel class Typ II Transmembranglykoproteinen, welche lediglich noch ein anderes homologes Protein, Chondromodulin I (Chm1), enthält. Für die antiangiogene Eigenschaft des Tnmd ist eine Spaltung des hochkonservierten C-Terminus und eine subsequente Sekretion nötig. Das *Tnmd* Transkript ist vorwiegend in hypovaskularisierten Geweben wie in Sehnen, Ligamente und im Auge exprimiert. Es zeigen sich zunehmend Beweise, dass Tnmd eine entscheidende Rolle in verschiedenen Geweben und deren Pathophysiologien einnimmt. Deshalb ist es essentiell, dessen Genfunktion bei der Sehnen Gewebsregeneration und Disci Intervertebrales (IVD) pathologischen Prozessen durch *Tnmd*-Knockout ($Tnmd^{-/-}$) Modelle zu untersuchen.

Um die anfängliche Sehnenheilung zu untersuchen, generierten wir eine Achillessehnenverletzung in 6 Monate alten $Tnmd^{-/-}$ Mäusen und wählten den 8. Tag nach Verletzung als Beobachtungszeitpunkt, eine Auswahl, die sich durch die Narbenbildung, Gefäß- und Entzündungszellinvasion, eine hohe allgemeine Zellmigration, Zellproliferation und robuste Extrazellulärmatrix (ECM)-Deposition, auszeichnet. Detaillierte Analysen zeigten nicht nur eine veränderte Narbenorganisation mit reduzierter Zellproliferation und verminderten Expressionsraten von Sehnen relevanten Transkriptionsfaktoren und ECM Genen, sondern auch eine gesteigerte Apoptose, sowie Akkumulation von Adipozyten und Gefäßendothel im Vergleich zu den Wildtyp (WT) Mäusen. Auch zeigte das $Tnmd^{-/-}$ Sehnengewebe ein verändertes Ablagerungsmuster der Matrixproteine Biglycan (Bgn), oligomeres Knorpelmatrixprotein (COMP) und Fibronectin (Fn), ein verändertes Makrophagenprofil mit vorherrschen von M1 Makrophagen und eine reduzierte Anzahl von CD146 positiven Zellen, welche sehnen-entstammende Stamm- und Progenitorzellen (TSPCs) kann sein. Eine Invitro Analyse zeigte, dass $Tnmd^{-/-}$ TSPCs ein signifikant reduziertes Migrations- und Proliferationspotential im Vergleich zu WT TSPCs aufweisen. Auch waren die Bgn und Fn Proteinlevel im Kulturmedium von $Tnmd^{-/-}$ TSPCs signifikant erhöht im Vergleich zu den WT TSPCs. Letztlich haben die $Tnmd^{-/-}$ TSPCs die adipogene Differenzierung beschleunigt, begleitend von einem signifikant erhöhtem mRNA Gehalt des Peroxisom proliferator-aktiviertem gamma Rezeptors (*Pparγ*) und der Lipoproteinlipase (*Lpl*). Zusammenbetrachtet zeigten unsere Ergebnisse, dass Tnmd für die Prävention von Adipozytenakkumulation und fibrovaskuläre Narbenformation in anfänglicher Sehnenheilung benötigt wird.

Um die IVD Degeneration zu untersuchen, führten wir zuerst Immunlokalisationen und dann Western Blot Analysen von IVD Gewebe aus WT Mäusen zu bestimmten Stadien der Skelettbildung durch. Dies diente zur Untersuchung der präzisen Verteilung des Tnmd in postnatalen und adulten IVD. Unsere Ergebnisse zeigten, dass Tnmd altersabhängig vorallem im äußeren Anulus fibrosus (AF) exprimiert wurde und entsprechend der frühen IVD Degeneration in Mäusen ab dem Alter von 6 Monaten herunterreguliert wird. Zusätzlich haben wir die TNMD Expression in humanen lumbalen IVD untersucht

und bestätigt, dass das TNMD Protein in der ECM des äußeren AF zu finden ist. Anschließend haben wir 6 Monate und 18 Monate alte *Tnmd*$^{-/-}$ und WT Mäuse verwendet um die Rolle des Tnmd in natürlich vorkommender IVD Degeneration zu untersuchen. Wir fanden heraus, dass *Tnmd*$^{-/-}$ Mäuse eine rapidere Progression der altersabhängingen IVD Degeneration aufweisen. Das beinhaltet auch kleinere Kollagenfibrillendurchmesser, eine niedrigere kompressive Steifigkeit, reduzierte IVD- und sehnen/ligament-abhängige Genexpression, erhöhte Angiogenese und Makrophageninfiltration in der äußeren AF und eine höhere Anzahl von hypertroph-like Chondrozyten im Nucleus pulposus (NP). Bei *Tnmd* und *Chm1* Doppelknockout Mäusen zeigten sich beschleunigte IVD Degenerationen und ektope Knochenformationen in der IVD. Um ein tieferes Verständnis für die Rolle des Tnmd in der IVD Homöostase zu erlangen, führten wir In vitro Experimente mit Zellen des äußeren AF durch, diese wurden von lumbalen IVDs von 12 Monate alten *Tnmd*$^{-/-}$ und WT Mäusen isoliert. Zuerst untersuchten wir den Phenotyp der äußeren AF Zellen und fanden heraus, dass ein Tnmd Verlust eine Reduktion des proliferativen und migratorischen Potentials, aber auch eine Erhöhung des Apopotoserisikos verursacht. Desweiteren zeigte sich eine p65 und Matrixmetalloproteinase (MMP) Hochregulation, sowie eine verstärkte Migrationsfähigkeit von humanen venösen Nabelschnurendothelzellen. Damit beweisen unsere Forschungsergebnisse, dass Tnmd als ein Angiogeneseinhibitor während IVD Homöostase wirkt und vor altersabhängiger IVD Degeneration schützt.

Zusammenfassend haben unsere Ergebnisse einen neuen Einblick in die Rolle des Tnmd bei der anfänglichen Sehnenheilung und IVD Homöostase gegeben. Bei einem Tnmd Verlust ist die Sehnenheilung eingeschränkt und dies stellt dementsprechend einen Risikofaktor für die altersabhängige IVD Degeneration dar. Das Verständnis für den Tnmd abhängigen Mechanismus wird die Herstellung von neuen therapeutischen Strategien für die Prävention und Behandlung von Sehnenerkrankungen und IVD Degeneration einleiten.

4. Publication I

Tenomodulin is essential for prevention of adipocyte accumulation and fibrovascular scar formation during early tendon healing

Dasheng Lin, Paolo Alberton, Manuel Delgado Caceres, Elias Volkmer, Matthias Schieker and Denitsa Docheva✉

Cell Death Dis. 2017;8(10):e3116. doi: 10.1038/cddis.2017.510.

OPEN

Citation: Cell Death and Disease (2017) 8, e3116; doi:10.1038/cddis.2017.510
Official journal of the Cell Death Differentiation Association

www.nature.com/cddis

Tenomodulin is essential for prevention of adipocyte accumulation and fibrovascular scar formation during early tendon healing

Dasheng Lin[1,2], Paolo Alberton[1], Manuel Delgado Caceres[3], Elias Volkmer[1,4], Matthias Schieker[1,5] and Denitsa Docheva*[,3]

Tenomodulin (*Tnmd*) is the best-known mature marker for tendon and ligament lineage cells. It is important for tendon maturation, running performance and has key implications for the resident tendon stem/progenitor cells (TSPCs). However, its exact functions during the tendon repair process still remain elusive. Here, we established an Achilles tendon injury model in a *Tnmd* knockout (*Tnmd*$^{-/-}$) mouse line. Detailed analyses showed not only a very different scar organization with a clearly reduced cell proliferation and expression of certain tendon-related genes, but also increased cell apoptosis, adipocyte and blood vessel accumulation in the early phase of tendon healing compared with their wild-type (WT) littermates. In addition, *Tnmd*$^{-/-}$ tendon scar tissue contained augmented matrix deposition of biglycan, cartilage oligomeric matrix protein (Comp) and fibronectin, altered macrophage profile and reduced numbers of CD146-positive cells. *In vitro* analysis revealed that *Tnmd*$^{-/-}$ TSPCs exhibited significantly reduced migration and proliferation potential compared with that of WT TSPCs. Furthermore, *Tnmd*$^{-/-}$ TSPCs had accelerated adipogenic differentiation accompanied with significantly increased peroxisome proliferator-activated receptor gamma (*Pparγ*) and lipoprotein lipase (*Lpl*) mRNA levels. Thus, our results demonstrate that Tnmd is required for prevention of adipocyte accumulation and fibrovascular scar formation during early tendon healing.

Cell Death and Disease (2017) **8,** e3116; doi:10.1038/cddis.2017.510; published online 12 October 2017

Tendon injuries are some of the most common orthopedic problems accounting for substantial pain, disability, and economic burden.[1] While many tendon injuries are acute, a very large number are chronic causing degenerative conditions.[2] Repair in either case results in the formation of fibrovascular scar, fat deposition or heterotopic ossification that never attains the gross, histological, or mechanical characteristics of normal tendon.[3–5] The precise mechanisms of matrix degeneration, tissue tearing, and the subsequent repair process remain poorly understood.[1] Tenomodulin (Tnmd) is a member of a novel class protein family of type II transmembrane glycoproteins with a highly conserved cleavable C-terminal cysteine-rich domain.[6,7] The *Tnmd* gene consists of seven exons localized on the X chromosome and accounts for an ~1.4 kb transcript and a predicted full-length protein consisting of 317 amino acids.[6,7] It is predominantly expressed in tendons and ligaments, but low levels of mRNA transcripts have also been identified in other tissues.[6–9] *Tnmd* is the best-known marker of the mature tendon and ligament lineage with a suggested dual role of its C-terminal domain, namely a pro-proliferative action with tendon/ligament cells and anti-angiogenic potential with vascular cells.[9,10] Interestingly, loss of *Tnmd* expression in gene targeted mice (*Tnmd*$^{-/-}$) abated tenocyte proliferation, led to reduced tenocyte density and to pathological thickening of collagen fibers in the tendon extracellular matrix (ECM) *in vivo* but caused no major changes in the tendon vasculature.[11] In our recent study, we subjected *Tnmd*$^{-/-}$ mice and their wild-type (WT) littermates to exhaustive running tests revealing significantly inferior running performance of the knockouts that further worsened with training.[12] *In vitro* analysis of *Tnmd*$^{-/-}$ tendon stem/progenitor cells (TSPCs) showed significantly reduced self-renewal, and augmented senescence paralleled by upregulated *p53* mRNA levels, which was confirmed *in vivo* by detecting an increased number of p53-positive tenocytes in *Tnmd*$^{-/-}$ Achilles tendons.[13] In addition, overexpression of *Tnmd* in murine mesenchymal stem cells (MSCs) inhibited their commitment towards the adipogenic, chondrogenic and osteogenic lineages, whilst promoting their tenogenic differentiation.[14] The above data motivated us to further examine the potential regulatory role of *Tnmd* gene in the early tendon healing stage when major cellular and ECM events take place,[3] such as vascular and inflammatory cell invasion, intrinsic cell activation, migration and proliferation, and ECM deposition. Hence, the objective of this study was to investigate the functions of Tnmd in early tendon healing *in vivo* and in wound healing assays *in vitro*, including careful tissue phenotyping and specific molecular target analyses, using the *Tnmd*$^{-/-}$ mouse strain.

[1]Experimental Surgery and Regenerative Medicine, Department of Surgery, Ludwig-Maximilians-University (LMU), Munich, Germany; [2]Orthopaedic Center of People's Liberation Army, Xiamen University Affiliated Southeast Hospital, Zhangzhou, China; [3]Experimental Trauma Surgery, Department of Trauma Surgery, University Regensburg Medical Centre, Regensburg, Germany; [4]Department of Hand, Plastic and Aesthetic Surgery, LMU, Munich, Germany and [5]Novartis Institutes for Biomedical Research (NIBR), Translational Medicine Musculoskeletal Disease, Basel, Switzerland

*Corresponding author: D Docheva, Experimental Trauma Surgery, Department of Trauma Surgery University Regensburg Medical Centre, Franz-Josef-Strauss-Allee 11, Regensburg, 93053 Germany. Tel: +49(0)9419431605; Fax: +49(0)9419431631; E-mail: denitsa.docheva@ukr.de

Received 10.3.17; revised 19.7.17; accepted 20.7.17; Edited by D Aberdam

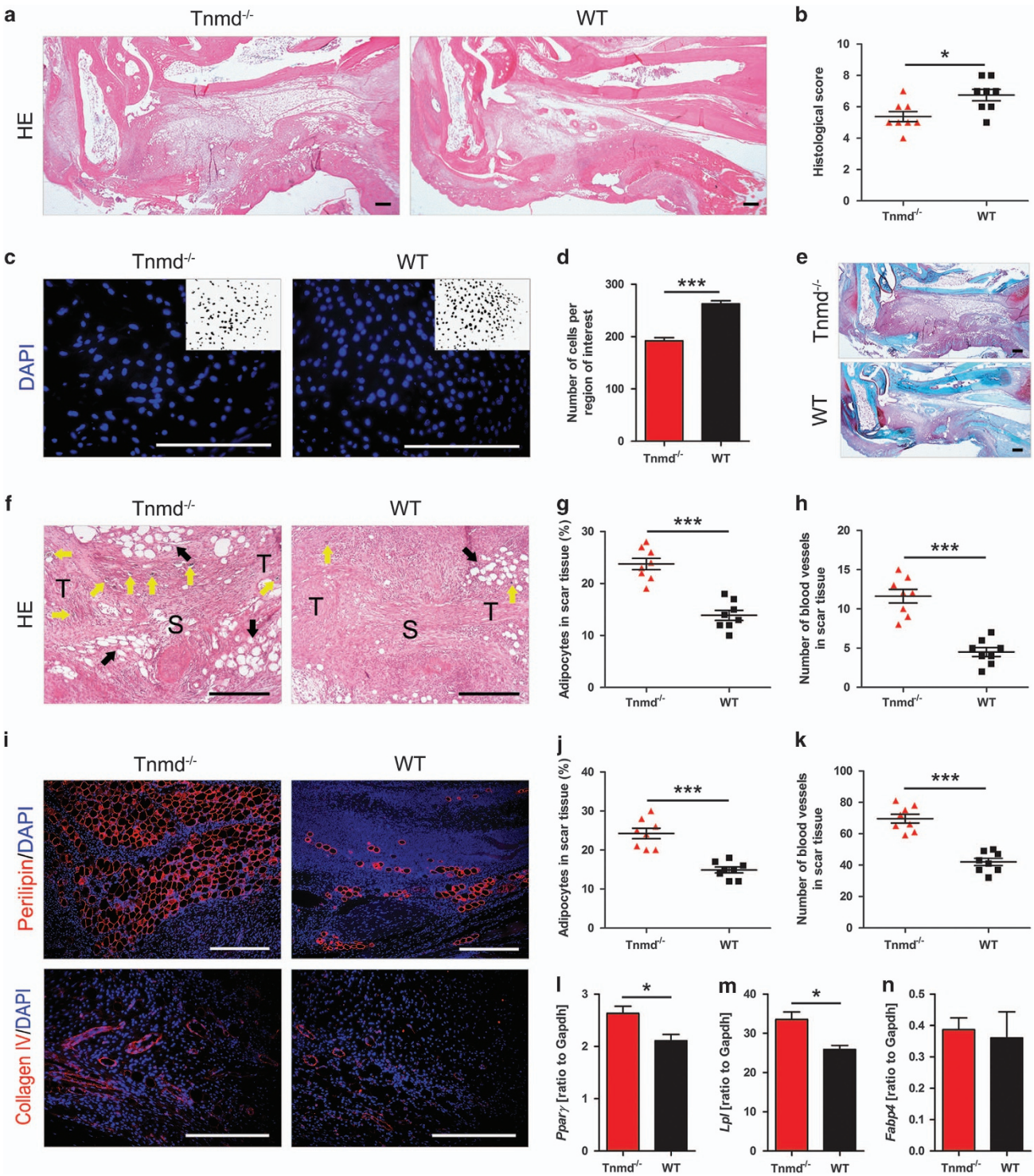

Results

***Tnmd*$^{-/-}$ tendon scars have inferior gross appearance, histological scores and cell density paralleled with increased accumulation of adipocytes and vessels.** To analyze Tnmd involvement during early tendon healing, we established a mouse model of full thickness Achilles tendon injury.[15] We analyzed the mice eight days after surgical repair, a time point characterized by scar formation, vascular and inflammatory cell invasion, high cell migration and proliferation as well as robust ECM secretory activity.[3,16] Hematoxylin–eosin (HE) staining of sectioned tendons revealed a very different scar organization in *Tnmd*$^{-/-}$ mice, as indicated by significantly inferior total histological scores[17] (Supplementary Table 1) compared with their WT littermates

Figure 1 *Tnmd* deficiency results in an inferior tendon repair process, lower cell density and increased adipocyte and vessel accumulation. (**a**) Low-magnification HE staining indicates a very different scar organization with clear adipocyte accumulation in *Tnmd*$^{-/-}$ mice. (**b**) Evaluation of tendon healing using an established histological scoring system revealed that *Tnmd*$^{-/-}$ mice had a significantly lower total histological score at 8 days postoperatively compared with WT mice. (**c**,**d**) Cell density in the healing region was significantly lower in *Tnmd*$^{-/-}$ *versus* WT mice. DAPI images were analyzed by computerized image analysis with ImageJ. (**e**) Ectopic endochondral ossification was not revealed by safranin O staining in the tendons of either genotype at day 8. (**f–h**) In HE-stained sections increased areas of adipocyte accumulation and numbers of large blood vessels were detected in the scar region of *Tnmd*$^{-/-}$ tendons compared with WT mice. (**i**) Visualization of adipocytes and blood vessels in *Tnmd*$^{-/-}$ and WT Achilles tendon scars via immunofluorescence staining for perilipin and collagen IV. (**j**,**k**) The perilipin-positive areas and number of collagen IV-labeled blood vessels were significantly higher by 8 days after surgery in *Tnmd*$^{-/-}$ *versus* WT mice. (**l–n**) qRT-PCR revealed upregulated mRNA levels of *Pparγ* and *Lpl*, but no changes in *Fabp4* expression in *Tnmd*$^{-/-}$ *versus* WT tendons. For quantification in (**b**, **d**, **g**, **h**, **j** and **k**), statistical significance was calculated using two-tailed non-parametric Mann–Whitney test, $n = 8$ (8 animals per group; each animal represented by 3 tissue sections). For qRT-PCR in (**l**, **m** and **n**), statistical significance between 2 groups was determined by unpaired Student's *t*-test (two-tailed) for 5 independent experiments. *$P < 0.05$; ***$P < 0.001$, compared with WT. S, scar; T, tendon; yellow arrows, blood vessels; black arrows, adipocytes. Scale bars: 200 μm

(Figures 1a and b). Quantitatively, total cell density was significantly lower in the *Tnmd*$^{-/-}$ mice at 8 postoperative days (Figures 1c and d). Ectopic ossification after tenotomy of rodent Achilles tendon at late stages of the tendon healing process has been reported in previous studies.[18–20] However, ectopic endochondral ossification was not detected in the scar tissues in either of the genotypes following safranin O staining at 8 days post-injury (Figure 1e). In contrast, the mean area of adipocyte accumulation, the number of blood vessels observed in HE staining analyses (Figures 1f–h) and validated by immunofluorescence staining and quantification for perilipin- (Figures 1i and j) and collagen IV-positive areas (Figures 1i and k), were significantly increased in the scar sites of *Tnmd*$^{-/-}$ mice compared with WT controls. We also found increased mRNA levels of the adipogenic marker genes, peroxisome proliferator-activated receptor gamma (*Pparγ*) and lipoprotein lipase (*Lpl*) in the tendons of *Tnmd*$^{-/-}$ mice through quantitative reverse transcriptase PCR (qRT-PCR) (Figures 1l and m). Expression of fatty acid-binding protein 4 (*Fabp4*), another adipogenic marker, was unaffected (Figure 1n). The above data revealed for the first time that the absence of *Tnmd* leads to an inferior morphological outcome and lower cellular density, whilst it activates adipocyte accumulation and adipose-related gene expression as well as vessel numbers in the early repair region of injured tendons.

***Tnmd*$^{-/-}$ tendons demonstrate reduced cell proliferation and CD146-positive cell numbers, downregulated levels of certain tendon-related genes, whilst increasing cell apoptosis and occurrence of p53-expressing cells.** To test whether the reduction in cell numbers was due to a decreased proliferation or increased apoptosis, we carried out proliferative and apoptotic assays by bromodeoxyuridine (BrdU) and terminal deoxynucleotidyl transferase-mediated dUTP-biotin nick end labeling (TUNEL) stainings. Furthermore, immunofluorescence staining was also performed for p53, which regulates the apoptosis in oxidative stress-exposed tenocytes,[21] and has been previously shown by us to be elevated in the tendons of uninjured *Tnmd*$^{-/-}$ mice.[11] BrdU analysis confirmed a lower number of proliferating cells at the scar site of injured Achilles tendons in *Tnmd*$^{-/-}$ than WT mice (Figures 2a and b). Furthermore, TUNEL assays and immunofluorescence staining for p53 showed that *Tnmd*$^{-/-}$ scars had an increased number of apoptotic cells (Figures 2c–f). In order to track activated local stem/progenitor cells at the scar site, we performed immunofluorescence analysis for CD146, which labels MSCs as well as the TSPCs.[22–24] The number of CD146-positive cells was significantly lower in *Tnmd*$^{-/-}$ compared with WT mice eight days after injury (Figures 2g and h). Following this, we analyzed how the absence of *Tnmd* affects the expression levels of tendon-associated gene markers using qRT-PCR of *Tnmd*$^{-/-}$ and WT tendon-derived mRNA. We observed significantly lower mRNA levels for early growth response protein 1 and 2 (*Egr1*, *Egr2*), collagens I, III and V (*Col1a1*, *Col3a1*, *Col5a1*), tenascin C (*Tnc*), thrombospondin 2 (*Thbs2*), alpha smooth muscle actin (*Acta2*) and transforming growth factor beta 1 (*Tgfb1*) in *Tnmd*$^{-/-}$ samples (Figure 2i). On the contrary, the relative expression levels of mohawk (*Mkx*), scleraxis (*Scx*), cartilage oligomeric protein (*Comp*) and lubricin (*Prg4*) displayed a dramatic increase, without affecting those of sine oculis homeobox homolog 1 (*Six1*), collagens VI and XII (*Col6a1*, *Col12a1*) and thrombospondin 4 (*Thbs4*) (Figure 2i). In sum, we concluded that the loss of *Tnmd* causes simultaneously reduced numbers of BrdU- and CD146-expressing cells, but an increased incidence of TUNEL- and p53-positive cells in the tendon scar tissue and dysregulated expression of key tendon-related transcription factors and ECM genes, which in turn can lead to altered tendon tissue composition during repair.

***Tnmd*$^{-/-}$ scar tissues are characterized by erroneous ECM deposition and abnormal macrophage profile.** The ECM of tendon tissue is composed primarily of collagen I, as well as collagen III, elastin and various proteoglycans and mucopolysaccharides.[3] Anomalies in the ECM composition of the scar tissue after tendon injury may contribute to a poor and delayed healing process resulting in compromised tissue quality.[20] Prompted by this observation and the gene expression changes in *Tnmd*$^{-/-}$ tendons, we carried out an ECM phenotyping of the scar tissues of both genotypes. First, we performed immunofluorescence staining with an anti-C-terminal Tnmd antibody visualizing Tnmd secretion in the ECM of WT mice Achilles tendon, but not in *Tnmd*$^{-/-}$ mice (Figures 3a and b). Surprisingly, three ECM proteins, namely biglycan, Comp and fibronectin, were more expressed in *Tnmd*$^{-/-}$ tendon healing sites than WT mice (Figures 3c–h). The increased protein deposition of Comp in *Tnmd*$^{-/-}$ samples was consistent with the qRT-PCR data showing higher Comp mRNA levels in this group (Figure 2i). However, collagens I and III, decorin, elastin, fibromodulin and lumican were not significantly affected (Supplementary Figure 1a). Nonetheless, picrosirious red-stained tendon sections analyzed by polarized light microscopy exhibited ECM containing thicker collagen fibers in the scar areas and tendon ends of

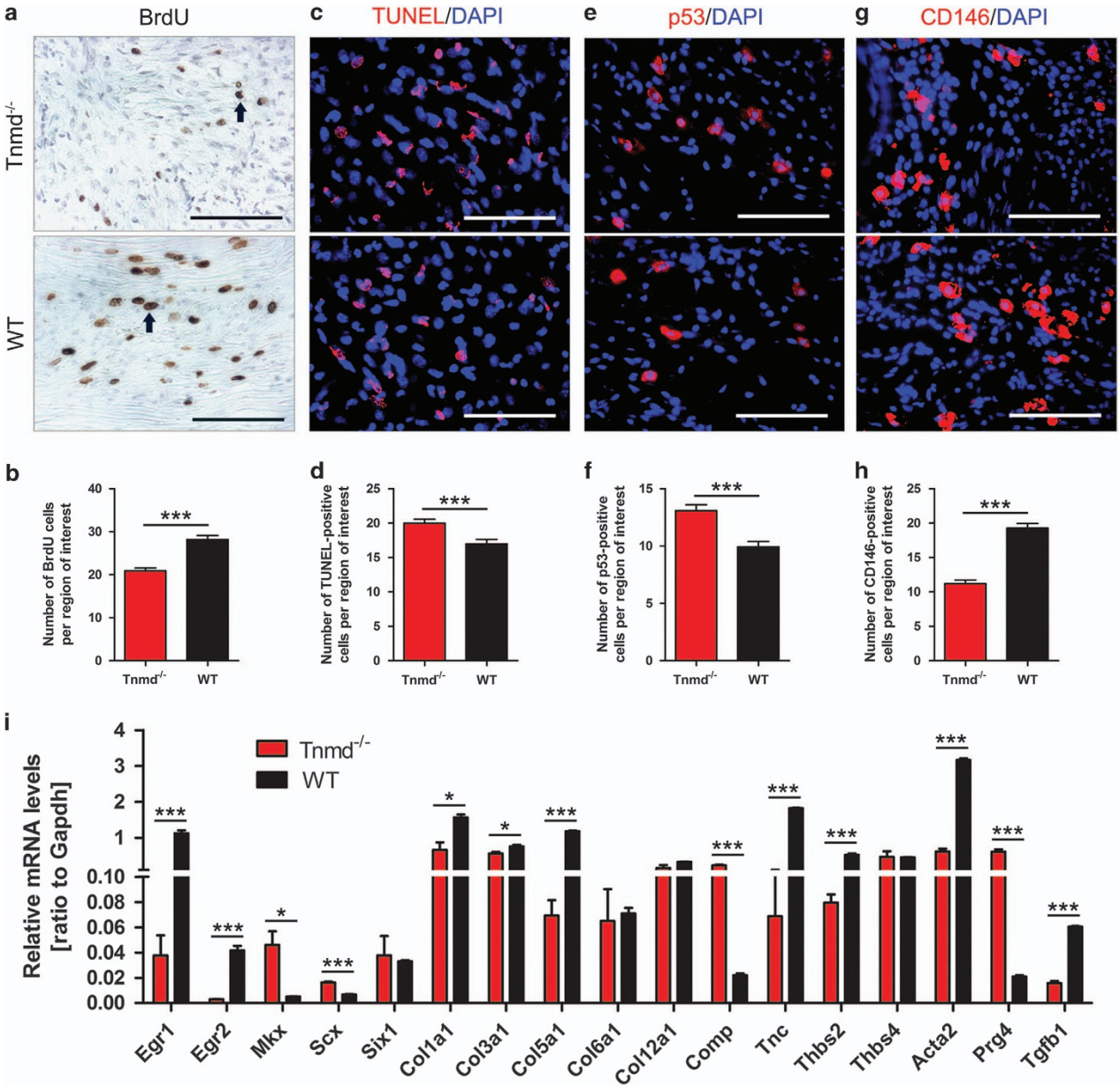

Figure 2 *Tnmd* deficiency results in reduced cell proliferation, CD146-positive cells, increased cell apoptosis and p53-expressing cells and an altered expression of certain tendon-related genes. (**a**,**b**) BrdU staining and quantification in the tendon scars revealed decreased proliferative cell numbers in *Tnmd*$^{-/-}$ *versus* WT mice at 8 days postoperatively. (**c**,**d**) TUNEL-based analyses detecting apoptotic cells showed increased cell apoptosis in *Tnmd*$^{-/-}$ mice compared with WT mice. (**e**,**f**) Increased number of p53-positive cells was found at day 8 in the tendons scar tissues of *Tnmd*$^{-/-}$ tendons compared with WT mice. (**g**,**h**) Immunofluorescence staining for CD146 showed that the number of CD146-expressing cells, corresponding to local MSCs and/or TSPCs was lower in *Tnmd*$^{-/-}$ mice than WT mice. (**i**) *Tnmd*$^{-/-}$ tendons displayed significantly lower expression levels for *Egr1*, *Egr2*, *Col1a1*, *Col3a1*, *Col5a1*, *Tnc*, *Thbs2*, *Acta2* and *Tgfb1* compared with WT mice. In contrast, the relative gene expression of *Mkx*, *Scx*, *Comp* and *Prg4* displayed a dramatic increase. No effect was found for *Six1*, *Col6a1*, *Col12a1* and *Thbs4*. For quantification in (**b**, **d**, **f** and **h**), statistical significance was calculated using two-tailed non-parametric Mann–Whitney test, $n = 8$ (8 animals per group; each animal represented by 3 tissue sections). For qRT-PCR in **i**, statistical significance between 2 groups was determined by unpaired Student's *t*-test (two-tailed) for 5 independent experiments. $^{*}P < 0.05$; $^{***}P < 0.001$, compared with WT. Black arrows, BrdU-positive cells. Scale bars: 100 μm

the *Tnmd*$^{-/-}$ than that of WT mice (Supplementary Figure 1b). Our observation of the increased erroneous ECM deposition in the repair sites of *Tnmd*$^{-/-}$ tendons motivated us to investigate by using target-specific ELISA whether *Tnmd*$^{-/-}$ TSPCs secrete higher amounts of biglycan and fibronectin proteins. The obtained quantitative data further confirmed our *in vivo* results by showing that the levels of both proteins were significantly increased in the supernatant of *Tnmd*$^{-/-}$ compared with WT TSPCs (Figures 3i–l).

The repair of injured tendons begins with an early inflammatory response that is associated with infiltration of pro-inflammatory, classically activated (M1) macrophages, whereas the secondary inflammatory response involves

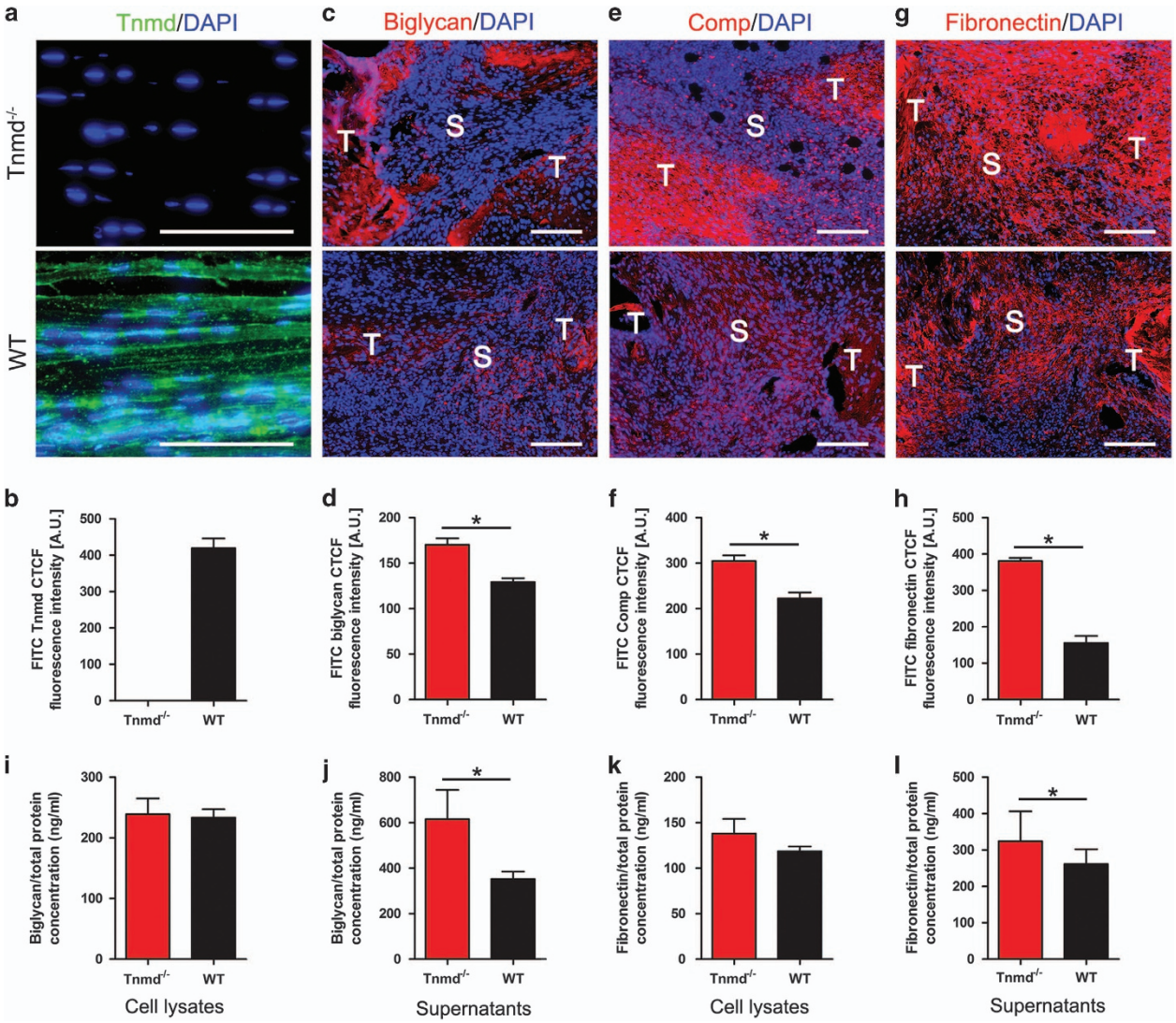

Figure 3 The absence of *Tnmd* increases erroneous ECM deposition. (**a**,**b**) Immunofluorescence staining with anti-Tnmd C-terminal antibody showed Tnmd secretion in the ECM of WT Achilles tendon, but not in *Tnmd*$^{-/-}$. (**c–h**) Biglycan, Comp and fibronectin protein deposition in the tendon scar, analyzed by fluorescent digital signal quantification, was clearly augmented in *Tnmd*$^{-/-}$ when compared with WT mice at 8 days postoperatively. (**i–l**) Biglycan and fibronectin protein levels from cell lysates and supernatant were assessed by ELISA and the levels of both proteins were significantly increased in the supernatant and slightly increased in the cell lysates of *Tnmd*$^{-/-}$ *versus* WT TSPCs. For quantification in (**b**, **d**, **f** and **h**), statistical significance was calculated using two-tailed non-parametric Mann–Whitney test, $n = 3$ (3 animals per group; each animal represented by 3 tissue sections). For ELISA in (**i**, **j**, **k** and **l**), statistical significance between 2 groups was determined by unpaired Student's *t*-test (two-tailed) for two independent experiments with two donors/genotypes. *$P < 0.05$ compared with WT. S, scar; T, tendon ends. Scale bars: 100 μm

anti-inflammatory, alternatively activated (M2) macrophages.[25] Recent evidence suggested that proper modulation of inflammation in the early stages of tendon repair may lead to improved healing.[26] Interestingly, in our model, the numbers of cells positive for CD68, (a prominent surface marker for M1 and tissue-resident macrophages), and CD80, (a M1 macrophage surface marker), were significantly increased (Figures 4a–d), whilst the number of cells expressing CD163, (a M2 macrophage surface marker), was significantly reduced in *Tnmd*$^{-/-}$ mice compared with WT mice eight days after injury (Figures 4e and f). These results were further substantiated by immunofluorescence staining of F4/80, a monoclonal antibody directed specifically against mouse macrophages, demonstrating a significant increase of labeled cells in the scar sites of *Tnmd*$^{-/-}$ mice (Figures 4g and h). Collectively, this set of data shows that *Tnmd* deficiency leads to erroneous ECM deposition *in vivo* and *in vitro* and leads to an abnormal macrophage profile with pre-dominating M1 macrophages in the repair site at day 8 of tendon healing.

***Tnmd*$^{-/-}$ TSPCs show significantly lesser migratory and proliferative capacities but have accelerated adipogenic differentiation rate and significantly upregulated *Pparγ* and *Lpl* mRNA expression.** Figures 1c and d and Figures 2a, b, g and h demonstrated that loss of *Tnmd* is associated with significantly lower cell density and numbers of BrdU- and CD146-positive cells in the scar tissues at day 8. These imply that Tnmd may regulate the migration and

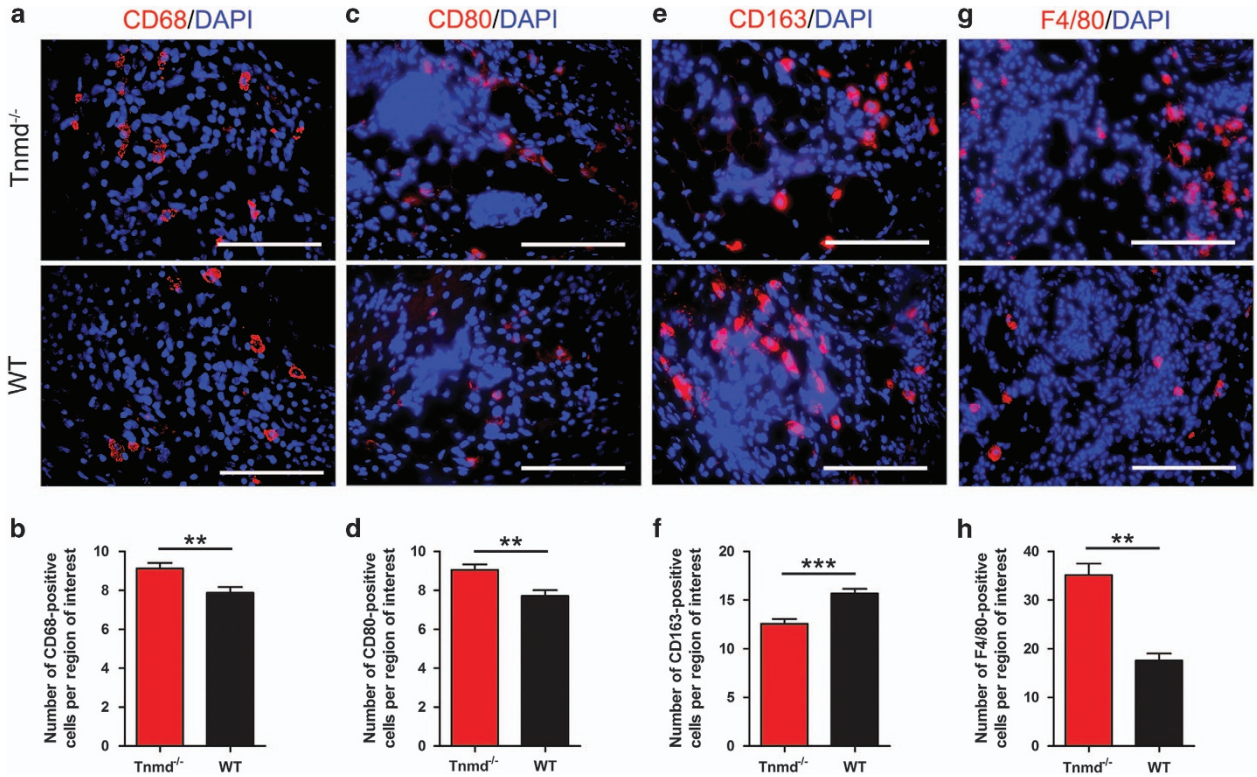

Figure 4 The lack of *Tnmd* alters the macrophage profile during early tendon healing. (**a–h**) The numbers of CD68-, CD80- and F4/80-positive cells were significantly increased, whereas the number of CD163-positive cells was significantly reduced in the *Tnmd*$^{-/-}$ tendon scar tissues compared with WT mice. For quantification in (**b**, **d**, **f** and **h**), statistical significance was calculated using two-tailed non-parametric Mann–Whitney test, $n = 8$ (8 animals per group; each animal represented by 3 tissue sections). $^{**}P < 0.01$; $^{***}P < 0.001$, compared with WT. Scale bars: 100 μm

self-renewal capacities of TSPCs. Therefore, we carried out scratch assays mimicking wound closure *in vitro*. To estimate the effect of ECM proteins and because of the increased fibronectin deposition in *Tnmd*$^{-/-}$ tendons, our scratch assays were performed on collagen I- and fibronectin-coated dishes. Quantification of scratch closure rate after 24 h, showed that the migration speed of *Tnmd*$^{-/-}$ TSPCs was significantly lower compared with WT TSPCs (Figures 5a–d). This finding was further solidified by random migration analysis after 48 h, in which forward migration index (FMI) of multiple single cells migrating on either of the ECM proteins was calculated (Figures 5e and f). Quantification of velocity, accumulated and Euclidean distance, also clearly indicated a significant reduction of *Tnmd*$^{-/-}$ TSPCs motility compared with WT (Figures 5g–l). Furthermore, during 12 days of culture, DNA-based CyQUANT assays at various time points showed that *Tnmd*$^{-/-}$ TSPCs proliferated significantly slower than WT TSPCs (Figure 5m), confirming and expanding our earlier report that Tnmd is a positive regulator of TSPC self-renewal.[13]

The observed adipocyte accumulation during early tendon healing prompted us to test whether the loss of *Tnmd* can accelerate TSPCs differentiation into adipocytes. Previously, we have observed an increased tendency of *in vitro* adipogenesis of *Tnmd*$^{-/-}$ TSPCs.[13] Here we again subjected TSPCs to adipocyte differentiation and examined the outcome in-depth. *Tnmd*$^{-/-}$ TSPCs grown in adipogenic medium had significantly more BODIPY 493/503 staining of neutral lipid droplets, indicating a higher adipogenic propensity than WT TSPCs after 7, 14 and 21 days, respectively (Figures 6a and b). Additional analysis, with the AdipoRed reagent revealed similar results (Figure 6c). Consistent with our *in vivo* results, semi-quantitative RT-PCR and densitometric PCR band evaluation showed that the expression levels of *Pparγ* and *Lpl*, but not *Fabp4*, were significantly increased in *Tnmd*$^{-/-}$ TSPCs compared with those of WT following 21 days of adipogenic stimulation (Figures 6d–f). We conclude that the lack of *Tnmd* in TSPCs negatively alters their migratory and proliferative capacities, whilst accelerating their commitment towards adipocytes and the expression of critical adipose regulatory genes such as *Pparγ* and *Lpl*.

Discussion

Effective strategies to speed up the healing process of tendon injuries are still not developed because the understanding of tendon biology lags far behind that of the other components of the musculoskeletal system, and the molecular mechanisms controlling the migration, proliferation and fate of TSPCs during tendon repair are not well understood.[1,9] Therefore, it is still very challenging to identify molecular targets that can be used to develop medicinal boosters for complete and timely repair of injured tendons or ligaments. *Tnmd* is a useful phenotypic marker of mature tenocytes and ligamentocytes that has been shown to have intriguing and diverse roles in developing tendons and those challenged by physical

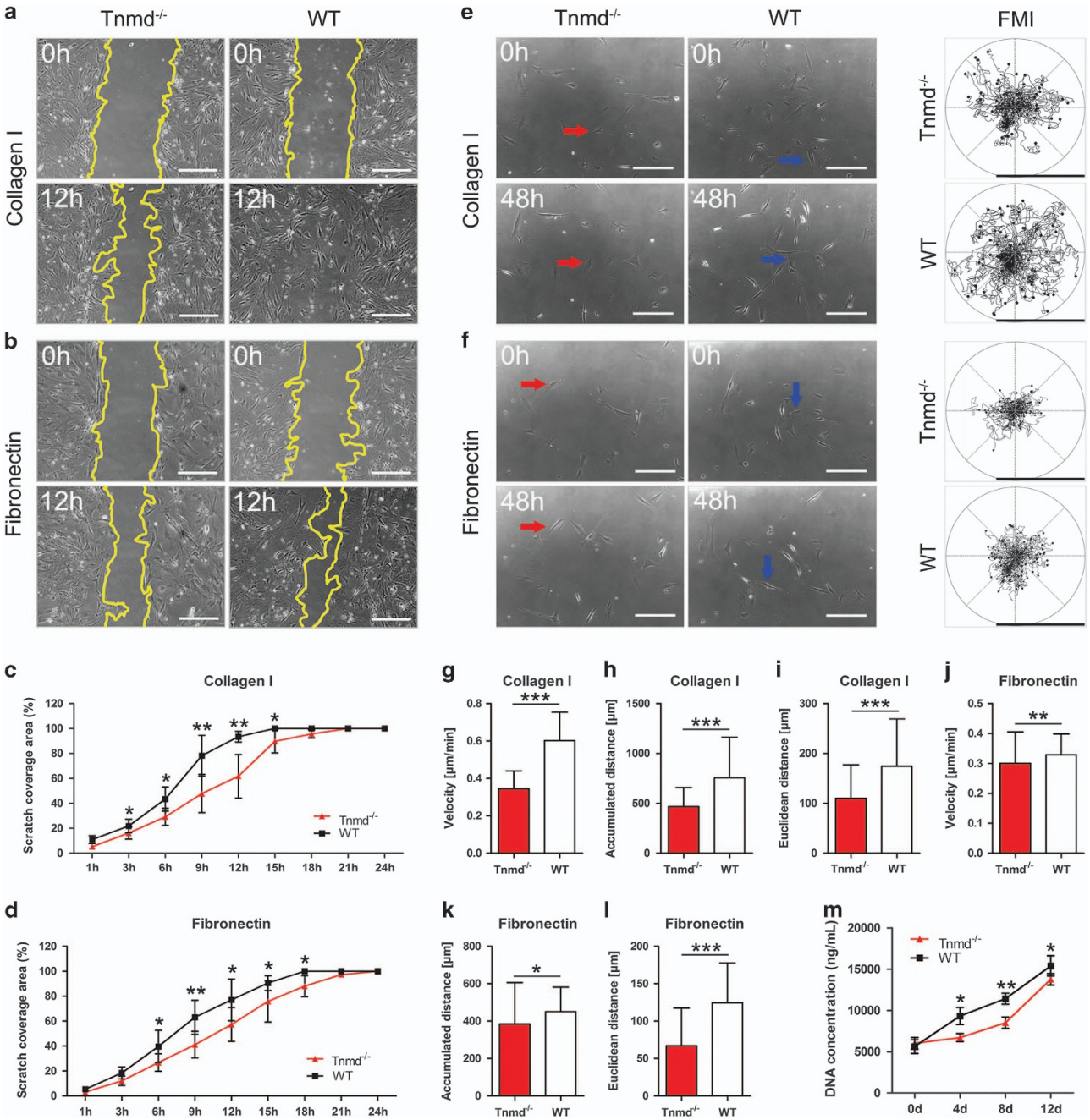

Figure 5 The absence of *Tnmd* in TSPCs leads to significantly reduced cell migration and proliferation. (**a**–**d**) *In vitro* wound healing assays on collagen I and fibronectin showed that *Tnmd*$^{-/-}$ TSPC scratch closure was significantly slower compared with WT TSPCs. The borders of the scratches are outlined with yellow lines. (**e**,**f**) Forward migration index (FMI) plots showed that *Tnmd*$^{-/-}$ TSPCs were indeed less migratory than WT TSPCs. Upper arrows on each type of matrix show the start point while lower arrows the end point of example migratory cells. (**g–l**) Quantification of velocity, accumulated and Euclidean distances further validated *Tnmd*$^{-/-}$ migratory deficiency. (**m**) During 0, 4, 8 and 12 days of culture cell growth kinetics were estimated by DNA-based CyQUANT assay revealing that the proliferation of *Tnmd*$^{-/-}$ TSPCs was significantly lower than that of WT TSPCs. For quantification in (**c**, **d** and **m**), $n = 4$ independent experiments per group. For quantifications in random migration, $n = 3$ independent experiments per group (total of 70–80 tracks per genotype). Statistical significance was calculated using two-tailed non-parametric Mann–Whitney test. *$P < 0.05$; **$P < 0.01$; ***$P < 0.001$, compared with WT. Blue arrows, WT TSPCs; d, day; h, hour; Red arrows, *Tnmd*$^{-/-}$ TSPCs; Scale bars: 200 μm

exercise.[9–12,27] Herein, we further explored the potential roles of Tnmd in the tendon healing process by subjecting *Tnmd*$^{-/-}$ mice to full thickness Achilles tendon injury and carrying out in-depth characterization of the scar tissues at day 8 as well as investigating certain TSPCs functions *in vitro*. The novel results of this study demonstrate for the first time that the absence of *Tnmd* causes inferior tendon repair process, as shown by adipocyte accumulation and fibrovascular scar formation during early tendon healing.

Efficient molecular modulation of tendon healing should accelerate cell proliferation and inhibit apoptosis, or at least not augment the number of apoptotic events.[28] We have

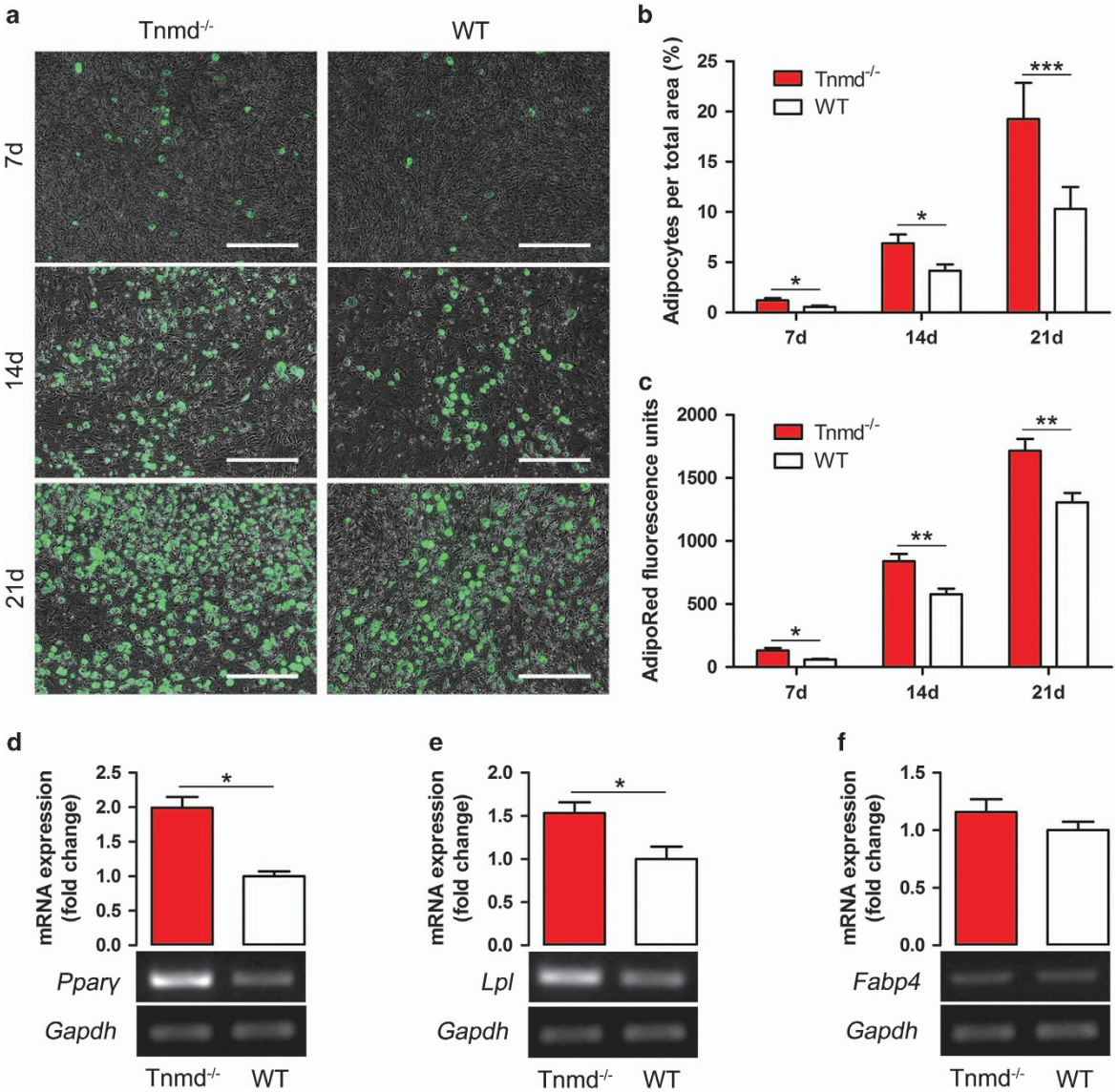

Figure 6 The absence of *Tnmd* in TSPCs leads to significantly accelerated adipogenic differentiation and upregulated *Pparγ* and *Lpl* expression levels. (**a**,**b**) *Tnmd*$^{-/-}$ TSPCs grown in adipogenic medium had significantly more BODIPY 493/503 staining of neutral lipid droplets, indicating a higher propensity of these cells to form adipocytes than WT TSPCs after 7, 14 and 21 days, respectively. (**c**) AdipoRed fluorescent quantitative assay confirmed these results. (**d–f**) Semi-quantitative RT-PCR and densitometric band analysis revealed that the expression of the two adipogenic marker genes *Pparγ* and *Lpl* was increased, while *Fabp4* levels were not significant changed in *Tnmd*$^{-/-}$ TSPCs after 21 days of adipogenic differentiation *versus* WT TSPCs. For quantification in **b** and **c** $n=4$ independent experiments. Statistical significance was calculated using two-tailed non-parametric Mann–Whitney test. For semi-quantitative RT-PCR, $n=5$ independent experiments per group. Statistical significance between 2 groups was determined by unpaired Student's *t*-test (2-tailed). *$P<0.05$; **$P<0.01$; ***$P<0.001$, compared with WT. Scale bars: 200 μm

already reported that the tendons of *Tnmd* knockout mice exhibit reduced cell density and proliferation[11] concomitant with apparent an *in vitro* phenotype of *Tnmd*$^{-/-}$ TSPCs, which were significantly less self-renewing, and more senescent.[13] Our current study provides further evidence that the loss of *Tnmd* expression in the healing tendon results in reduced cell density and proliferation and lower numbers of CD146-expressing cells, as well as augmented cell apoptosis and higher numbers of p53-positive cells. Furthermore, we show for the first time that *Tnmd*$^{-/-}$ TSPCs also have significant migratory deficits in two different experimental set-ups. Hence, we suggest that Tnmd has anti-apoptotic and anti-senescence roles and has important regulatory roles in cell migration and proliferation during the early stage of tendon repair. The positive association of *Tnmd* expression with advancement of tendon healing was previously suggested by Tokunaga *et al.*[29] in a growth factor-dependent model of rotator cuff healing.

Adipocyte accumulation and fibrovascular scar are common pathological changes that occur in ruptured tendons and ligaments.[30–34] They often do not properly remodel and in some cases continue to worsen even after surgical repair and physiotherapy. However, little is known of the pathophysiological pathways behind these phenomena.[30–34] Persistent or unresolved inflammation is considered a major trigger in many fibrotic diseases and in tendon healing has been associated with abnormal fibrogenesis.[35–37] Recent *in vivo* large animal

studies showed that inflammatory factors are dramatically upregulated within the first week after tendon injury, which in turn stimulate the production of proteases, cause apoptosis of tendon cells, impede the intrinsic repair process, and promote adhesion formation.[38–42] During inflammation, macrophages have essential roles in both promoting and resolving inflammation and in both facilitating and modulating tissue repair. In an injury setting, M1 cells predominate early, whereas M2 cells accumulate later. Hence, in tendon injury, it could be postulated that M1 macrophages promote repair by stimulating ECM production and that M2 macrophages enter the process to repress inflammation and clear excess ECM, a concept that is consistent with experimental evidence.[26] Disturbing the balance between these macrophage subtypes may result in abnormal scar formation, a defective repair process and impaired tissue function.[26] In our model, *Tnmd*$^{-/-}$ scars at day 8 exhibited higher numbers of vessels than WT scars, and displayed a macrophage profile of predominantly M1 cells with lower M2 numbers. This finding may help to explain the excess ECM protein deposition of biglycan, Comp and fibronectin, seen in *Tnmd*$^{-/-}$ tendons. Similarly, some recent reports dealing with tendon healing demonstrated higher expression of biglycan and Comp in the ectopic chondro-ossification sites in injured tendon tissues.[20,43] In addition, Spiegelman *et al.*[44] found that fibronectin protein can regulate adipogenic gene expression. Furthermore, a study focusing on stem cell-based therapy of tendon injuries suggested that a lower M2 macrophage number leads to less accumulation of CD146-positive cells and more erroneous matrix deposition at the repair site.[45] Thus, we suggest that the absence of *Tnmd* leads to enhanced vascular invasion, a prolonged inflammatory response, aggravated deposition or delayed clearing of excessive erroneous ECM. A deficiency of our study is that we do not describe the precise molecular mechanism by which Tnmd regulates the above processes. At present, we are unable to elucidate the exact Tnmd mode of action because we do not yet know the binding partners of this protein. Future studies are needed if we are to decipher the Tnmd signaling pathways. It will also be important to compare our small animal model with clinical tendon pathologies, for example by investigating *Tnmd* expression levels in different tendinopathy forms.

Interestingly, many recent studies have focused on understanding *Tnmd* involvement in obesity and diabetes.[46–52] Of interest, Senol-Cosar *et al.*[46] suggested that *Tnmd* facilitates pre-adipocyte terminal differentiation while Jiang *et al.*[14] showed that overexpression of *Tnmd* actually inhibits adipogenesis of murine MSCs. These data suggest that Tnmd might have cell type-specific modes of action; a suggestion reinforced by the contrasting observations that Tnmd causes proliferation of tendon-derived cells but inhibits proliferation of vascular-derived cells.[9] Our results are in line with the study of Jiang *et al.*[14] as we showed *Tnmd*$^{-/-}$ scars had significantly higher adipocyte accumulation and also that *Tnmd*$^{-/-}$ TSPCs had a higher rate of differentiation into adipocytes. We propose that the different regulatory mechanisms of the Tnmd signaling pathway are involved in different cell types, which will be revealed when the *Tnmd* molecular network is finally mapped.

Pparγ is a transcriptional master regulator of adipogenic differentiation and stimulates adipogenesis.[53–56] Here, we showed that concomitantly with the higher adipocyte numbers, the lack of *Tnmd* significantly enhanced the expression levels of *Pparγ* and *Lpl in vivo and in vitro*. Furthermore, we observed that the absence of *Tnmd* results in dysregulated expression of key tendon transcription factors and ECM genes and proteins, which in turn may lead to altered scar composition and thereby increased lipid accumulation. Gehwolf *et al.*[57] revealed that loss of the expression of the ECM protein Sparc drives adipocyte differentiation in tendons. Our study does not differentiate whether the pathways underlying the induction of adipogenesis either by *Pparγ* upregulation or by changes in ECM properties operate independently of each other or in an interdependent manner.[57,58] We can not provide a conclusive answer to this question, but we propose that *Tnmd* may strongly influence adipogenesis during tendon healing through the regulation of *Pparγ* expression, ECM composition and/or by preventing TSPC adipocyte commitment.

In summary, we created an Achilles tendon injury model in *Tnmd*$^{-/-}$ mice, that showed that loss of *Tnmd* results in inferior tendon repair characterized by increased adipocyte accumulation, reduced cell density, proliferation and CD146-positive cells, increased apoptotic and p53-expressing cells, M1:M2 macrophage ratio changes, abnormal expression of tendon-related genes, and augmented fibrovascular scar composition. Concomitant *in vitro* analysis of *Tnmd*$^{-/-}$ TSPCs revealed significantly reduced migratory and proliferative capacities, but upregulated adipogenic gene marker levels and accelerated differentiation down this lineage. Thus, our results suggest that Tnmd is required for prevention of adipocyte accumulation and fibrovascular scar formation during the early phase of tendon healing.

Materials and Methods

Animal model and surgical procedure. *Tnmd*$^{-/-}$ mice and their WT littermates were used in this study. The generation of the *Tnmd*$^{-/-}$ mice and their primary phenotype were described by Docheva and co-workers.[11–13] All the mice were on a C57BL/6 J background. Surgical procedures were performed as previously described by Palmes *et al.*[15] with 6-month old mice that had reached skeletal maturity. In brief, (1) after anesthesia, the skin above the left Achilles tendon was opened from the gastrocnemius muscle to the calcaneus; (2) using sterile scissors, the tendon proper (~5 mm above the calcaneus) of the Achilles tendon was fully resected; (3) the tendon ends were then connected with modified Kirchmayr 8-0 Dermalon suture and further supported with single 10-0 Dermalon circular suture; (4) in order to avoid suture failure due to overstretching of the operated tendons, the movement of the talocrural joint was restricted by a cerclage that was inserted through the tibiofibular fork and fixed between the calcaneus and the plantar aponeurosis. This assured a more limited degree of talocrural joint extension (~30%) but still allowed a tensile load to be actively transferred to the healing Achilles tendon; and (5) the skin was closed. The tendons were given eight days for repair, corresponding to the early phase of tendon healing, after which the animals were euthanized and the whole hind limb including the Achilles tendon-gastrocnemius muscle-calcaneus complexes were dissected and histologically processed as described below. All procedures for animal handling prior, during and after surgery were approved by the Animal Care and Use Committee of the Bavarian Government (Grant Nr. 55.2-1-54-2531-57-08). Bio-statistical design of the group size was based on the default values of $\alpha = 0.05$ and $\beta = 0.8$ for type one error and for the power as well as on pilot histological data for each genotype, resulting in eight animals per group.

Histomorphometry. Achilles tendons within the hind limbs were fixed in 4% paraformaldehyde (PFA; Merck, Darmstadt, Germany) overnight at 4 °C. After fixation, specimens were decalcified in 10% ethylene diamine tetraacetic acid (EDTA)/phosphate buffered saline (PBS) pH 8.0 (Sigma-Aldrich, Munich, Germany) for 7 days, and embedded in paraffin or cryogenic media and then sectioned at 5 or

10 μm for paraffin and frozen specimens, respectively. Every 10th slide was stained with HE and slides with comparable regional planes between genotypes (where the whole complex of gastrocnemius muscle-Achilles tendon-calcaneus was exposed) were selected for in-depth investigation. To analyze the total histological scores on HE-stained slides we used the established histological scoring system of Stoll *et al.*[17] given in Supplementary Table 1. To reveal the ectopic endochondral ossification in the scar tissue, safranin O staining was applied using the standard histological protocol.

For immunofluorescence, the tissue sections were treated with 2 mg/ml hyaluronidase (Sigma-Aldrich, Steinheim, Germany) for 30 min at 37 °C in order to increase antibody permeability. After washing and blocking with 2% bovine serum albumin (BSA)/PBS (Sigma-Aldrich), primary antibodies against biglycan, CD68, CD80, CD146, CD163, collagen I, collagen III, collagen IV, Comp, decorin, elastin, fibromodulin, fibronectin, F4/80, lumican, perilipin, p53 and Tnmd (all from Abcam, Cambridge, UK; except for Tnmd, which was provided by Denitsa Docheva) were applied overnight at 4 °C. Next day, corresponding Alexa Fluor 546-labeled secondary antibodies (all from Life technology, Carlsbad, CA, USA) were applied for 1 h. Then, sections were counter-stained with 4',6-diamidino-2-phenylindole (DAPI) (Life Technology) and mounted with fluoroshield (Sigma-Aldrich). To detect proliferating cells, 90 min prior to euthanasia all mice received intraperitoneal injection with BrdU (50 μg/g body weight). BrdU detection was performed with a BrdU kit according to the manufacturer's instructions (Roche Applied Science, Penzberg, Germany). To analyze apoptotic cells numbers, TUNEL assay was performed according to the manufacturer's instructions (Abcam). Photo-micrographs were taken on the Observer Z1 microscope equipped with the Axiocam MRm camera (Carl Zeiss, Jena, Germany). In general, all histomorphometry experiments, unless specified otherwise in the text, were reproduced in with 8 animals per group and representative images are shown.

In order to analyze biglycan, Comp and fibronectin levels, an automated quantitative image analysis was performed as described in the literature.[18] In brief, using ImageJ (National Institutes of Health, Bethesda, MD, USA), the following algorithm was applied: (1) area of interest was manually designated using the 'drawing/selection' tool; (2) 'set measurements for area, integrated density and mean gray value' was selected from the analyze menu; (3) the corrected total cryosection fluorescence (CTCF) representing the biglycan, Comp and fibronectin expression detected were calculated as follows CTCF = media of integrated density – (media of area of selected area × mean fluorescence). Three animals per group were analyzed.

Scar nuclear density was determined on DAPI staining with ImageJ according to Hsieh and co-workers.[18] All cell nuclei (DAPI) in 3 images per scar from 3 sections per animal with 8 animals per group were counted. To analyze adipocytes (perilipin), blood vessels (collagen IV), cell proliferation (BrdU), apoptotic cells (TUNEL and p53), TSPC/MSC cells (CD146) and macrophages (CD68, CD80, CD163, and F4/80) quantification of labeled cell per scar tissue was carried out for each staining on 8 animals per group. Each animal was represented with 3 different tissue sections with comparable planes between genotypes. The results were averaged per animal and shown as final mean and standard deviation (S.D.) between the 8 animals per group. The above information is given in the figure legends (8 animals per group; each animal represented by 3 tissue sections).

Mouse TSPCs isolation and cell culture. Mouse TSPCs were isolated as previously described by Alberton and co-workers[13] from tendons of two uninjured *Tnmd*$^{-/-}$ and WT 6-month-old mice. Tendon tissues were enzymatically treated overnight with collagenase II (Worthington, Lakewood, NJ, USA) in Dulbecco's modified Eagle's medium (DMEM)/Ham's F-12 (1:1) (Biochrom, Berlin, Germany) supplemented with 10% fetal bovine serum (FBS), 1% l-ascorbic-acid-2-phosphate (both from Sigma-Aldrich, Steinheim, Germany), 1% minimum essential medium (MEM)-Amino Acid and 1% penicillin/streptomycine (Pen/Strep) (both from Biochrom, Berlin, Germany). Then, the cell suspension was filtered through 70 μm nylon mesh, centrifuged at 500 × *g* for 5 min, and resuspended in fresh culture media. TSPCs were grown at 37 °C and 5% CO_2 and passaged when 70% confluent with the culture media changed every third day. Cells in passages 1–3 were used for experiments.

***In vitro* wound healing assay.** These experiments were carried out according to our previously published protocol.[59] Shortly, 1×10^4 cells per cm^2 were plated on collagen I- (20 μg/Ml; Millipore, Billerica, MA, USA) or fibronectin-coated (10 μg/Ml; Sigma-Aldrich, Steinheim, Germany) 6-well plates in low serum (2%) medium and were allowed to form confluent cell layers for 48 h. Prior to imaging, the layers were scratched multiple times. Time lapse photography was performed at 4 frames per h for 24 h. For each group, the areas of 12 scratches were measured at 9 different time points from 4 independent experiments using the ImageJ 'wound healing' tool.

Migration analysis. Migration analysis was performed similarly to our previous studies.[59,60] For random migration, 1.5×10^3 cells/cm^2 of *Tnmd*$^{-/-}$ and WT TSPCs were seeded on collagen I- (20 μg/ml) or fibronectin-coated (10 μg/ml) 6-well plates and incubated for 2 h before imaging. Time lapse photography was performed at 4 frames per h for 48 h. The image data was extracted with AxioVisionLE software (Carl Zeiss, Jena, Germany) and individual cell tracks were analyzed with ImageJ. Random migration was expressed by calculating the forward migration index (FMI; the ratio of the vector length to the migratory starting point), velocity, and accumulated (cumulative track length) and Euclidian (the ordinary straight-line length between two points) distances. Results of random TSPCs migration measurements consist of 3 independent time lapse movies of two *Tnmd*$^{-/-}$ and WT TSPC donors as a total number of 70–80 TSPC per genotype were tracked.

CyQUANT assays. 1.5×10^3 cells per well were plated in 6-well plates, and the CyQUANT assay detection was performed according to the manufacturer's instructions (Invitrogen, Eugene, OR, USA) after 0, 4, 8 and 12 days of cell culture, respectively. CyQUANT assay was repeated independently in 4 experiments per time point with two TSPC donors/genotypes.

Adipogenic differentiation assays. These experiments were carried out according to our previously published protocol.[13] Briefly, 8×10^3 cells/cm^2 TSPCs were seeded in triplicates in 6-well plates, and were cultivated in an induction media for 5 days (DMEM-high glucose with 10% FBS, 1 μM dexamethasone, 200 μM indomethacin, 0.01 mg/ml insulin, and 500 μM 3-isobutyl-1-methylxanthine; all from Sigma-Aldrich, Steinheim, Germany) followed by 2 days in preservation media (DMEM-high glucose medium supplemented with 10% FBS, 0.01 mg/ml insulin). The process was repeated for 21 days. The adipogenic differentiation was estimated by BODIPY 493/503 staining of neutral lipid droplets (Thermo Fisher Scientific, Waltham, MA, USA) and AdipoRed assay (Lonza, Walkersville, MA, USA). Staining was carried out according to the manufacturer's instructions. Using the automatic color pixel quantification tool in the Adobe Photoshop CS5 software, the BODIPY 493/503 staining-positive areas were estimated and calculated as a percentage of the image total pixel size. Using a fluorimeter (Tecan, Männedorf, Switzerland), AdipoRed assays were measured with excitation at 485 nm and emission at 572 nm. BODIPY 493/503 staining and AdipoRed assay were repeated in 4 independent experiments.

ELISA. The protein levels of biglycan and fibronectin were analyzed by ELISA. TSPCs (8×10^3 cells/cm^2) were seeded in 6-well plates. After 3 days, the cell supernatant and cell RIPA protein lysates were collected and frozen. Before ELISA, the total protein of all samples was measured via DC protein assays (BioRad, Munich, Germany). Secreted biglycan and fibronectin were determined using mouse biglycan and fibronectin ELISA kits (Cloud-Clone Corp, Katy, TX, USA; and Aviva Systems Biology, San Diego, CA, USA; respectively) according to the manufacturer's instructions. Two independent ELISA measurements were done with two donors/genotypes. The data was expressed as target-specific concentration to total protein content.

Semi-quantitative and qRT-PCR. Total RNA from tendon tissue and adipogenic-stimulated TSPCs was isolated with Qiagen RNeasy Mini kit (Qiagen, Hilden, Germany) and used for semi-quantitative and qRT-PCR. For cDNA synthesis, 1 μg total RNA and AMV First-Strand cDNA Synthesis Kit (Invitrogen) were used. Semi-quantitative PCR was performed with Taq DNA Polymerase (Invitrogen) in MGResearch instrument (BioRad, Munich, Germany). For Primer sequences and PCR conditions: *Pparγ* forward 5′ctccgtgatggaagaccactc3′, reverse 5′agactcggaactcaatggc3′; *Lpl* forward 5′gtctggctgacactggacaa3′, reverse 5′ tgggccattagattcctcac3′; *Fabp4* forward 5′gaagcttgtctccagtcaaaa3′, reverse 5′ agtcacgcctttcataacacat3′; *Gapdh* forward 5′gagaggccctatcccaactc3′, reverse 5′ gtgggtgcagcgaactttat3′; PCR was performed with incubation at 94 °C for 5 min followed by 30 cycles of a three step temperature program of 1 min at 94 °C, 20 s at 60 °C, and 30 s at 72 °C. The PCR reaction was terminated after a 7 min extension at 70 °C. The band intensity of the amplified products in the gel was visualized, photographed and analyzed using a gel imager (Vilber Lourmat, Eberhardzell, Germany). The relative gene expression was quantified by densitometry and normalized to the amount of Gapdh with ImageJ and presented as fold-change to

WT. Quantitative RT-PCR of adipogenic and tenogenic associated gene markers was performed using RealTime Ready Custom Panel 96–32+ plates (https://configurator.realtimeready.roche.com) according to the manufacturer's instructions (Roche Applied Science, Mannheim, Germany). Briefly, PCR reactions were pipetted on ice and each well contained 10 μl LightCycler 480 probes master mix, 0.2 μl cDNA and 9.8 μl PCR grade water. Plates were subsequently sealed and centrifuged down for 15 s at 2100 rpm. The relative gene expression was calculated as describe by Dex and co-workers.[12] All PCR results have been reproduced independently in five experiments.

Statistical analysis. Statistical differences between two groups were determined using two-tailed unpaired Student's *t*-test, or two-tailed non-parametric Mann–Whitney test. Sample size and experimental reproduction are indicated for each method. Results are presented as mean $\pm$ S.D. Differences were considered statistically significant according to values of $^{*}P<0.05$, $^{**}P<0.01$ and $^{***}P<0.001$.

Conflict of Interest

The authors declare no conflict of interest.

Acknowledgements. DD acknowledges the German Research Foundation (Grant No. DO1414/3-1) and the National Institutes of Health (Grant No. GM089820). DL acknowledges the National Natural Science Foundation of China (Grant No. 81600696). We are thankful to CF Hsieh, S Dex and D Drenkard for experimental help. We also thank Dr G Pattappa and Professor B Johnstone for proof-reading of the manuscript.

Author contributions

DL designed, performed and analyzed experiments and wrote the manuscript; PA assisted with the operations, performed tissue dissections and analyses; MDC performed ELISA and semi-quantitative RT-PCR; EV performed tendon surgery; MS approved manuscript; DD conceived the study, designed, and analyzed experiments and wrote the manuscript.

Publisher's Note

1. Nourissat G, Berenbaum F, Duprez D. Tendon injury: from biology to tendon repair. *Nat Rev Rheumatol* 2015; **11**: 223–233.
2. Galatz LM, Gerstenfeld L, Heber-Katz E, Rodeo SA. Tendon regeneration and scar formation: the concept of scarless healing. *J Orthop Res* 2015; **33**: 823–831.
3. Docheva D, Müller SA, Majewski M, Evans CH. Biologics for tendon repair. *Adv Drug Deliv Rev* 2015; **84**: 222–239.
4. Gaspar D, Spanoudes K, Holladay C, Pandit A, Zeugolis D. Progress in cell-based therapies for tendon repair. *Adv Drug Deliv Rev* 2015; **84**: 240–256.
5. Aslan H, Kimelman-Bleich N, Pelled G, Gazit D. Molecular targets for tendon neoformation. *J Clin Invest* 2008; **118**: 439–444.
6. Brandau O, Meindl A, Fässler R, Aszódi A. A novel gene, tendin, is strongly expressed in tendons and ligaments and shows high homology with chondromodulin-I. *Dev Dyn* 2001; **221**: 72–80.
7. Shukunami C, Oshima Y, Hiraki Y. Molecular cloning of tenomodulin, a novel chondromodulin-I related gene. *Biochem Biophys Res Commun* 2001; **280**: 1323–1327.
8. Yamana K, Wada H, Takahashi Y, Sato H, Kasahara Y, Kiyoki M. Molecular cloning and characterization of CHM1L, a novel membrane molecule similar to chondromodulin-I. *Biochem Biophys Res Commun* 2001; **280**: 1101–1106.
9. Dex S, Lin D, Shukunami C, Docheva D. Tenogenic modulating insider factor: Systematic assessment on the functions of tenomodulin gene. *Gene* 2016; **587**: 1–17.
10. Oshima Y, Sato K, Tashiro F, Miyazaki J, Nishida K, Hiraki Y *et al.* Anti-angiogenic action of the C-terminal domain of tenomodulin that shares homology with chondromodulin-I. *J Cell Sci* 2004; **117**: 2731–2744.
11. Docheva D, Hunziker EB, Fässler R, Brandau O. Tenomodulin is necessary for tenocyte proliferation and tendon maturation. *Mol Cell Biol* 2005; **25**: 699–705.
12. Dex S, Alberton P, Willkomm L, Söllradl T, Bago S, Milz S *et al.* Tenomodulin is required for tendon endurance running and collagen I fibril adaptation to mechanical load. *EBioMedicine* 2017; **20**: 240–254.
13. Alberton P, Dex S, Popov C, Shukunami C, Schieker M, Docheva D. Loss of tenomodulin results in reduced self-renewal and augmented senescence of tendon stem/progenitor cells. *Stem Cells Dev* 2015; **24**: 597–609.
14. Jiang Y, Shi Y, He J, Zhang Z, Zhou G, Zhang W *et al.* Enhanced tenogenic differentiation and tendon-like tissue formation by tenomodulin overexpression in murine mesenchymal stem cells. *J Tissue Eng Regen Med* 2016; **11**: 2525–2536.
15. Palmes D, Spiegel HU, Schneider TO, Langer M, Stratmann U, Budny T *et al.* Achilles tendon healing: long-term biomechanical effects of postoperative mobilization and immobilization in a new mouse model. *J Orthop Res* 2002; **20**: 939–946.
16. Dyment NA, Hagiwara Y, Matthews BG, Li Y, Kalajzic I, Rowe DW. Lineage tracing of resident tendon progenitor cells during growth and natural healing. *PLoS One* 2014; **9**: e96113.
17. Stoll C, John T, Conrad C, Lohan A, Hondke S, Ertel W *et al.* Healing parameters in a rabbit partial tendon defect following tenocyte/biomaterial implantation. *Biomaterials* 2011; **32**: 4806–4815.
18. Hsieh CF, Alberton P, Loffredo-Verde E, Volkmer E, Pietschmann M, Müller PE *et al.* Periodontal ligament cells as alternative source for cell-based therapy of tendon injuries: in vivo study of full-size Achilles tendon defect in a rat model. *Eur Cell Mater* 2016; **32**: 228–240.
19. Fang Z, Zhu T, Shen WL, Tang QM, Chen JL, Yin Z *et al.* Transplantation of fetal instead of adult fibroblasts reduces the probability of ectopic ossification during tendon repair. *Tissue Eng Part A* 2014; **20**: 1815–1826.
20. Lui PP, Cheuk YC, Lee YW, Chan KM. Ectopic chondro-ossification and erroneous extracellular matrix deposition in a tendon window injury model. *J Orthop Res* 2012; **30**: 37–46.
21. Poulsen RC, Knowles HJ, Carr AJ, Hulley PA. Cell differentiation versus cell death: extracellular glucose is a key determinant of cell fate following oxidative stress exposure. *Cell Death Dis* 2014; **5**: e1074.
22. Bi Y, Ehirchiou D, Kilts TM, Inkson CA, Embree MC, Sonoyama W *et al.* Identification of tendon stem/progenitor cells and the role of the extracellular matrix in their niche. *Nat Med* 2007; **13**: 1219–1227.
23. Lee CH, Lee FY, Tarafder S, Kao K, Jun Y, Yang G *et al.* Harnessing endogenous stem/progenitor cells for tendon regeneration. *J Clin Invest* 2015; **125**: 2690–2701.
24. Yin Z, Hu JJ, Yang L, Zheng ZF, An CR, Wu BB *et al.* Single-cell analysis reveals a nestin+ tendon stem/progenitor cell population with strong tenogenic potentiality. *Sci Adv* 2016; **2**: e1600874.
25. Chazaud B. Macrophages: supportive cells for tissue repair and regeneration. *Immunobiology* 2014; **219**: 172–178.
26. Thomopoulos S, Parks WC, Rifkin DB, Derwin KA. Mechanisms of tendon injury and repair. *J Orthop Res* 2015; **33**: 832–839.
27. Shukunami C, Yoshimoto Y, Takimoto A, Yamashita H, Hiraki Y. Molecular characterization and function of tenomodulin, a marker of tendons and ligaments that integrate musculoskeletal components. *Jpn Dent Sci Rev* 2016; **52**: 84–92.
28. Wu YF, Chen CH, Cao Y, Avanessian B, Wang XT, Tang JB. Molecular events of cellular apoptosis and proliferation in the early tendon healing period. *J Hand Surg Am* 2010; **35**: 2–10.
29. Tokunaga T, Shukunami C, Okamoto N, Taniwaki T, Oka K, Sakamoto H *et al.* FGF-2 stimulates the growth of tenogenic progenitor cells to facilitate the generation of Tenomodulin-positive tenocytes in a rat rotator cuff healing model. *Am J Sports Med* 2015; **43**: 2411–2422.
30. Kang JR, Gupta R. Mechanisms of fatty degeneration in massive rotator cuff tears. *J Shoulder Elbow Surg* 2012; **21**: 175–180.
31. Oak NR, Gumucio JP, Flood MD, Saripalli AL, Davis ME, Harning JA *et al.* Inhibition of 5-LOX, COX-1, and COX-2 increases tendon healing and reduces muscle fibrosis and lipid accumulation after rotator cuff repair. *Am J Sports Med* 2014; **42**: 2860–2868.
32. Gladstone JN, Bishop JY, Lo IK, Flatow EL. Fatty infiltration and atrophy of the rotator cuff do not improve after rotator cuff repair and correlate with poor functional outcome. *Am J Sports Med* 2007; **35**: 719–728.
33. Zhou Z, Akinbiyi T, Xu L, Ramcharan M, Leong DJ, Ros SJ *et al.* Tendon-derived stem/progenitor cell aging: defective self-renewal and altered fate. *Aging Cell* 2010; **9**: 911–915.
34. Kannus P, Józsa L. Histopathological changes preceding spontaneous rupture of a tendon. A controlled study of 891 patients. *J Bone Joint Surg Am* 1991; **73**: 1507–1525.
35. Nanthakumar CB, Hatley RJ, Lemma S, Gauldie J, Marshall RP, Macdonald SJ. Dissecting fibrosis: therapeutic insights from the small-molecule toolbox. *Nat Rev Drug Discov* 2015; **14**: 693–720.
36. Pellicoro A, Ramachandran P, Iredale JP, Fallowfield JA. Liver fibrosis and repair: immune regulation of wound healing in a solid organ. *Nat Rev Immunol* 2014; **14**: 181–194.
37. Wynn TA, Ramalingam TR. Mechanisms of fibrosis: therapeutic translation for fibrotic disease. *Nat Med* 2012; **18**: 1028–1040.
38. Chen S, Jiang S, Zheng W, Tu B, Liu S, Ruan H *et al.* RelA/p65 inhibition prevents tendon adhesion by modulating inflammation, cell proliferation, and apoptosis. *Cell Death Dis* 2017; **8**: e2710.
39. Shen H, Kormpakis I, Havlioglu N, Linderman SW, Sakiyama-Elbert SE, Erickson IE *et al.* The effect of mesenchymal stromal cell sheets on the inflammatory stage of flexor tendon healing. *Stem Cell Res Ther* 2016; **7**: 144.
40. Manning CN, Havlioglu N, Knutsen E, Sakiyama-Elbert SE, Silva MJ, Thomopoulos S *et al.* The early inflammatory response after flexor tendon healing: a gene expression and histological analysis. *J Orthop Res* 2014; **32**: 645–652.
41. Geary MB, Orner CA, Bawany F, Awad HA, Hammert WC, O'Keefe RJ *et al.* Systemic EP4 inhibition increases adhesion formation in a murine model of flexor tendon repair. *PLoS One* 2015; **10**: e0136351.

42. Beredjiklian PK. Biologic aspects of flexor tendon laceration and repair. *J Bone Joint Surg Am* 2003; **85-A**: 539–550.
43. Korntner S, Kunkel N, Lehner C, Gehwolf R, Wagner A, Augat P *et al.* A high-glucose diet affects Achilles tendon healing in rats. *Sci Rep* 2017; **7**: 780.
44. Spiegelman BM, Ginty CA. Fibronectin modulation of cell shape and lipogenic gene expression in 3T3-adipocytes. *Cell* 1983; **35**: 657–666.
45. Gelberman RH, Linderman SW, Jayaram R, Dikina AD, Sakiyama-Elbert S, Alsberg E *et al.* Combined administration of ASCs and BMP-12 promotes an M2 macrophage phenotype and enhances tendon healing. *Clin Orthop Relat Res* **475**: 2318–23312017.
46. Senol-Cosar O, Flach RJ, DiStefano M, Chawla A, Nicoloro S, Straubhaar J *et al.* Tenomodulin promotes human adipocyte differentiation and beneficial visceral adipose tissue expansion. *Nat Commun* 2016; **7**: 10686.
47. Tolppanen AM, Pulkkinen L, Herder C, Koenig W, Kolehmainen M, Lindström J *et al.* The genetic variation of the tenomodulin gene (TNMD) is associated with serum levels of systemic immune mediators–the Finnish Diabetes Prevention Study. *Genet Med* 2008; **10**: 536–544.
48. Saiki A, Olsson M, Jernås M, Gummesson A, McTernan PG, Andersson J *et al.* Tenomodulin is highly expressed in adipose tissue, increased in obesity, and down-regulated during diet-induced weight loss. *J Clin Endocrinol Metab* 2009; **94**: 3987–3994.
49. Tolppanen AM, Kolehmainen M, Pulkkinen L, Uusitupa M. Tenomodulin gene and obesity-related phenotypes. *Ann Med* 2010; **42**: 265–275.
50. Tolppanen AM, Pulkkinen L, Kuulasmaa T, Kolehmainen M, Schwab U, Lindström J *et al.* The genetic variation in the tenomodulin gene is associated with serum total and LDL cholesterol in a body size-dependent manner. *Int J Obes* 2008; **32**: 1868–1872.
51. Johansson LE, Danielsson AP, Parikh H, Klintenberg M, Norström F, Groop L *et al.* Differential gene expression in adipose tissue from obese human subjects during weight loss and weight maintenance. *Am J Clin Nutr* 2012; **96**: 196–207.
52. Kolehmainen M, Salopuro T, Schwab US, Kekäläinen J, Kallio P, Laaksonen DE *et al.* Weight reduction modulates expression of genes involved in extracellular matrix and cell death: the GENOBIN study. *Int J Obes* 2008; **32**: 292–303.
53. Kawai M, Rosen CJ. PPARγ: a circadian transcription factor in adipogenesis and osteogenesis. *Nat Rev Endocrinol* 2010; **6**: 629–636.
54. Ahmadian M, Suh JM, Hah N, Liddle C, Atkins AR, Downes M *et al.* PPARγ signaling and metabolism: the good, the bad and the future. *Nat Med* 2013; **19**: 557–566.
55. Cao Y, Gomes SA, Rangel EB, Paulino EC, Fonseca TL, Li J *et al.* S-nitrosoglutathione reductase-dependent PPARγ denitrosylation participates in MSC-derived adipogenesis and osteogenesis. *J Clin Invest* 2015; **125**: 1679–1691.
56. Rosen ED, MacDougald OA. Adipocyte differentiation from the inside out. *Nat Rev Mol Cell Biol* 2006; **7**: 885–896.
57. Gehwolf R, Wagner A, Lehner C, Bradshaw AD, Scharler C, Niestrawska JA *et al.* Pleiotropic roles of the matricellular protein Sparc in tendon maturation and ageing. *Sci Rep* 2016; **6**: 32635.
58. Nobusue H, Onishi N, Shimizu T, Sugihara E, Oki Y, Sumikawa Y *et al.* Regulation of MKL1 via actin cytoskeleton dynamics drives adipocyte differentiation. *Nat Commun* 2014; **5**: 3368.
59. Kohler J, Popov C, Klotz B, Alberton P, Prall WC, Haasters F *et al.* Uncovering the cellular and molecular changes in tendon stem/progenitor cells attributed to tendon aging and degeneration. *Aging Cell* 2013; **12**: 988–999.
60. Popov C, Kohler J, Docheva D. Activation of EphA4 and EphB2 reverse signaling restores the age-associated reduction of self-renewal, migration, and actin turnover in human tendon stem/progenitor cells. *Front Aging Neurosci* 2016; **7**: 246.

Supplementary Information accompanies this paper on Cell Death and Disease website (http://www.nature.com/cddis)

5. Publication II

Loss of tenomodulin expression is a risk factor for age-related intervertebral disc degeneration

Dasheng Lin, Paolo Alberton, Manuel Delgado Caceres, Carina Prein, Hauke Clausen-Schaumann, Jian Dong, Attila Aszodi, Chisa Shukunami, James C Iatridis and Denitsa Docheva✉

Aging Cell. 2020;19(3):e13091. doi: 10.1111/acel.13091.

Received: 30 October 2019 | Accepted: 21 November 2019

DOI: 10.1111/acel.13091

ORIGINAL ARTICLE

Aging Cell WILEY

Loss of tenomodulin expression is a risk factor for age-related intervertebral disc degeneration

Dasheng Lin[1,2] | Paolo Alberton[1] | Manuel Delgado Caceres[3] | Carina Prein[4] | Hauke Clausen-Schaumann[4] | Jian Dong[5] | Attila Aszodi[1] | Chisa Shukunami[6] | James C Iatridis[7] | Denitsa Docheva[3]

[1]Experimental Surgery and Regenerative Medicine, Clinic for General, Trauma and Reconstructive Surgery, Ludwig-Maximilians-University (LMU), Munich, Germany

[2]Orthopaedic Center of People's Liberation Army, The Affiliated Southeast Hospital of Xiamen University, Zhangzhou, China

[3]Experimental Trauma Surgery, Department of Trauma Surgery, University Regensburg Medical Centre, Regensburg, Germany

[4]Center for Applied Tissue Engineering and Regenerative Medicine (CANTER), Munich University of Applied Sciences and Center for Nanoscience (CeNS), Munich, Germany

[5]Department of Orthopaedic Surgery, Zhongshan Hospital, Fudan University, Shanghai, China

[6]Department of Molecular Biology and Biochemistry, Graduate School of Biomedical & Health Sciences, Hiroshima University, Hiroshima, Japan

[7]Leni and Peter W. May Department of Orthopaedics, Icahn School of Medicine at Mount Sinai, New York, NY, USA

Correspondence
Denitsa Docheva, Department of Trauma Surgery, University Regensburg Medical Centre, Franz-Josef-Strauss-Allee 11, 93053 Regensburg, Germany.
Email: denitsa.docheva@ukr.de

Funding information
Deutsche Forschungsgemeinschaft, Grant/Award Number: DO1414/3-1; EU H2020-WIDESPREAD-Twinning Grant Achilles, Grant/Award Number: 810850; National Natural Science Foundation of China, Grant/Award Number: 81600696; National Institutes of Health, Grant/Award Number: GM089820

Abstract

The intervertebral disc (IVD) degeneration is thought to be closely related to ingrowth of new blood vessels. However, the impact of anti-angiogenic factors in the maintenance of IVD avascularity remains unknown. Tenomodulin (*Tnmd*) is a tendon/ligament-specific marker and anti-angiogenic factor with abundant expression in the IVD. It is still unclear whether Tnmd contributes to the maintenance of IVD homeostasis, acting to inhibit vascular ingrowth into this normally avascular tissue. Herein, we investigated whether IVD degeneration could be induced spontaneously by the absence of *Tnmd*. Our results showed that Tnmd was expressed in an age-dependent manner primarily in the outer annulus fibrous (OAF) and it was downregulated at 6 months of age corresponding to the early IVD degeneration stage in mice. *Tnmd* knockout ($Tnmd^{-/-}$) mice exhibited more rapid progression of age-related IVD degeneration. These signs include smaller collagen fibril diameter, markedly lower compressive stiffness, reduced multiple IVD- and tendon/ligament-related gene expression, induced angiogenesis, and macrophage infiltration in OAF, as well as more hypertrophic-like chondrocytes in the nucleus pulposus. In addition, *Tnmd* and chondromodulin I (*Chm1*, the only homologous gene to *Tnmd*) double knockout ($Tnmd^{-/-}Chm1^{-/-}$) mice displayed not only accelerated IVD degeneration, but also ectopic bone formation of IVD. Lastly, the absence of *Tnmd* in OAF-derived cells promoted p65 and matrix metalloproteinases upregulation, and increased migratory capacity of human umbilical vein endothelial cells. In sum, our data provide clear evidences that Tnmd acts as an angiogenic inhibitor in the IVD homeostasis and protects against age-related IVD degeneration. Targeting Tnmd may represent a novel therapeutic strategy for attenuating age-related IVD degeneration.

KEYWORDS

angiogenesis, annulus fibrous, intervertebral disc degeneration, knockout mice, nucleus pulposus, tenomodulin

1 | INTRODUCTION

Intervertebral disc (IVD) degeneration is a common condition and is thought to be an initiating factor for back pain (Nguyen, Poiraudeau, & Rannou, 2015). The pathogenesis of IVD degeneration is a complex, multifactorial process with large contribution from both genetic and environmental components (Annunen et al., 1999; Pye, Reid, Adams, Silman, & O'Neill, 2007; Song et al., 2013; Stokes & Iatridis, 2004; Williams et al., 2013; Williams et al., 2011). The IVD is the largest avascular tissue in the body and has poor self-healing potential (Huang, Urban, & Luk, 2014). Under pathological conditions, the IVDs express pro-angiogenic factors leading to neovascularization (Cornejo, Cho, Giannarelli, Iatridis, & Purmessur, 2015; de Vries, van Doeselaar, Meij, Tryfonidou, & Ito, 2018; Freemont et al., 1997; Purmessur, Freemont, & Hoyland, 2008). However, the impact of anti-angiogenic factors in the maintenance of IVD avascularity remains unknown.

Tenomodulin (Tnmd), a tendon/ligament-specific marker and anti-angiogenic molecule, is a member of a novel class protein family of type II transmembrane glycoproteins containing only one other homologous protein, namely chondromodulin I (Chm1) that is abundant in cartilage tissue (Brandau, Meindl, Fässler, & Aszódi, 2001; Dex, Lin, Shukunami, & Docheva, 2016; Docheva, Hunziker, Fässler, & Brandau, 2005; Kimura et al., 2008; Shukunami, Oshima, & Hiraki, 2001). The cleavage of the highly conserved C-terminal cysteine-rich domain of Tnmd and subsequent secretion are required for the anti-angiogenic activities of the protein (Oshima et al., 2004). *Tnmd* transcript is predominantly expressed in hypovascular tissues, such as tendons, ligaments, as well as eyes (Brandau et al., 2001; Shukunami et al., 2001). Interestingly, Minogue, Richardson, Zeef, Freemont, and Hoyland (2010) have demonstrated that *Tnmd* mRNA has abundant expression in the annulus fibrous (AF) and the nucleus pulposus (NP). Concomitantly, Nakamichi et al. (2016) showed that *Mohawk* (*Mkx*), an upstream gene of *Tnmd* (Ito et al., 2010), promotes the maintenance and regeneration of the outer annulus fibrous (OAF) of IVD suggesting that *Tnmd* may be involved in IVD homeostasis. To date, however, this hypothesis has not been investigated in detail.

In our previous studies, we compared *Tnmd* knockout ($Tnmd^{-/-}$) mice with their wild-type (WT) littermates and showed that the absence of *Tnmd* causes reduced tendon cell proliferation and density in vivo (Docheva et al., 2005), coupled with significantly lower self-renewal and augmented senescence of tendon-derived stem/progenitor cells (TSPCs) in vitro (Alberton et al., 2015). Furthermore, we observed the pathological thickening and stiffening of collagen I (Col I) fibers in $Tnmd^{-/-}$ Achilles tendons resulting in running distance and time failure in $Tnmd^{-/-}$ mice challenged by running tests (Dex et al., 2017). Interestingly, the local absence of *Tnmd* in the cardiac chordae tendineae cordis (CTC) promoted angiogenesis and matrix metalloproteinases (MMPs) activation (Kimura et al., 2008), a phenomenon also observed when $Tnmd^{-/-}$ mice were subjected to surgically induced Achilles tendon rupture. In this model, we detected that genetic ablation of *Tnmd* leads to blood vessel accumulation accompanied by abnormal extracellular matrix (ECM) composition and macrophage profile during the early repair phase of injured tendons (Lin et al., 2017).

Cumulatively, the aforementioned data reveal that *Tnmd* plays an important regulatory role in the avascular tendogenic/ligamentogenic tissue homeostasis. Therefore, we hypothesized that Tnmd in the IVD may act to inhibit vascular ingrowth into this normally avascular tissue and maintain homeostasis. Here, we investigated the exact functional role of Tnmd in IVD in vivo and in vitro by phenotypization of *Tnmd*-deficient IVD tissues and IVD-derived cells. Lastly, to rule out possible compensatory effects between the two homologs, we investigated the IVDs of *Tnmd* and *Chm1* double knockout ($Tnmd^{-/-}Chm1^{-/-}$) mice.

2 | RESULTS

2.1 | Tnmd is expressed in the IVD OAF and NP

Tnmd expression was observed by us, along with other researchers, in tendons, ligaments, eyes, and CTC (Brandau et al., 2001; Kimura et al., 2008; Shukunami et al., 2001). In the vertebral column, previous studies have localized *Tnmd* gene expression to areas of the IVD (Minogue et al., 2010; Nakamichi et al., 2016), as well as Tnmd immunostainings carried out in neonate mice detected robust protein expression in the OAF (Yoshimoto et al., 2017). To further determine the precise distribution of Tnmd in the postnatal and adult IVD, we first performed immunolocalization studies on IVD tissues from WT mice at distinct stages of skeletal development ranging

FIGURE 1 Tnmd is mainly expressed in OAF, and its loss leads to age-related IVD degeneration. (a and b) Immunofluorescence of Tnmd protein expression in developing adult and aged IVDs of WT mice shows that Tnmd is mainly expressed in OAF and to a lower extent in the NP, and as expected, Tnmd was not detected in $Tnmd^{-/-}$ IVDs. Fluorescence intensity analysis revealed an expression peak at 1 month and expression downregulation from 6 months onwards (n = 3–5 animals). (c) Western blot confirmed that Tnmd protein expression is higher at 1 month than at 6 months (n = 3 animals). (d and e) IHC of the human IVDs confirmed that TNMD protein is mainly found in the OAF and to a lesser extended in the NP (two-tailed nonparametric Mann–Whitney test; n = 5 samples). (f) Representative H&E stainings of human IVD (n = 5 samples). (g) H&E staining demonstrates greater degenerative changes in $Tnmd^{-/-}$ IVDs when compared to WT at 6 and 18 months. (h) Safranin O staining reveals small roundish chondrocyte-like cells in IAF and NP of $Tnmd^{-/-}$ IVDs. (i and j) Histological grading and disc height index calculation show in $Tnmd^{-/-}$ mice significantly widespread degeneration compared to WT at both examined stages (two-tailed nonparametric Mann–Whitney test; 6-month-old mice, n = 5 animals; 18-month-old mice, n = 3 animals). $^{**}p < .01$; $^{***}p < .001$. d, day; H&E, hematoxylin–eosin; IAF, inner annulus fibrous; IHC, immunohistochemistry; IVD, intervertebral disc; mo, month; NB, newborn; NP, nucleus pulposus; OAF, outer annulus fibrous; WT, wild-type. Scale bar, 200 μm

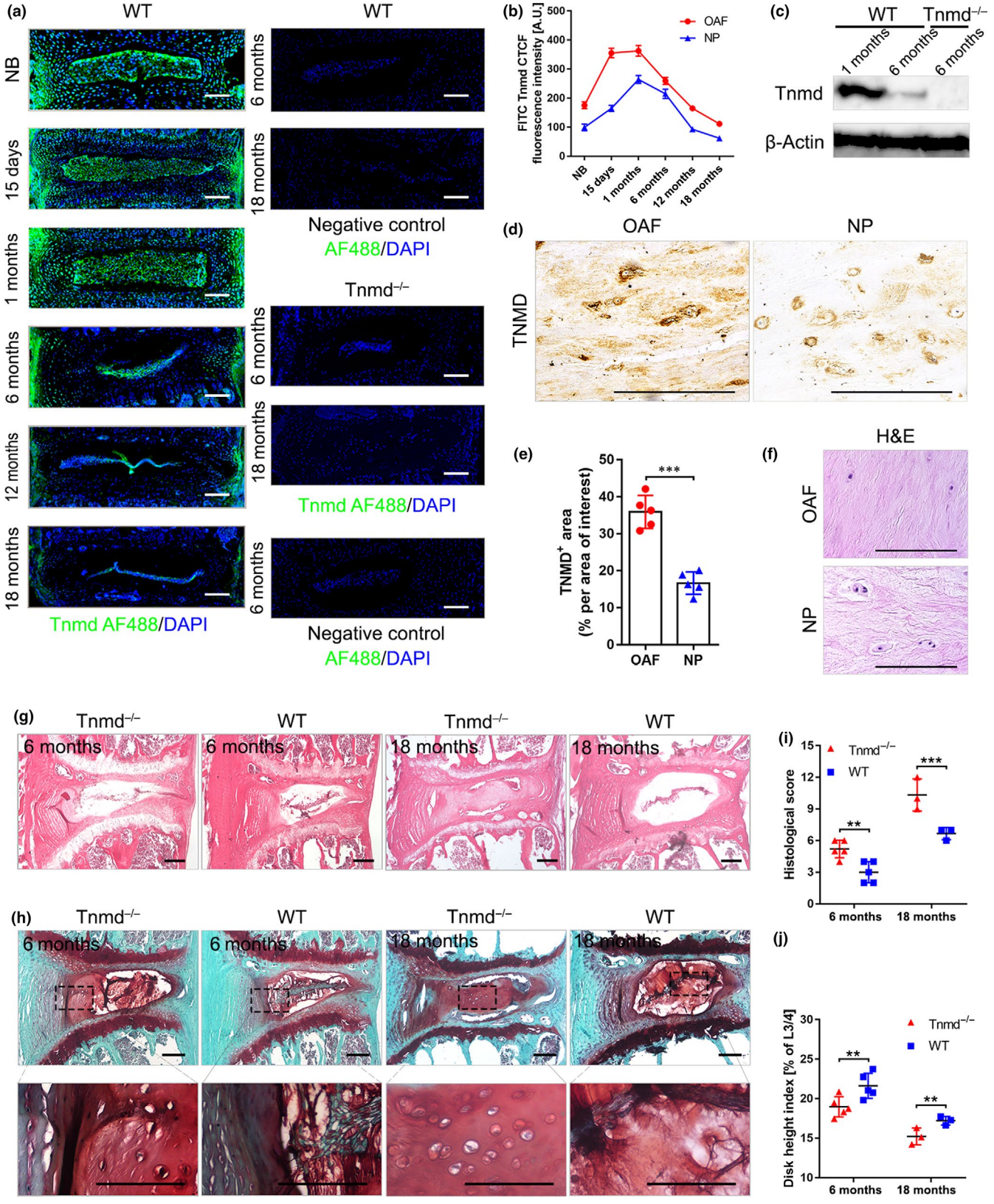

from newborn to 18 months of age. We observed that Tnmd is predominantly produced and deposited in the ECM of the OAF, as well as to a lesser extent in the NP regions. Scarce positive signals in the inner annulus fibrous (IAF) and the cartilaginous endplate (EP) were also detected; however, those were primarily cellular and not in the ECM (Figure 1a). Notably, Tnmd signals in the OAF and the NP gradually peaked at 1 month of age, while it dropped at 6 months of age corresponding to the early IVD degeneration stage in mice,

and then further decreased at 12 and 18 months (Figure 1b). As expected, Tnmd was not detected in *Tnmd*$^{-/-}$ IVDs (Figure 1a). Western blotting of IVD tissue protein extracts confirmed that the protein levels of Tnmd are higher at 1 month, when compared to 6 months (Figure 1c) as well as that in the IVD; similar to Achilles tendon and CTC, Tnmd is fully processed to its 16 kDa C-terminal portion. We also assessed the expression of TNMD in human lumbar discs (Table S1). Consistent with the observation in mice, TNMD protein was predominantly found in the ECM of the OAF and to a lesser extent in the NP regions (Figure 1d–f).

2.2 | The absence of Tnmd leads to age-related IVD degeneration

To analyze the potential involvement of Tnmd during naturally occurring IVD degeneration in mouse, 6- and 18-month-old lumbar IVDs were first examined by hematoxylin–eosin (H&E) and safranin O staining for pathological changes. Importantly, *Tnmd*$^{-/-}$ mice showed higher levels of degenerative changes compared to WT mice. Lamellae appeared thinner, looser, and fibrillated in *Tnmd*$^{-/-}$ AF (Figure 1g). In the IAF and NP areas of *Tnmd*$^{-/-}$ IVDs, small round cells, morphologically resembling chondrocytes, were visible. Cumulatively, such abnormalities are often described as degenerative changes (Nakamichi et al., 2016), and they were even more evident in the *Tnmd*$^{-/-}$ discs at 18 months (Figure 1h). By implementing the histological scoring system for mouse IVD (Tam et al., 2018), we detected higher degenerative scores at 6 and 18 months in *Tnmd*$^{-/-}$ mice, reflective of a significantly widespread IVD degeneration compared to WT (Figure 1i). In addition, calculation of disc height index (Masuda et al., 2005) showed lower values for *Tnmd*$^{-/-}$ IVDs at both examined stages (Figure 1j). Thus, our results demonstrate that Tnmd is associated with IVD homeostasis and its loss leads to profound tissue degeneration that advances during the aging process.

2.3 | Tnmd deficiency results in abnormal diameters and biomechanical properties of IVD collagen fibrils, accompanied by reduced expression of multiple IVD- and tendon/ligament-related genes in the OAF

Since Tnmd is highly expressed in the OAF and a disorganized OAF morphology characterized by thinner collagen fibers (Figure S1a,b) was observed in *Tnmd*$^{-/-}$ mice, we next examined the nanotopographical and biomechanical properties of 6-month-old *Tnmd*$^{-/-}$ and WT IVDs. We applied indentation-type atomic force microscopy (IT-AFM) to quantitatively assess collagen fibril diameters and compressive stiffness of AF. Height images revealed that the collagen fibrils of *Tnmd*$^{-/-}$ OAF were more frayed and interrupted by gaps, and vertical deflection images indicated that the collagenous network of *Tnmd*$^{-/-}$ OAF was less dense compared to WT (Figure 2a). The fibril diameters in OAF and IAF were significantly smaller in *Tnmd*$^{-/-}$ than in WT mice (Figure 2b). Indentation measurements on native IVD tissues indicated a bimodal stiffness distribution in both genotypes (Figure 2c). In *Tnmd*$^{-/-}$ OAF and IAF, the proteoglycan stiffness peaks were detected at 1.240 ± 0.098 and 0.272 ± 0.004 MPa and those of collagen network at 2.972 ± 0.033 and 0.532 ± 0.049 MPa, respectively. In WT OAF and IAF, the average proteoglycan stiffness peaks were 8.134 ± 0.307 and 0.285 ± 0.013 MPa, while the collagen stiffness peaks were 14.019 ± 0.493 and 0.581 ± 0.0063 MPa, respectively. In sum, the overall compressive stiffness of OAF was markedly lower in *Tnmd*$^{-/-}$ than WT mice, but the IAF biomechanical properties were not significantly different between genotypes.

Changes in expression levels of ECM and cross-linking molecules can lead to loss of mechanical properties and, thus, impaired ability of the OAF to resist compression delivered to the IVD and particularly the NP (Feng, Danfelter, Strömqvist, & Heinegård, 2006). Therefore, we analyzed how the ablation of *Tnmd* affects the expression levels of IVD- and tendon/ligament-related genes using quantitative real-time PCR (qRT–PCR) on *Tnmd*$^{-/-}$ and WT lumbar OAF tissue-derived mRNA. We observed downregulation of multiple IVD- and tendon/ligament-related genes including scleraxis (*Scx*), *Mkx*, collagens I, V, XII, XIV, and XV (*Col1a1*, *Col5a1*, *Col12a1*, *Col14a1*, *Col15a1*), early growth response protein 1 and 2 (*Egr1*, *Egr2*), tenascin C (*Tnc*), thrombospondin 2 and 4 (*Thbs2*, *Thbs4*), transforming growth factor beta 1 (*Tgfb1*), alpha smooth muscle actin (*Acta2*), ephrin type-A receptor 4 (*Epha4*), asporin (*Aspn*), and fibromodulin (*Fmod*), without affecting those of collagens III and VI (*Col3a1*, *Col6a1*), eyes absent homolog 1 and 2 (*Eya1*, *Eya2*), sine oculis homeobox homolog 1 and 2 (*Six1*, *Six2*), cartilage oligomeric protein (*Comp*), lubricin (*Prg4*), biglycan (*Bgn*), decorin (*Dcn*), fibronectin (*Fn*), lysyl oxidase (*Lox*), lumican (*Lum*), procollagen-lysine, 2-oxoglutarate-5-dioxygenase 1 (*Plod1*), and transglutaminase 2 (*Tgm2*) in *Tnmd*$^{-/-}$ compared to WT mice (Figure 2d). Additionally, we compared the mRNA levels of IVD- and tendon/ligament-related genes between tendon and OAF tissues from both genotypes, and showed that the absence of *Tnmd* in the tendon and the OAF causes opposite effects on the mRNA expression levels of *Scx*, *Mkx*, *Col14a1*, *Col15a1*, and *Prg4* (Figure S1c) suggesting tissue-specific regulation.

Taken together, these findings demonstrate that *Tnmd* is a critical factor required to maintain the structural and biomechanical properties of the OAF collagen fibrils likely through the modulation of ECM gene expression.

2.4 | Increased angiogenesis, macrophages infiltration, and apoptosis in Tnmd$^{-/-}$ OAF

The AF and EP are natural barriers resistant to vascular invasion due to intrinsic angiogenic inhibitors. IVD degeneration is often marked by blood vessel ingrowth, infiltration of inflammatory cells, and increased cell apoptosis (de Vries, van Doeselaar, Meij, Tryfonidou, & Ito, 2018; Freemont et al., 1997; McCann & Séguin, 2016; Phillips, Jordan-Mahy, Nicklin, & Le Maitre, 2013). For this reason, we then focused our investigation on the OAF zone in 6-month-old mice in

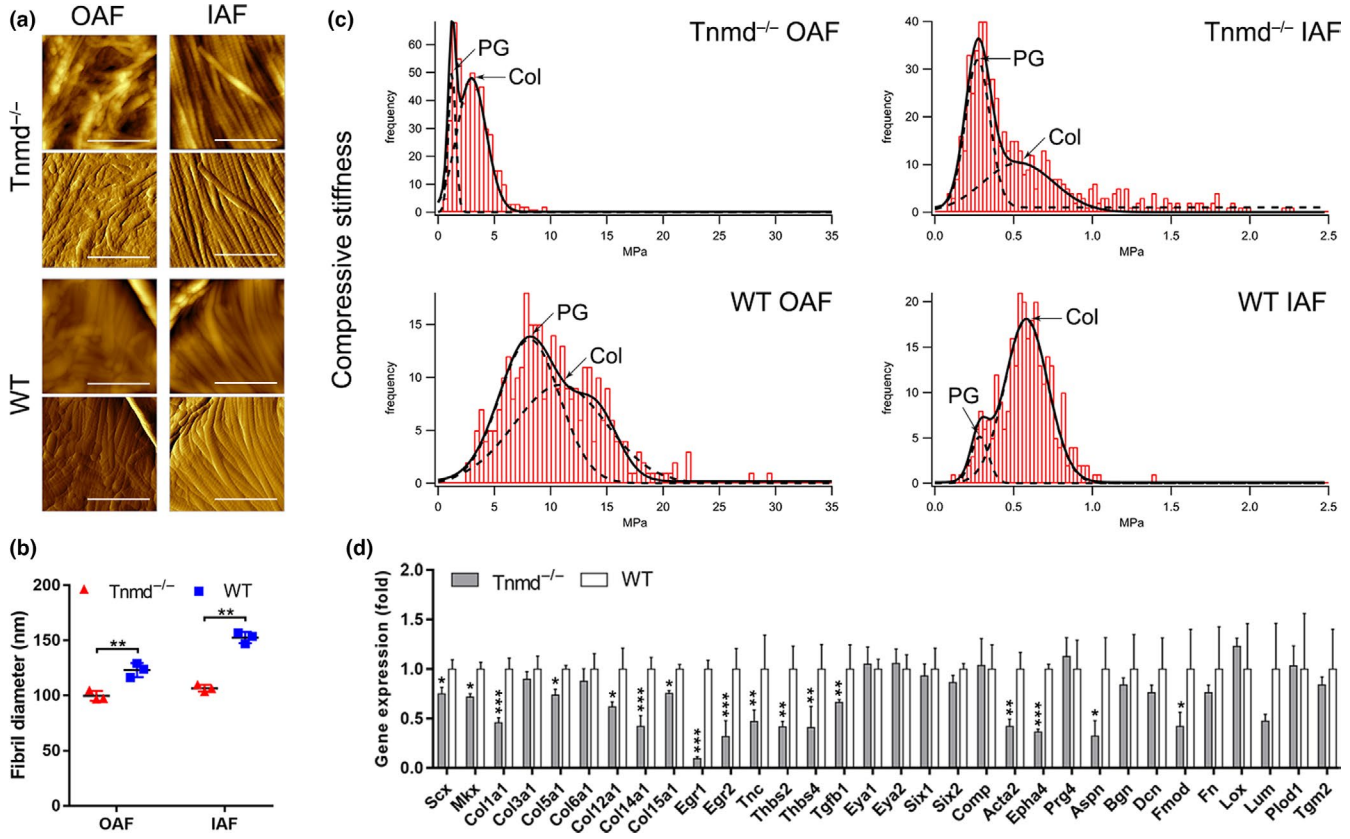

FIGURE 2 *Tnmd* deficiency causes altered ECM nanostructure and mechanical properties of the OAF in 6-month-old mice. (a) AFM height images (upper panels for both genotypes) show that the collagen fibrils in *Tnmd*$^{-/-}$ OAF were more frayed and interrupted by gaps, and vertical deflection images (lower panels) demonstrate that the collagen network in this region was less dense in *Tnmd*$^{-/-}$ compared to WT. (b) Comparison of the collagen fibril diameters reveals significantly smaller average size in *Tnmd*$^{-/-}$ than in WT AF (two-tailed unpaired Student's *t* test; *n* = 3 animals, and 200 fibrils were analyzed per genotype). (c) Plots of compressive stiffness data obtained by indentation AFM demonstrated that ECM compressive stiffness was markedly lower in the OAF regions of *Tnmd*$^{-/-}$ IVDs but not noticeably different in the IAF regions (two-tailed unpaired Student's *t* test; *n* = 3 animals). (d) Significant downregulation of numerous IVD- and tendon/ligament-related genes was detected in *Tnmd*$^{-/-}$ OAF by qRT–PCR analysis. For calculation of fold changes, WT was set to 1 (two-tailed unpaired Student's *t* test; *n* = 3 animals). $^{*}p < .05$; $^{**}p < .01$; $^{***}p < .001$. AF, annulus fibrous; Col, collagen; ECM, extracellular matrix; IAF, inner annulus fibrous; IVD, intervertebral disc; OAF, outer annulus fibrous; PG, proteoglycan; qRT–PCR, quantitative real-time PCR; WT, wild-type. Scale bar, 1 μm

order to reveal if *Tnmd* contributes to the maintenance of avascularity. We found that the occurrence of CD31-labeled vessels was increased in the OAF of *Tnmd*$^{-/-}$ mice when compared with WT mice (Figure 3a,b). Infiltration of macrophages was confirmed by staining with F4/80 monoclonal antibody directed specifically against mouse macrophages, demonstrating a significant increase in macrophage number in the OAF zone of *Tnmd*$^{-/-}$ IVDs (Figure 3c,d). We also performed in situ terminal deoxynucleotidyl transferase-mediated dUTP-biotin nick end labeling (TUNEL) assay and immunofluorescent staining for p53, to detect if apoptotic and senescent cells are present in the OAF of *Tnmd*$^{-/-}$ mice, landmarks of IVD degenerative processes (Feng et al., 2016). We observed a higher number of TUNEL- and p53-positive cells in *Tnmd*$^{-/-}$ compared to WT OAF (Figure 3e,f, Figure S1d,e). Lastly, we carried out immunofluorescent staining for the proliferative marker, PCNA, which confirmed a lower number of dividing cells in the OAF zone of 6-month-old *Tnmd*$^{-/-}$ than WT IVDs (Figure 3g,h). Taken together, the above findings indicate the essential role of the locally expressed *Tnmd* in IVD homeostasis, its loss led to induced angiogenesis, macrophage infiltration, and apoptosis, while cell proliferation was significantly reduced.

2.5 | Manifestation of hypertrophic chondrocytes and Col X-rich matrix in the NP of Tnmd$^{-/-}$ mice

It has been shown that ectopic calcifications in IVDs are a known characteristic of IVD degeneration (Hristova et al., 2011; Illien-Jünger et al., 2016). The observed small round cells, resembling chondrocyte morphology, in the *Tnmd*$^{-/-}$ NP prompted us to test whether the loss of *Tnmd* is accelerating hypertrophic chondrocyte-like occurrence. The major proteoglycan of the NP is aggrecan (Acan), which due to its highly anionic glycosaminoglycan content provides osmotic properties, enabling the NP to maintain height and turgor against compressive loads (Bedore et al., 2013).

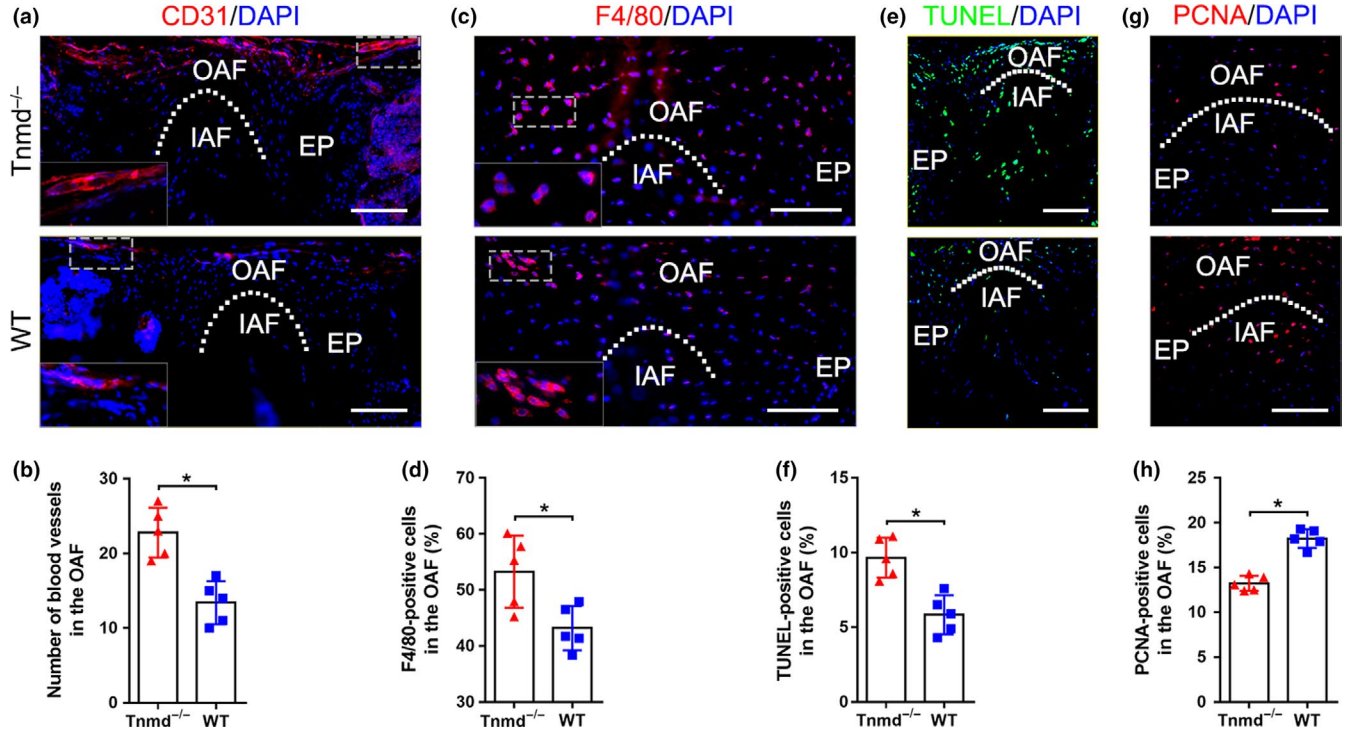

FIGURE 3 Loss of *Tnmd* results in blood vessel ingrowth, macrophage infiltration, and increased cell apoptosis in the OAF. (a and b) Immunofluorescence staining with anti-CD31 antibody reveals increased vessel number in the OAF of *Tnmd*$^{-/-}$ than WT. (c and d) Higher number of F4/80-positive macrophages was detected in the OAF of *Tnmd*$^{-/-}$ versus WT. (e and f) TUNEL staining demonstrates increased number of apoptotic cells in *Tnmd*$^{-/-}$ OAF than WT. (g and h) Reduced number of proliferating cells was observed in *Tnmd*$^{-/-}$ compared to WT mice by PCNA immunofluorescence staining. All quantitative histomorphometry data were assessed by two-tailed nonparametric Mann–Whitney test; $n = 5$ animals. $^{*}p < .05$. EP, endplate; IAF, inner annulus fibrous; OAF, outer annulus fibrous; TUNEL, transferase-mediated dUTP-biotin nick end labeling; WT, wild-type; white dotted line, OAF-IAF boundary. Scale bar, 200 μm

Therefore, we explored Acan expression by immunohistochemistry (IHC) in IVD sections from both genotypes. At 6 months, no noticeable change in Acan localization was found in *Tnmd*$^{-/-}$ NP compared to WT NP. However, the deposition of Acan was significantly decreased in Tnmd-deficient NP at 18 months (Figure 4a,b). More specifically, it has been proposed that Acan production ratio within the NP to hyaline cartilage is approximately 27:2 (Mwale, Roughley, & Antoniou, 2004). Hence, Acan downregulation can lead to appearance of hypertrophic-like chondrocytes, which subsequently contribute to calcification, due to the available free calcium ions (Hristova et al., 2011). In order to track hypertrophic chondrocyte-like differentiation in the NP, we next implemented immunofluorescence analysis for Sox9, the key pro-chondrogenic transcription factor (Takimoto, Oro, Hiraki, & Shukunami, 2012), and Runx2 and Col X, markers of hypertrophic chondrocytes (van der Kraan & van den Berg, 2012). *Tnmd*$^{-/-}$ NP showed compositional alterations associated with increased levels of Sox9- and Runx2-positive cells and Col X deposition at 18 months of age in contrast to WT mice (Figure 4c–h). These protein data together with the observed transcriptional changes of multiple genes (Figure 2d) suggested that *Tnmd* deficiency alters the balance in the expression of ECM molecules and is manifested by accumulation of hypertrophic chondrocytes and Col X-rich matrix in the NP, indicating clearly substantial IVD cell dysfunction.

2.6 | Tnmd and Chm1 double mutant mice display not only accelerated IVD degeneration but also ectopic bone formation

Our findings suggest that Tnmd contributes to protect the IVD from vascularization and inflammation. However, our present data do not exclude the possibility of the existence of other anti-angiogenic factors. Chm1, the only Tnmd homologous protein (Brandau et al., 2001; Shukunami et al., 2001), is a cartilage-specific angiogenesis inhibitor (Hiraki et al., 1997; Yoshioka et al., 2006) that has been previously shown to be also highly expressed in the IVD during the gestational period and gradually downregulated after maturation (Takao, Iwaki, Kondo, & Hiraki, 2000). Immunofluorescence staining for Chm1 in IVD showed that it is deposited in the ECM of NP, as well as expressed in cells from EP and OAF (Figure 5a). Western blotting and densitometric analyses of Chm1-positive areas revealed that Chm1 levels are decreased in *Tnmd*$^{-/-}$ IVD when compared with WTs (Figure 5b,c). These lines of evidence suggest that the expression of *Tnmd* and *Chm1* may be coordinated between the cell populations of NP, AF, and EP. Therefore, we carried out a pilot investigation of *Tnmd*$^{-/-}$*Chm1*$^{-/-}$ mouse model to elucidate for the first time the relationship between both proteins and IVD degeneration. Interestingly, H&E and safranin O staining demonstrated that *Tnmd*$^{-/-}$*Chm1*$^{-/-}$ mice display more severe

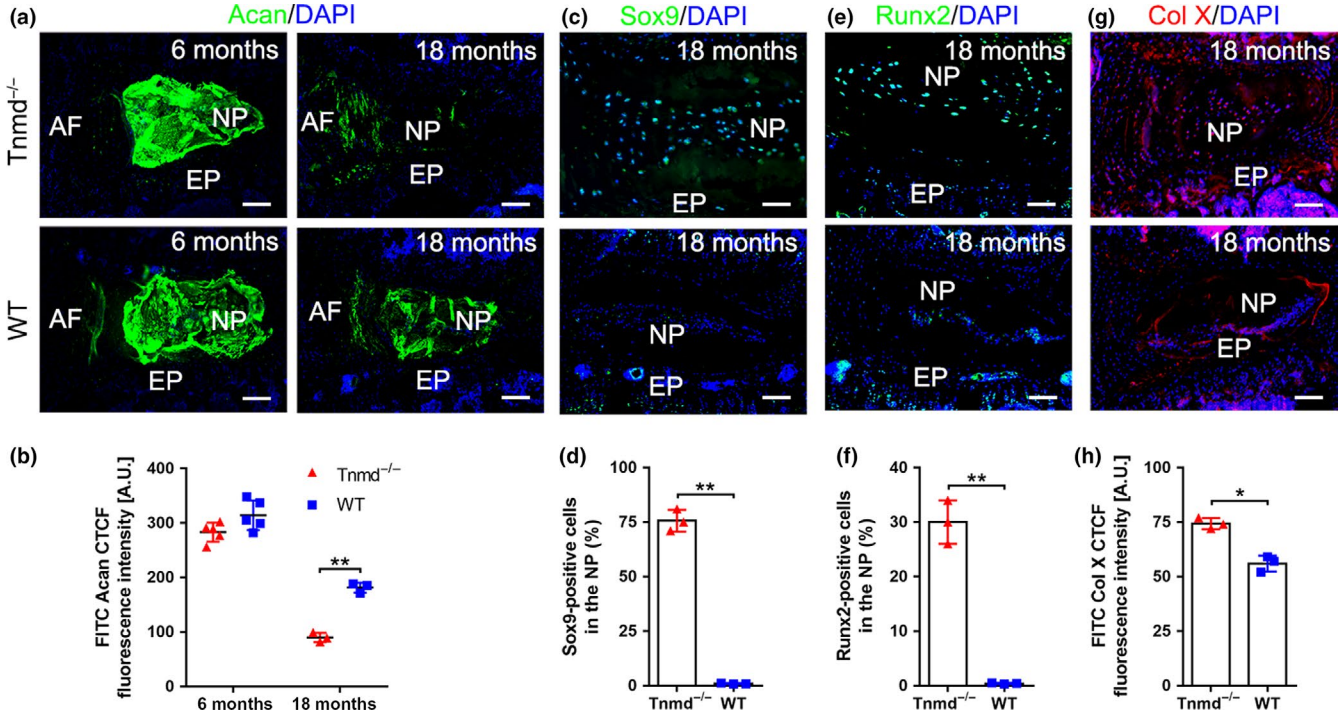

FIGURE 4 Accumulation of hypertrophic chondrocyte-like alterations in the NP of *Tnmd*$^{-/-}$ mice. (a and b) Significant downregulation of Acan protein expression was detected at 18 months by immunofluorescent imaging and fluorescence intensity analysis in *Tnmd*$^{-/-}$ NP compared to WT. (c–h) Immunofluorescence stainings with anti-Sox9, anti-Runx2 and anti-Col X antibodies reveal increased expression levels of the three hypertrophy markers in *Tnmd*$^{-/-}$ NPs compared with WT at 18 months. All quantitative histomorphometry data were assessed by two-tailed nonparametric Mann–Whitney test; 6-month-old mice, $n = 5$ animals; 18-month-old mice, $n = 3$ animals. $^{*}p < .05$; $^{**}p < .01$. AF, annulus fibrous; EP, endplate; mo, month; NP, nucleus pulposus; WT, wild-type. Scale bar, 200 μm

IVD degeneration associated with ectopic bone formation in the IVDs at 18 months when compared with *Tnmd*$^{-/-}$ and WT mice (Figure 5d–f). Immunofluorescence of CD31 showed that the OAF of *Tnmd*$^{-/-}$*Chm1*$^{-/-}$ mice contained many capillary-like structures (Figure 5g). Furthermore, multiple F4/80-labeled macrophages were distributed in the AF and NP regions (Figure 5h) and, lastly, ectopic ossification sites were detected with osteopontin (Opn, bone-specific marker) antibody in *Tnmd*$^{-/-}$*Chm1*$^{-/-}$ IVDs Figure 5i). Based on our novel data, we concluded that simultaneous loss of *Tnmd* and *Chm1* causes a more progressive IVD degenerative phenotype than *Tnmd* single knockout. It remains to be investigated to what extent these mutant variants compare to *Chm1* single knockout.

2.7 | Loss of Tnmd in OAF cells suppresses their proliferation and promotes cell apoptosis

To further understand the mechanisms underlying the roles of *Tnmd* in IVD homeostasis, we performed in vitro studies with OAF cells isolated from 12-month-old *Tnmd*$^{-/-}$ or WT lumbar IVDs (Figure S2a). First, we characterized the obtained cell populations by immunofluorescence staining and RT–PCR. Fmod, an accepted AF-specific marker in rodent (Leung, Tam, Chan, Chan, & Cheung, 2011; Smits & Lefebvre, 2003), was expressed in both genotypes, but its immunostaining signal was weaker in *Tnmd*$^{-/-}$ OAF cells compared with WTs (Figure S2b,g).

WT OAF cells were strongly expressing Tnmd, while as expected Tnmd was not produced by *Tnmd*$^{-/-}$ cells (Figure S2c). To analyze whether the synthesis of ECM proteins by the OAF cells is altered due to *Tnmd* deficiency, we next performed immunofluorescence analysis for Col I, which is the main protein component of OAF; Fn, which plays a pivotal role in facilitating AF cell attachment and fiber alignment (Attia, Santerre, & Kandel, 2011); and Lum, which interacts with collagen fibrils and contributes to AF mechanical properties (Sztrolovics, Alini, Mort, & Roughley, 1999). In vitro, only a slight decrease in the expression of the three proteins was observed in *Tnmd*$^{-/-}$ OAF cells (Figure S2d–g). Semiquantitative RT–PCR revealed that *Tnmd* mRNA could not be detected, while *Chm1* mRNA levels were reduced in *Tnmd*$^{-/-}$ OAF cells (Figure S2h).

To further evaluate the role of *Tnmd* in OAF cell behavior, we carried out time-lapse imaging of random migration, followed by plotting of forward migration index (FMI). Our results showed that *Tnmd*$^{-/-}$ OAF cells were less migratory than WT cells (Figure S3a,b). Quantification of velocity, accumulated and Euclidean distance clearly indicated that the observed effect was significant (Figure S3c,d). Furthermore, during 0, 3, 5, and 7 days of culture, DNA-based CyQUANT assays showed that the proliferation of *Tnmd*$^{-/-}$ OAF cells was significantly reduced compared to that of WT cells (Figure S3e). Lastly, TUNEL assays demonstrated that *Tnmd*$^{-/-}$ OAF

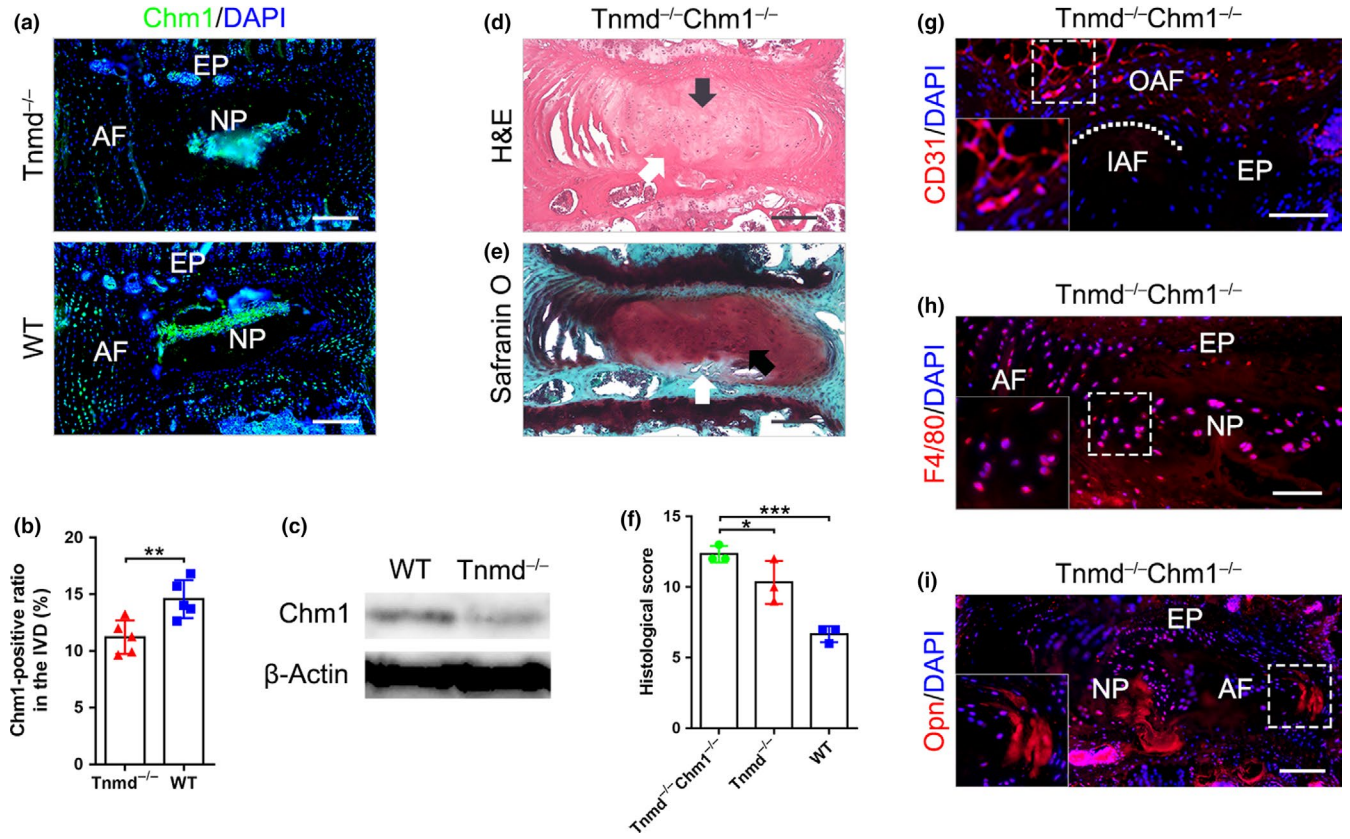

FIGURE 5 Double knockout for *Tnmd* and *Chm1* lead to accelerated IVD degeneration coupled with ectopic bone formation. (a and b) Immunofluorescence analysis of Chm1 expression shows Chm1 major localization in the NP as well as lower protein levels in $Tnmd^{-/-}$ than WT IVD at 6 months (two-tailed nonparametric Mann–Whitney test; $n = 5$ animals). (c) Western blotting confirmed the downregulation of Chm1 protein in $Tnmd^{-/-}$ compared to WT IVD ($n = 3$ animals). (d-f) H&E and safranin O staining reveal advanced IVD degeneration and ectopic bone formation in $Tnmd^{-/-}Chm1^{-/-}$ mice, and histological grading shows significantly worsened scores at 18 months in $Tnmd^{-/-}Chm1^{-/-}$ mice compared to $Tnmd^{-/-}$ and WT mice (one-way ANOVA was followed by Bonferroni post hoc correction, $n = 3$ animals). (g) Immunofluorescence analysis for CD31 demonstrate that $Tnmd^{-/-}Chm1^{-/-}$ OAF contain many capillary-like structures ($n = 3$ animals). (h) Immunofluorescence analysis for F4/80 shows many macrophages were distributed in and around the NP of $Tnmd^{-/-}Chm1^{-/-}$ mice ($n = 3$ animals). (i) Multiple sites of ectopic ossifications in $Tnmd^{-/-}Chm1^{-/-}$ IVD were observed by carrying out Opn immunostaining ($n = 3$ animals). $^{*}p < .05$; $^{**}p < .01$; $^{***}p < .001$. AF, annulus fibrous; EP, endplate; H&E, hematoxylin–eosin; IAF, inner annulus fibrous; IVD, intervertebral disc; NP, nucleus pulposus; OAF, outer annulus fibrous; WT, wild-type; black arrows, chondrocyte-like cells; white arrows, ectopic ossifications; white dotted line, OAF-IAF boundary. Scale bar: 200 μm

cell population contained increased number of apoptotic cells compared to WT cell population (Figure S3f,g). Taken together, we validated the OAF phenotype of our isolated cells and concluded that the loss of *Tnmd* causes reduction in their proliferative and migratory potential but an increase in apoptotic risk.

2.8 | Human umbilical vein endothelial cells migrate more toward $Tnmd^{-/-}$ OAF cells which exhibit elevation in p65 and MMPs expression levels

Following our observation of increased angiogenesis and macrophage infiltration in $Tnmd^{-/-}$ OAF, we investigated the human umbilical vein endothelial cells (HUVECs) migratory capacity toward WT or $Tnmd^{-/-}$ OAF cells by implementing transwell assays and found that loss of Tnmd in OAF supernatant promoted their migratory capacity compared to co-culture with WT OAF cells (Figure 6a–c). Immunofluorescence analysis revealed that the number of nuclei positive for p65, a key regulator of nuclear factor-kappa-B activation and function, was significantly increased in $Tnmd^{-/-}$ compared with WT OAF cells (Figure 6d,e), which was in parallel with elevated expression of MMP-3 and MMP-9 in $Tnmd^{-/-}$ OAF cells compared with WT OAF cells (Figure 6f–i). Thus, our results suggest that Tnmd-deficient OAF cells exhibit elevated p65, MMP-3, and MMP-9 expression and that the absence of secreted Tnmd by these cells significantly promotes HUVECs migration.

3 | DISCUSSION

Low back pain is an enormous medical and socioeconomic burden in modern society. Although there are many etiologies for the development of low back pain, a main component appears to be IVD degeneration, including neovascularization and inflammatory element

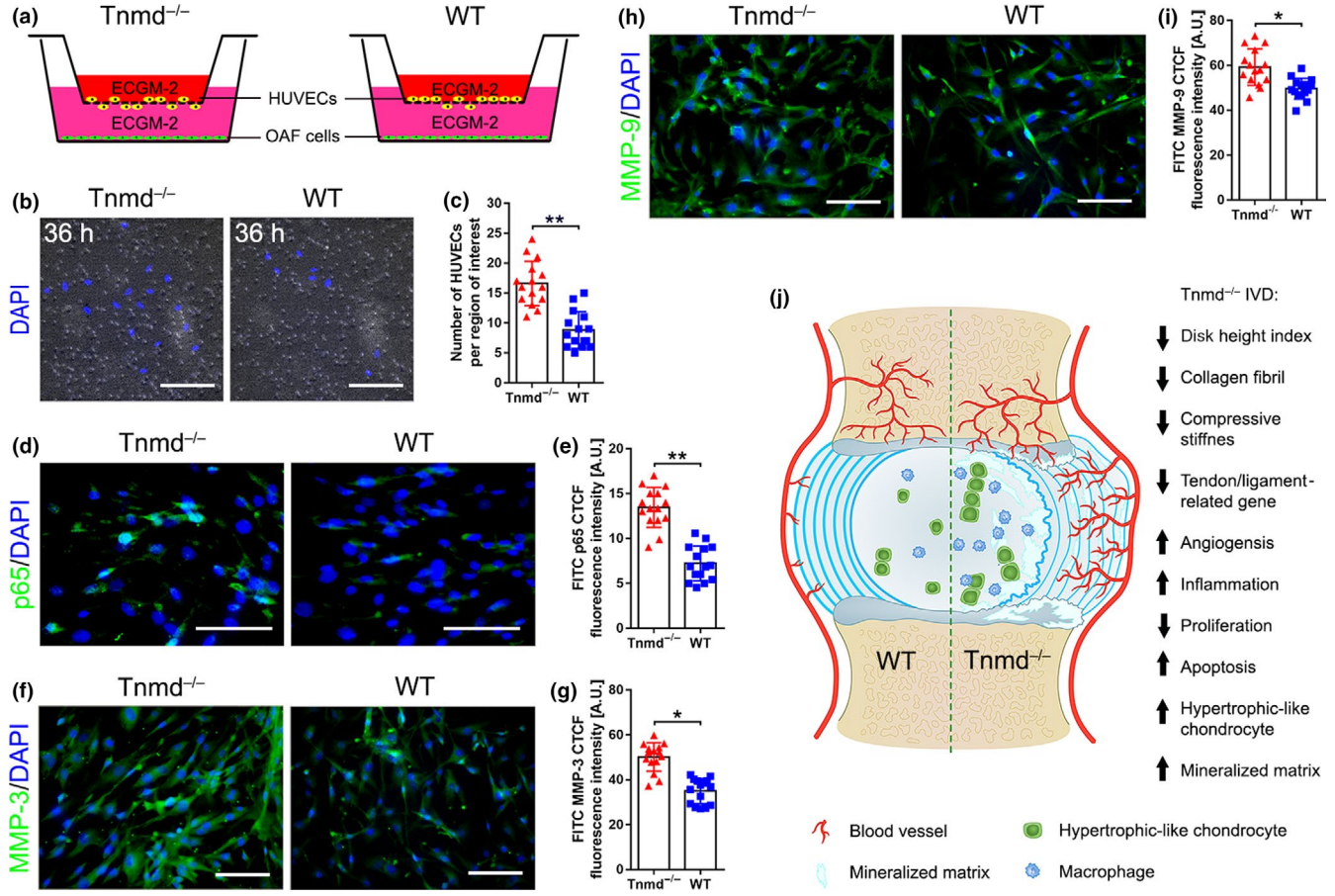

FIGURE 6 *Tnmd*$^{-/-}$ OAF cells promote HUVECs migration and have elevated p65 and MMPs expression. (a) Experimental design of HUVECs-OAF cells co-culture experiments. (b and c) Significantly increased migration of HUVECs toward *Tnmd*$^{-/-}$ OAF cells. Representative images of the bottom side of the transwell membrane taken after 36 hr of co-culturing (n = 3 independent experiments). (d–i) *Tnmd*$^{-/-}$ OAF cells exhibit upregulated protein expression of p65 (component NF-κB complex), MMP-3, and MMP-9 compared with WT cells (two-tailed nonparametric Mann–Whitney test; n = 3 independent experiments). (j) Cartoon highlighting the hallmarks of *Tnmd*$^{-/-}$ IVD phenotype. $^{*}p < .05$; $^{**}p < .01$. Scale bar: 100 μm. HUVEC, human umbilical vein endothelial cells; IVD, intervertebral disc; MMP, matrix metalloproteinases; NF-κB, nuclear factor-kappa-B; OAF, outer annulus fibrous; WT, wild-type

(Cornejo, Cho, Giannarelli, Iatridis, & Purmessur, 2015; Freemont et al., 1997; Kwon, Moon, Kwon, Park, & Kim, 2017; Risbud & Shapiro, 2014). In the present study, we demonstrate the important role of *Tnmd* in prevention of IVD degeneration by maintaining the avascular nature of the IVD (Figure 6j).

Based on our initial investigation at the protein level, we could show that Tnmd is strongly expressed in the ECM of the OAF, while Chm1 is predominantly found in the NP. We could detect to a lower extent a signal for Tnmd also in the NP; however, this should be taken with caution considering the highly conserved C-terminus between both proteins against which the primary antibody was raised. Moreover, we could show, similar to the Achilles tendon and CTC (Dex et al., 2016), that Tnmd processing in the IVD undergoes a proteolytic cleavage at its 16kDa C-terminal portion. Thus, we report for the first time the expression pattern of Tnmd protein in the ECM of the IVD, but also revealing that Tnmd is downregulated at 6 months of age.

Neovascularization allows the infiltration of macrophages into the IVD triggering inflammation (Fontana, See, & Pandit, 2015; Nakazawa et al., 2018; Walker & Anderson, 2004), which in turn can further amplify the vascularization (Cornejo, Cho, Giannarelli, Iatridis, & Purmessur, 2015; Lee et al., 2011), thereby triggering a self-perpetuating process. Here, we revealed that the absence of *Tnmd* activates angiogenesis and macrophage infiltration in the IVD in vivo, as well as HUVECs migration in an in vitro co-culture setting with OAF-derived cells. Furthermore, we also provide direct evidence that both *Tnmd* and *Chm1* act as anti-angiogenic cues in the IVD due to the observed severe IVD phenotype in the double mutant animals. We detected not only pronounced vascularization and infiltration of inflammatory cells into the matrix of the IVD but also unusual calcification. These data provide a new insight into the molecular mechanisms underlying the maintenance of IVD avascularity and implicate that disruption of its homeostasis leads to pathological status.

The ECM composition and organization are very important for IVD structure and function; hence, alterations in the ECM can also contribute to IVD degeneration (Cs-Szabo et al., 2002; Hoogendoorn et al., 2008; Liu et al., 2017; Zhang et al., 2013).

In general, IVD degeneration starts with proteoglycan breakdown leading to diminished water retention and disc dehydration. Our previous nanostructural and biomechanical analyses of the collagen matrix in Achilles tendons demonstrated that the absence of *Tnmd* causes thickening and stiffening of the collagen fibrils (Docheva et al., 2005). Therefore, we analyzed whether the lack of *Tnmd* affects the collagen fibrils of the AF. In contrast to our previous results, we found out that *Tnmd*$^{-/-}$ OAF contain collagen fibrils with smaller calibers and lower compressive stiffness, which cannot provide enough strength and proper load distribution over large parts of the OAF. According to these results and our previous finding that *Tnmd* is a mechanosensitive and mechanoregulated gene (Dex et al., 2017), we propose that the above-described phenotypic differences between tendon and IVD tissues are the consequence of the different biomechanical environments, namely IVDs are subjected mainly to compressive stress while tendons to tensile forces.

Altered OAF matrix can hinder the ability of the tissue to withstand mechanical load and in turn can increase the likelihood of tear formation (Gruber & Hanley, 1998; Guterl et al., 2013; Iatridis, Nicoll, Michalek, Walter, & Gupta, 2013; Roberts et al., 2008; Shukunami et al., 2018). Interestingly, the absence of *Tnmd* in tendon versus OAF tissues caused the opposite effect on the mRNA expression levels of several ECM genes such as *Col14a1*, *Col15a1*, and *Prg4*, as well as the transcription factors *Scx*, a direct transactivator of Tnmd (Shukunami et al., 2018), and *Mkx*, both known to regulate collagens. Furthermore, we detected elevated expression of MMP-3 and MMP-9 in *Tnmd*$^{-/-}$ OAF cells; thus, soluble matrix proteins can be extruded from the tissue by mechanical loading and enhance the degenerative process (Kamper et al., 2016). Notably, the glycosaminoglycan to hydroxyproline ratio within the NP of young adults is approximately 27:1, whereas the ratio within the hyaline cartilage of the same individuals is about 2:1 (Mwale et al., 2004). In our study, decreased Acan content in the *Tnmd*$^{-/-}$ NP, paralleled by increased Sox9, Runx2, and Col X levels, is indicative for a transition from a hydrated gel-like NP to a more hypertrophic chondrocyte-like matrix that is involved in IVD degeneration. Altogether, in such circumstances, sprouting of blood vessels in the abnormal OAF matrix and further toward the center of the IVD can facilitate ectopic ossification via intermediate hypertrophy state (Roberts et al., 2008).

Apoptosis is known to be a component of IVD degeneration (Gruber & Hanley, 1998). Previously, we have reported a reduced proliferative rate in *Tnmd*$^{-/-}$ tendon tissues and derived cells, as well as an increased number of p53-positive cells in *Tnmd*$^{-/-}$ Achilles tendons (Alberton et al., 2015; Docheva et al., 2005). Therefore, another important point that we examined was the effect of *Tnmd* on cell proliferation and apoptosis in the IVD. Interestingly and similar to tendon tissues, our in vivo and in vitro investigations convincingly prove that *Tnmd* is a positive regulator of cell proliferation and its loss accelerates apoptosis, which in turn leads to propagation of IVD aging and degenerative process. However, our study is impeded in providing an explanation of the exact molecular mode of action of *Tnmd*, due to lack of known binding partners. Therefore, further studies are promptly required to determine the signaling pathways in which *Tnmd* participates during IVD homeostasis.

Taken together, our findings provide new insights into the protective role of *Tnmd* in IVD degeneration. Understanding the precise *Tnmd*-dependent mechanisms can form the basis of developing new therapeutic strategies for prevention or treatment of IVD degeneration.

4 | EXPERIMENTAL PROCEDURES

4.1 | Animals

Tnmd$^{-/-}$, *Tnmd*$^{-/-}$*Chm1*$^{-/-}$, and their WT littermates mice were used in this study. The generation of the *Tnmd*$^{-/-}$, *Tnmd*$^{-/-}$*Chm1*$^{-/-}$ mice, and their primary phenotype tendon tissues and cells were described by Docheva and co-workers (Alberton et al., 2015; Dex et al., 2017; Docheva et al., 2005; Lin et al., 2017). All the mice were backcrossed to a C57BL/6J strain.

4.2 | Human samples

Samples comprising 5 IVDs (Table S1) were collected from 5 patients undergoing vertebral reconstruction (IVD tissues are removed and discarded) due to burst fractures or lumbar tumors in the Orthopaedic Center of People's Liberation Army, the Affiliated Southeast Hospital of Xiamen University. There were 3 males and 2 females (21–32 years of age). All patients received magnetic resonance imaging scans to confirm intact and healthy status of the IVDs. Samples were fixed immediately after removal in 4% paraformaldehyde (PFA; Merck) overnight at 4°C and then embedded in paraffin. From each patient, an informed consent was obtained. Sample collection and experimental methods were authorized by the Ethics Committee of the Xiamen University.

4.3 | Cell culture

Mouse OAF cells were isolated according to Nakamichi and colleagues (Nakamichi et al., 2016). Briefly, *Tnmd*$^{-/-}$ or WT mice were euthanized and lumbar discs (12-month-old, L1/2-5/6, 6 animals per group) were dissected under laminar flow. The discs were trimmed, and pieces of OAF tissues were obtained, then enzymatically treated overnight with 0.04% collagenase II (Worthington) in Dulbecco's modified Eagle's medium (DMEM)/Ham's F-12 (1:1) (Biochrom) supplemented with 10% fetal bovine serum (FBS) (Sigma-Aldrich) and 1% penicillin/streptomycin (PS) (Biochrom). Cell suspension was filtered through 70-µm nylon mesh (VWR International) and centrifuged at 500 g for 5 min. Isolated cells were grown in DMEM/Ham's F-12 (1:1) with 10% FBS, 1%

l-ascorbic-acid-2-phosphate (Sigma-Aldrich), 1% minimum essential medium (MEM)-amino acid (Biochrom), and 1% PS until day 5, at which point the medium was changed for the first time. Cells between passages 1–3 were used for experiments. HUVECs (Lonza) were cultured in the endothelial cell growth medium 2 (ECGM-2) (PromoCell). Cells in passages 7–8 were used for experiments. Both cell types were cultured at 37°C and 5% CO_2, kept up to 70% confluency and supplemented with fresh culture media every third day.

4.4 | Histology, immunohistology, and histomorphometry

Mouse spines were obtained after euthanasia (newborn, 15 days, 1 month, 12 months, and 18 months of age: n = 3 animals; 6 months of age: n = 5 animals). The samples were fixed in 4% PFA overnight at 4°C. Following fixation, specimens were decalcified in 10% ethylene diamine tetraacetic acid (EDTA)/phosphate-buffered saline (PBS) pH 8.0 (Sigma-Aldrich, Munich, Germany) for 14 days, and embedded into paraffin or cryo-media, and then the mouse and human samples were sectioned with 6 µm (paraffin) or 10 µm (cryo), and stained with H&E and safranin O using standard protocols. Quantification of histological score was based on a new scoring system specialized on histomorphology of mouse IVD (Tam et al., 2018). In brief, the scoring system included the following evaluation: NP structure (0 point, single-cell mass; 1 point, cell clusters <50%; 2 points, cell clusters >50%; 3 points, matrix-rich with little cells NP; 4 points, mineralized NP), NP clefts/fissures (0 point, none; +1 point, mild; +2 points, severe), AF/NP boundary (0 point, clear cut boundary; 1 point, round chondrocyte cells at the boundary; 2 points, loss of boundary), AF structure (0 point, concentric lamellar structure; 1 point, serpentine, widened or rounded AF lamellae; 2 points, reversal of lamellae; 3 points, undefinable lamellar structure or penetrating the NP; 4 points, mineralized or lost AF), and AF clefts/fissures (0 point, none; +1 point, mild; +2 points, severe). Quantification of disc height index was performed on H&E images (Masuda et al., 2005). In general, all histology, immunohistology, and histomorphometry experiments, unless specified otherwise in the text, were reproduced in 3 sections per sample with 5 or 3 samples per group for investigation.

For immunofluorescence staining, the sections were treated with 2 mg/ml hyaluronidase (Sigma-Aldrich) for 30 min at 37°C in order to increase antibody permeability. After washing and blocking with 2% bovine serum albumin/PBS (Sigma-Aldrich), primary antibodies against Acan (Abcam, 1:100, ab36861), CD31 (Abcam, 1:50, ab28364), Chm1 (Santa Cruz Biotechnology, 1:200, sc-33563), Col I (Abcam, 1:50, ab34710), Col X (Abcam, 1:50, ab58632), Fmod (Abcam, 1:200, ab81443), Fn (Abcam, 1:50, ab2413), F4/80 (Abcam, 1:100, ab100790), Lum (Abcam, 1:50, ab168348), MMP-3 (Novus Biologicals, 1:100, NB110-57221), MMP-9 (Millipore, 1:100, AB19016), Opn (Abcam, 1:200, ab8448), PCNA (Invitrogen, 1:100, 13-3900), p53 (Abcam, 1:100, ab61241), p65 (Abcam, 1:1000, ab16502), Runx2 (Abcam, 1:200, ab102711), Sox9 (Abcam, 1:400, ab3697), and Tnmd (Metabion, PAB 201603-00002, 1:100) were applied overnight at 4°C. Corresponding Alexa Fluor 488- or 546-labeled secondary antibodies (all from Life technology) were used for 1h at room temperature. Then, sections were shortly counter-stained with via 4′,6-diamidino-2-phenylindole (DAPI) (Life technology) and mounted with fluoroshield (Sigma-Aldrich). To analyze apoptotic cells numbers, TUNEL kit was applied following the manufacturer's instructions (Abcam, ab66110). Photomicrographs were taken on the Observer Z1 microscope equipped with the Axiocam MRm camera (Carl Zeiss). Quantitative histomorphometry was carried out via an automated quantitative image analysis according to algorithms from literature (Hsieh et al., 2016; Lin et al., 2017). In brief, using ImageJ (National Institutes of Health), the following algorithm was applied: (a) area of interest was manually designated using the "drawing/selection" tool; (b) "set measurements" for area, integrated density and mean gray value was selected from the analyze menu; and (c) lastly, the corrected total cryosections fluorescence (CTCF) representing the Acan, Col I, Col X, Fmod, Fn, Lum, MMP3, MMP-9, p65, and Tnmd expression were exported and calculated in Excel (Microsoft) as follows CTCF = media of integrated density − (media of area of selected area × mean fluorescence). To analyze Chm1-positive ratio of IVD, automatic color pixel quantification tool in the Adobe Photoshop CS5 software (Adobe System) was calculated in percentage to the image total pixel size. For IHC of the human IVDs, sections were deparaffinized in xylene, dehydrated in ethanol, and incubated with 0.3% hydrogen peroxide in absolute methanol for 30 min at room temperature to inhibit endogenous peroxidase. To enhance the immunoreactivity toward TNMD, the sections were treated with 0.05% citraconic anhydride (Sigma-Aldrich) in PBS for 30 min at 60°C. After washing with Tris-HCl buffer (50 mmol/L Tris-HCl, pH 7.6), the sections were incubated with primary antibody (Anti-TNMD antibody, Sigma-Aldrich, 1:100, HPA034961) at 4°C overnight, followed by corresponding biotinylated secondary antibody and horseradish peroxidase-labeled streptavidin. The colored reaction product was developed with 3,3′-diaminobenzidine tetrahydrochloride. Finally, the sections were counter-stained with hematoxylin. For quantification of the TNMD-positive area, image analysis of the OAF or NP areas stained in brown was carried out using ImageJ (TNMD-positive area/per area of interest [%]).

4.5 | IT-AFM

Indentation-type atomic force microscopy was performed on 14 µm-thick frozen tissue sections from 6-month-old *Tnmd*$^{-/-}$ and WT mice (3 animals per group; each animal represented by 3 tissue sections). Measurements were taken with NanoWizard AFM instrument (JPK Instruments) mounted on an inverted optical microscope (Axiovert 200, Zeiss) as described in detail previously (Dex et al., 2017; Gronau et al., 2017; Kamper et al., 2016). Briefly, 625 indentation curves per sample were recorded in 2 × 2 µm^2 area using pyramidal tips with nominal radius of 20 nm and silicon nitride cantilevers (MLCT microcantilever, Bruker). The spring constant of each cantilever was

determined prior to the experiment using the thermal noise method, and the sample stiffness was determined via a modified Hertz model using the JPK Data Processing software (V4.2.20, JPK Instruments), as described in detail previously (Gronau et al., 2017; Kamper et al., 2016). Based on these results, histograms were plotted and the two maxima were identified by fitting a linear combination of two Gaussian functions using OriginLab software (version 6). As previously reported, the lower stiffness peak attributes to the proteoglycan moiety, while the higher stiffness peak relates to collagen fibrils (Gronau et al., 2017; Kamper et al., 2016).

4.6 | Western blot analysis

Mouse IVDs from WT (1 and 6 months of age) and Tnmd$^{-/-}$ (6 months of age) animals were snap-frozen in liquid nitrogen. Using a mortar and pestle, the tissue was pulverized and resuspended in 8 M urea, 50 mM Tris-HCl (pH 8.0), 1 mM dithiothreitol, and 1 mM EDTA. Protein (22 μg) aliquots were loaded on a 12% SDS-polyacrylamide gel and transferred to Immobilon-p transfer membrane (Merck Millipore). The membrane was blocked for 90 min with 5% Milk/TBS-T buffer. Anti-Tnmd (1:500), anti-Chm1 (1:500), and anti-β-Actin (Abcam, 1:1,000, ab8227) antibodies were added. After overnight incubation with the primary antibodies at 4°C, membranes were washed and probed with corresponding horseradish peroxidase-conjugated goat anti-rabbit IgG (Thermo Fischer Scientific). Protein bands were visualized using SuperSignal West Dura Extended Duration Substrate (Thermo Fischer Scientific) and film paper. Western blot was independently reproduced with two separate preparation of IVDs from 1- and 6-month-old *Tnmd*$^{-/-}$ and WT animals.

4.7 | Semiquantitative and qRT–PCR

Total RNAs from OAF tissues (n = 3 animals) and OAF cells were isolated with Qiagen RNeasy Mini kit (Qiagen) and used for standard semiquantitative and qRT–PCR. For cDNA synthesis, 1 μg total RNA and AMV First-Strand cDNA Synthesis Kit (Invitrogen) were implemented. Semiquantitative PCR was performed with Taq DNA Polymerase (Invitrogen) in MGResearch instrument (BioRad, Munich, Germany). Primer sequences and PCR conditions were as follows: *Tnmd* forward 5′gaaaccatggcaaagaatcctccagag3′, reverse 5′ttagactctcccaagcatgcgggc3′; *Chm1* forward 5′atggtagggcctgaggacgttg3′, reverse 5′gctgcatggcatgacgactctg3′; *Gapdh* forward 5′gagaggccctatcccaactc3′, reverse 5′gtgggtgcagcgaactttat3′; PCR was performed with incubation at 94°C for 5 min followed by 30 cycles of a three-step temperature program of 1 min at 94°C, 20 s at 57°C, and 30 s at 72°C. The PCR reaction was terminated after a 7 min extension at 70°C. The band intensity of the amplified products in the gel was visualized, photographed, and analyzed using a gel imager (Vilber Lourmat). The relative gene expression was quantified by densitometry and normalized to the amount of *Gapdh* with ImageJ and presented as fold change to WT. Quantitative PCR of tendon-associated genes was performed using RealTime Ready Custom Panel 96 – 32+ plates (https://configurator.realtimeready.roche.com) according to the manufacturer's instructions (Roche Applied Science). Briefly, PCR reactions were pipetted on ice and each well contained 10 μl LightCycler 480 probes master mix, 0.2 μl cDNA (diluted 1:5) and 9.8 μl PCR grade water. Plates were subsequently sealed and centrifuged down for 15 s. at 2,100 rpm. The relative gene expression was calculated as a ratio to *Gapdh*. All PCR results have been reproduced in three independent experiments.

4.8 | Migration analysis

Migration analysis was performed similarly to our previous study (Popov, Kohler, & Docheva, 2016). For random migration, 1.5 × 10^3 cells/cm^2 of *Tnmd*$^{-/-}$ and WT OAF cells were seeded on Col I-coated (20 μg/Ml; Millipore) 6-well plates and incubated for 2 hr prior imaging. Time lapse was performed with 4 frames per 20 min for 24 hr. The image data were extracted with AxioVisionLE software (Carl Zeiss), and individual cell tracks were analyzed with ImageJ. Random migration was expressed by calculation of the forward migration index (FMI; the ratio of the vector length to the migratory starting point), velocity, and accumulated (cumulative track length) and Euclidian (the ordinary straight-line length between two points) distances. Results of random OAF cells migration measurements consist of 3 independent time-lapse movies of two *Tnmd*$^{-/-}$ and WT OAF cells donors as a total number of 20–25 OAF cells per genotype were tracked.

4.9 | CyQUANT assays

A total of 1.5 × 10^3 cells (passage 1) per well were plated in 6-well plates, and CyQUANT assay detection was performed according to the manufacturer's instructions (Invitrogen) after 0, 3, 5, and 7 days cell culture. CyQUANT assay was repeated independently in 3 experiments per time point.

4.10 | HUVECs-OAF cells co-culture

Co-cultures were performed using Boyden chambers with membrane containing 8.0 μm pores inserted in 24-well plates (Becton Dickinson Labware) as described previously (Kimura et al., 2008). In brief, *Tnmd*$^{-/-}$ or WT OAF cells (1 × 10^4 cells per well) were seeded on the bottom of the wells and cultured in DMEM/Ham's F-12 (1:1) with 10% FBS, 1% l-ascorbic-acid-2-phosphate, 1% MEM-amino acid, and 1% PS for 24 hr, and then, the medium was replaced with ECGM-2. Before seeding HUVECs into the upper chamber, the membrane was coated with Col I (10 μg/Ml; Millipore), kept in a humidified incubator overnight, and filled with ECGM-2 an hour before introducing the 5 × 10^3 HUVECs per well. After 36 hr co-culturing, HUVECs that have migrated through the pores and adhered to the lower side

of the membrane were fixed with 4% PFA and stained with DAPI. The cell nuclei were counted using the Observer Z1 microscope equipped with the Axiocam MRm camera. *Tnmd*$^{-/-}$ or WT OAF cells in the lower chamber were analyzed for p65, MMP-3, and MMP-9 by immunofluorescence staining. The interactions of the co-cultures assays were repeated independently in 3 experiments. All cell nuclei (DAPI) in 3 images per well from 5 wells per plate were counted.

4.11 | Statistical analysis

In this study, each animal was represented with 3 different tissue sections with comparable planes between genotypes. The results were averaged per animal were presented as mean ± *SD* between the 3–5 animals per group. Exact animal number and experimental reproducibility is given for each result in the figure legends. Statistical differences between two groups were determined using two-tailed unpaired Student's *t* test, or two-tailed nonparametric Mann–Whitney test. In multiple comparisons, one-way ANOVA was followed by Bonferroni post hoc correction. Differences were considered statistically significant at the values of $^{*}p < .05$, $^{**}p < .01$, and $^{***}p < .001$.

ACKNOWLEDGMENTS

D.D. acknowledges the German Research Foundation (Grant Nr. DO1414/3-1), the EU Twinning Grant Achilles (H2020-WIDESPREAD-05-2017-Twinning Grant Nr. 810850) and the National Institutes of Health (Grant Nr. GM089820). D.L. acknowledges the National Natural Science Foundation of China (Grant Nr. 81600696). We are thankful to Dr. C.F. Hsieh, MSc. S. Dex and P. Li for experimental help, Dr. D. Luo for his guidance with statistical analyses, and Dr. Girish Pattappa for English proof-reading.

CONFLICT OF INTEREST

The authors declare no conflict of interest.

AUTHOR CONTRIBUTIONS

D.L. designed, performed, and analyzed experiments and wrote the manuscript; P.A. performed co-culture experiments; C.P. and H.C-S. carried out AFM analyses; M.D.C. performed Western blotting and RT–PCR; J.D., A.A., C.S. and J.C.I. approved manuscript; D.D. conceived the study, designed, and analyzed experiments and wrote the manuscript.

ETHICS APPROVAL

Mouse husbandry, handling, and euthanasia were strictly carried out according to the guidelines of the Bavarian authorities. Animals were euthanized with CO_2 and dissected for collection of whole spine and tail tendon tissues. Human sample collection and experimental methods were authorized by the Ethics Committee of the Xiamen University.

ORCID

Denitsa Docheva https://orcid.org/0000-0002-7588-1290

REFERENCES

Alberton, P., Dex, S., Popov, C., Shukunami, C., Schieker, M., & Docheva, D. (2015). Loss of tenomodulin results in reduced self-renewal and augmented senescence of tendon stem/progenitor cells. *Stem Cells and Development*, *24*(5), 597–609. https://doi.org/10.1089/scd.2014.0314

Annunen, S., Paassilta, P., Lohiniva, J., Perälä, M., Pihlajamaa, T., Karppinen, J., … Ala-Kokko, L. (1999). An allele of COL9A2 associated with intervertebral disc disease. *Science*, *285*(5426), 409–412. https://doi.org/10.1126/science.285.5426.409

Attia, M., Santerre, J. P., & Kandel, R. A. (2011). The response of annulus fibrosus cell to fibronectin-coated nanofibrous polyurethane-anionic dihydroxyoligomer scaffolds. *Biomaterials*, *32*(2), 450–460. https://doi.org/10.1016/j.biomaterials.2010.09.010

Bedore, J., Sha, W., McCann, M. R., Liu, S., Leask, A., & Séguin, C. A. (2013). Impaired intervertebral disc development and premature disc degeneration in mice with notochord-specific deletion of CCN2. *Arthritis & Rheumatology*, *65*(10), 2634–2644. https://doi.org/10.1002/art.38075

Brandau, O., Meindl, A., Fässler, R., & Aszódi, A. (2001). A novel gene, tendin, is strongly expressed in tendons and ligaments and shows high homology with chondromodulin-I. *Developmental Dynamics*, *221*(1), 72–80. https://doi.org/10.1002/dvdy.1126

Cornejo, M. C., Cho, S. K., Giannarelli, C., Iatridis, J. C., & Purmessur, D. (2015). Soluble factors from the notochordal-rich intervertebral disc inhibit endothelial cell invasion and vessel formation in the presence and absence of pro-inflammatory cytokines. *Osteoarthritis and Cartilage*, *23*(3), 487–496. https://doi.org/10.1016/j.joca.2014.12.010

Cs-Szabo, G., Ragasa-San Juan, D., Turumella, V., Masuda, K., Thonar, E. J., & An, H. S. (2002). Changes in mRNA and protein levels of proteoglycans of the anulus fibrosus and nucleus pulposus during intervertebral disc degeneration. *Spine*, *27*(20), 2212–2219. https://doi.org/10.1097/00007632-200210150-00006

de Vries, S. A. H., van Doeselaar, M., Meij, B. P., Tryfonidou, M. A., & Ito, K. (2018). Notochordal cell matrix: An inhibitor of neurite and blood vessel growth? *Journal of Orthopaedic Research*, *36*(12), 3188–3195. https://doi.org/10.1002/jor.24114

Dex, S., Alberton, P., Willkomm, L., Söllradl, T., Bago, S., Milz, S., … Docheva, D. (2017). Tenomodulin is required for tendon endurance running and collagen I fibril adaptation to mechanical load. *EBioMedicine*, *20*, 240–254. https://doi.org/10.1016/j.ebiom.2017.05.003

Dex, S., Lin, D., Shukunami, C., & Docheva, D. (2016). Tenogenic modulating insider factor: Systematic assessment on the functions of tenomodulin gene. *Gene*, *587*(1), 1–17. https://doi.org/10.1016/j.gene.2016.04.051

Docheva, D., Hunziker, E. B., Fässler, R., & Brandau, O. (2005). Tenomodulin is necessary for tenocyte proliferation and tendon maturation. *Molecular and Cellular Biology*, *25*(2), 699–705. https://doi.org/10.1128/MCB.25.2.699-705.2005

Feng, C., Liu, H., Yang, M., Zhang, Y., Huang, B., & Zhou, Y. (2016). Disc cell senescence in intervertebral disc degeneration: Causes and molecular pathways. *Cell Cycle*, *15*(13), 1674–1684. https://doi.org/10.1080/15384101.2016.1152433

Feng, H., Danfelter, M., Strömqvist, B., & Heinegård, D. (2006). Extracellular matrix in disc degeneration. *The Journal of Bone and Joint Surgery-American*, *88*(Suppl 2), 25–29. https://doi.org/10.2106/JBJS.E.01341

Fontana, G., See, E., & Pandit, A. (2015). Current trends in biologics delivery to restore intervertebral disc anabolism. *Advanced Drug Delivery Reviews*, *84*, 146–158. https://doi.org/10.1016/j.addr.2014.08.008

Freemont, A. J., Peacock, T. E., Goupille, P., Hoyland, J. A., O'Brien, J., & Jayson, M. I. (1997). Nerve ingrowth into diseased intervertebral disc in chronic back pain. *The Lancet*, *350*(9072), 178–181. https://doi.org/10.1016/S0140-6736(97)02135-1

Gronau, T., Krüger, K., Prein, C., Aszodi, A., Gronau, I., Iozzo, R. V., … Dreier, R. (2017). Forced exercise-induced osteoarthritis is attenuated in mice lacking the small leucine-rich proteoglycan decorin. *Annals of the Rheumatic Diseases*, *76*(2), 442–449. https://doi.org/10.1136/annrheumdis-2016-209319

Gruber, H. E., & Hanley, E. N. Jr. (1998). Analysis of aging and degeneration of the human intervertebral disc. *Spine*, *23*(7), 751–757. https://doi.org/10.1097/00007632-199804010-00001

Guterl, C. C., See, E. Y., Blanquer, S., Pandit, A., Ferguson, S. J., Benneker, L. M., … Grad, S. (2013). Challenges and strategies in the repair of ruptured annulus fibrosus. *European Cells and Materials*, *25*, 1–21. https://doi.org/10.22203/eCM.v025a01

Hiraki, Y., Inoue, H., Iyama, K.-I., Kamizono, A., Ochiai, M., Shukunami, C., … Kondo, J. (1997). Identification of chondromodulin I as a novel endothelial cell growth inhibitor. Purification and its localization in the avascular zone of epiphyseal cartilage. *Journal of Biological Chemistry*, *272*(51), 32419–32426. https://doi.org/10.1074/jbc.272.51.32419

Hoogendoorn, R., Doulabi, B. Z., Huang, C. L., Wuisman, P. I., Bank, R. A., & Helder, M. N. (2008). Molecular changes in the degenerated goat intervertebral disc. *Spine*, *33*(16), 1714–1721. https://doi.org/10.1097/BRS.0b013e31817d2468

Hristova, G. I., Jarzem, P., Ouellet, J. A., Roughley, P. J., Epure, L. M., Antoniou, J., & Mwale, F. (2011). Calcification in human intervertebral disc degeneration and scoliosis. *Journal of Orthopaedic Research*, *29*(12), 1888–1895. https://doi.org/10.1002/jor.21456

Hsieh, C.-F., Alberton, P., Loffredo-Verde, E., Volkmer, E., Pietschmann, M., Müller, P. E., … Docheva, D. (2016). Periodontal ligament cells as alternative source for cell-based therapy of tendon injuries: In vivo study of full-size Achilles tendon defect in a rat model. *European Cells and Materials*, *32*, 228–240. https://doi.org/10.22203/eCM.v032a15

Huang, Y. C., Urban, J. P., & Luk, K. D. (2014). Intervertebral disc regeneration: Do nutrients lead the way? *Nature Reviews Rheumatology*, *10*(9), 561–566. https://doi.org/10.1038/nrrheum.2014.91

Iatridis, J. C., Nicoll, S. B., Michalek, A. J., Walter, B. A., & Gupta, M. S. (2013). Role of biomechanics in intervertebral disc degeneration and regenerative therapies: What needs repairing in the disc and what are promising biomaterials for its repair? *The Spine Journal*, *13*(3), 243–262. https://doi.org/10.1016/j.spinee.2012.12.002

Illien-Jünger, S., Torre, O. M., Kindschuh, W. F., Chen, X., Laudier, D. M., & Iatridis, J. C. (2016). AGEs induce ectopic endochondral ossification in intervertebral discs. *European Cells and Materials*, *32*, 257–270. https://doi.org/10.22203/eCM.v032a17

Ito, Y., Toriuchi, N., Yoshitaka, T., Ueno-Kudoh, H., Sato, T., Yokoyama, S., … Asahara, H. (2010). The Mohawk homeobox gene is a critical regulator of tendon differentiation. *Proceedings of the National Academy of Sciences*, *107*, 10538–10542. https://doi.org/10.1073/pnas.1000525107

Kamper, M., Hamann, N., Prein, C., Clausen-Schaumann, H., Farkas, Z., Aszodi, A., … Zaucke, F. (2016). Early changes in morphology, bone mineral density and matrix composition of vertebrae lead to disc degeneration in aged collagen IX -/- mice. *Matrix Biology*, *49*, 132–143. https://doi.org/10.1016/j.matbio.2015.09.005

Kimura, N., Shukunami, C., Hakuno, D., Yoshioka, M., Miura, S., Docheva, D., … Fukuda, K. (2008). Local tenomodulin absence, angiogenesis, and matrix metalloproteinase activation are associated with the rupture of the chordae tendineae cordis. *Circulation*, *118*(17), 1737–1747. https://doi.org/10.1161/CIRCULATIONAHA.108.780031

Kwon, W. K., Moon, H. J., Kwon, T. H., Park, Y. K., & Kim, J. H. (2017). The role of hypoxia in angiogenesis and extracellular matrix regulation of intervertebral disc cells during inflammatory reactions. *Neurosurgery*, *81*(5), 867–875. https://doi.org/10.1093/neuros/nyx149

Lee, J. M., Song, J. Y., Baek, M. J., Jung, H.-Y., Kang, H., Han, I. B., … Shin, D. E. (2011). Interleukin-1β induces angiogenesis and innervation in human intervertebral disc degeneration. *Journal of Orthopaedic Research*, *29*(2), 265–269. https://doi.org/10.1002/jor.21210

Leung, V. Y., Tam, V., Chan, D., Chan, B. P., & Cheung, K. M. (2011). Tissue engineering for intervertebral disk degeneration. *Orthopedic Clinics of North America*, *42*(4), 575–583. https://doi.org/10.1016/j.ocl.2011.07.003

Lin, D., Alberton, P., Caceres, M. D., Volkmer, E., Schieker, M., & Docheva, D. (2017). Tenomodulin is essential for prevention of adipocyte accumulation and fibrovascular scar formation during early tendon healing. *Cell Death and Disease*, *8*(10), e3116. https://doi.org/10.1038/cddis.2017.510

Liu, W., Liu, D., Zheng, J., Shi, P., Chou, P.-H., Oh, C., … Chee, A. (2017). Annulus fibrosus cells express and utilize C-C chemokine receptor 5 (CCR5) for migration. *The Spine Journal*, *17*(5), 720–726. https://doi.org/10.1016/j.spinee.2017.01.010

Masuda, K., Aota, Y., Muehleman, C., Imai, Y., Okuma, M., Thonar, E. J., An, H. S. (2005). A novel rabbit model of mild, reproducible disc degeneration by an anulus needle puncture: correlation between the degree of disc injury and radiological and histological appearances of disc degeneration. *Spine*, *30*(1), 5–14. https://doi.org/10.1097/01.brs.0000148152.04401.20

McCann, M. R., & Séguin, C. A. (2016). Notochord cells in intervertebral disc development and degeneration. *Journal of Developmental Biology*, *4*(1), 1–18. https://doi.org/10.3390/jdb4010003

Minogue, B. M., Richardson, S. M., Zeef, L. A., Freemont, A. J., & Hoyland, J. A. (2010). Transcriptional profiling of bovine intervertebral disc cells: Implications for identification of normal and degenerate human intervertebral disc cell phenotypes. *Arthritis Research & Therapy*, *12*(1), R22. https://doi.org/10.1186/ar2929

Mwale, F., Roughley, P., & Antoniou, J. (2004). Distinction between the extracellular matrix of the nucleus pulposus and hyaline cartilage: A requisite for tissue engineering of intervertebral disc. *European Cells and Materials*, *8*, 58–63. https://doi.org/10.22203/eCM.v008a06

Nakamichi, R., Ito, Y., Inui, M., Onizuka, N., Kayama, T., Kataoka, K., … Asahara, H. (2016). Mohawk promotes the maintenance and regeneration of the outer annulus fibrosus of intervertebral discs. *Nature Communications*, *7*, 12503. https://doi.org/10.1038/ncomms12503

Nakazawa, K. R., Walter, B. A., Laudier, D. M., Krishnamoorthy, D., Mosley, G. E., Spiller, K. L., & Iatridis, J. C. (2018). Accumulation and localization of macrophage phenotypes with human intervertebral disc degeneration. *The Spine Journal*, *18*(2), 343–356. https://doi.org/10.1016/j.spinee.2017.09.018

Nguyen, C., Poiraudeau, S., & Rannou, F. (2015). From Modic 1 vertebral-endplate subchondral bone signal changes detected by MRI to the concept of 'active discopathy'. *Annals of the Rheumatic Diseases*, *74*(8), 1488–1494. https://doi.org/10.1136/annrheumdis-2015-207317

Oshima, Y., Sato, K., Tashiro, F., Miyazaki, J., Nishida, K., Hiraki, Y., … Shukunami, C. (2004). Anti-angiogenic action of the C-terminal domain of tenomodulin that shares homology with chondromodulin-I. *Journal of Cell Science*, *117*(Pt 13), 2731–2744. https://doi.org/10.1242/jcs.01112

Phillips, K. L., Jordan-Mahy, N., Nicklin, M. J., & Le Maitre, C. L. (2013). Interleukin-1 receptor antagonist deficient mice provide insights into pathogenesis of human intervertebral disc degeneration. *Annals of the Rheumatic Diseases*, *72*(11), 1860–1867. https://doi.org/10.1136/annrheumdis-2012-202266

Popov, C., Kohler, J., & Docheva, D. (2016). Activation of EphA4 and EphB2 reverse signaling restores the age-associated reduction of self-renewal, migration, and actin turnover in human tendon stem/progenitor cells. *Frontiers in Aging Neuroscience*, *7*, 246. https://doi.org/10.3389/fnagi.2015.00246

Purmessur, D., Freemont, A. J., & Hoyland, J. A. (2008). Expression and regulation of neurotrophins in the nondegenerate and degenerate

human intervertebral disc. *Arthritis Research & Therapy*, *10*(4), R99. https://doi.org/10.1186/ar2487

Pye, S. R., Reid, D. M., Adams, J. E., Silman, A. J., & O'Neill, T. W. (2007). Influence of weight, body mass index and lifestyle factors on radiographic features of lumbar disc degeneration. *Annals of the Rheumatic Diseases*, *66*(3), 426–427. https://doi.org/10.1136/ard.2006.057166

Risbud, M. V., & Shapiro, I. M. (2014). Role of cytokines in intervertebral disc degeneration: Pain and disc content. *Nature Reviews Rheumatology*, *10*(1), 44–56. https://doi.org/10.1038/nrrheum.2013.160

Roberts, S., Evans, H., Trivedi, J., & Menage, J. (2008). Histology and pathology of the human intervertebral disc. *The Journal of Bone and Joint Surgery-American*, *88*(Suppl 2), 10–14. https://doi.org/10.2106/JBJS.F.00019

Shukunami, C., Oshima, Y., & Hiraki, Y. (2001). Molecular cloning of tenomodulin, a novel chondromodulin-I related gene. *Biochemical and Biophysical Research Communications*, *280*(5), 1323–1327. https://doi.org/10.1006/bbrc.2001.4271

Shukunami, C., Takimoto, A., Nishizaki, Y., Yoshimoto, Y., Tanaka, S., Miura, S., … Hiraki, Y. (2018). Scleraxis is a transcriptional activator that regulates the expression of tenomodulin, a marker of mature tenocytes and ligamentocytes. *Scientific Reports*, *8*(1), 3155. https://doi.org/10.1038/s41598-018-21194-3

Smits, P., & Lefebvre, V. (2003). Sox5 and Sox6 are required for notochord extracellular matrix sheath formation, notochord cell survival and development of the nucleus pulposus of intervertebral discs. *Development*, *130*(6), 1135–1148. https://doi.org/10.1242/dev.00331

Song, Y.-Q., Karasugi, T., Cheung, K. M. C., Chiba, K., Ho, D. W. H., Miyake, A., … Chan, D. (2013). Lumbar disc degeneration is linked to a carbohydrate sulfotransferase 3 variant. *Journal of Clinical Investigation*, *123*(11), 4909–4917. https://doi.org/10.1172/JCI69277

Stokes, I. A., & Iatridis, J. C. (2004). Mechanical conditions that accelerate intervertebral disc degeneration: overload versus immobilization. *Spine*, *29*(23), 2724–2732. https://doi.org/10.1097/01.brs.0000146049.52152.da

Sztrolovics, R., Alini, M., Mort, J. S., & Roughley, P. J. (1999). Age-related changes in fibromodulin and lumican in human intervertebral discs. *Spine*, *24*(17), 1765–1771. https://doi.org/10.1097/00007632-199909010-00003

Takao, T., Iwaki, T., Kondo, J., & Hiraki, Y. (2000). Immunohistochemistry of chondromodulin-I in the human intervertebral discs with special reference to the degenerative changes. *The Histochemical Journal*, *32*(9), 545–550. https://doi.org/10.1023/A:1004150211097

Takimoto, A., Oro, M., Hiraki, Y., & Shukunami, C. (2012). Direct conversion of tenocytes into chondrocytes by Sox9. *Experimental Cell Research*, *318*(13), 1492–1507. https://doi.org/10.1016/j.yexcr.2012.04.002

Tam, V., Chan, W. C. W., Leung, V. Y. L., Cheah, K. S. E., Cheung, K. M. C., Sakai, D., … Chan, D. (2018). Histological and reference system for the analysis of mouse intervertebral disc. *Journal of Orthopaedic Research*, *36*(1), 233–243. https://doi.org/10.1002/jor.23637

van der Kraan, P. M., & van den Berg, W. B. (2012). Chondrocyte hypertrophy and osteoarthritis: Role in initiation and progression of cartilage degeneration? *Osteoarthritis and Cartilage*, *20*(3), 223–232. https://doi.org/10.1016/j.joca.2011.12.003

Walker, M. H., & Anderson, D. G. (2004). Molecular basis of intervertebral disc degeneration. *The Spine Journal*, *4*(6 Suppl), 158S–166S. https://doi.org/10.1016/j.spinee.2004.07.010

Williams, F. M. K., Bansal, A. T., van Meurs, J. B., Bell, J. T., Meulenbelt, I., Suri, P., … Spector, T. D. (2013). Novel genetic variants associated with lumbar disc degeneration in northern Europeans: A meta-analysis of 4600 subjects. *Annals of the Rheumatic Diseases*, *72*(7), 1141–1148. https://doi.org/10.1136/annrheumdis-2012-201551

Williams, F. M., Popham, M., Sambrook, P. N., Jones, A. F., Spector, T. D., & MacGregor, A. J. (2011). Progression of lumbar disc degeneration over a decade: A heritability study. *Annals of the Rheumatic Diseases*, *70*(7), 1203–1207. https://doi.org/10.1136/ard.2010.146001

Yoshimoto, Y., Takimoto, A., Watanabe, H., Hiraki, Y., Kondoh, G., & Shukunami, C. (2017). Scleraxis is required for maturation of tissue domains for proper integration of the musculoskeletal system. *Scientific Reports*, *7*, 45010. https://doi.org/10.1038/srep45010

Yoshioka, M., Yuasa, S., Matsumura, K., Kimura, K., Shiomi, T., Kimura, N., … Fukuda, K. (2006). Chondromodulin-I maintains cardiac valvular function by preventing angiogenesis. *Nature Medicine*, *12*(10), 1151–1159. https://doi.org/10.1038/nm1476

Zhang, D., Jin, L., Reames, D. L., Shen, F. H., Shimer, A. L., & Li, X. (2013). Intervertebral disc degeneration and ectopic bone formation in apolipoprotein E knockout mice. *Journal of Orthopaedic Research*, *31*(2), 210–217. https://doi.org/10.1002/jor.22216

SUPPORTING INFORMATION

Additional supporting information may be found online in the Supporting Information section.

How to cite this article: Lin D, Alberton P, Delgado Caceres M, et al. Loss of tenomodulin expression is a risk factor for age-related intervertebral disc degeneration. *Aging Cell*. 2020;19:e13091. https://doi.org/10.1111/acel.13091

6. References

Abraham AC, Shah SA, Golman M, *et al*. (2019) Targeting the NF-κB signaling pathway in chronic tendon disease. *Sci Transl Med* 11(481).

Ackerman JE, Nichols AE, Studentsova V, Best KT, Knapp E, Loiselle AE (2019) Cell non-autonomous functions of S100a4 drive fibrotic tendon healing. *Elife* 8. pii: e45342.

Alberton P, Dex S, Popov C, Shukunami C, Schieker M, Docheva D (2015) Loss of tenomodulin results in reduced self-renewal and augmented senescence of tendon stem/progenitor cells. *Stem Cells Dev* 24:597-609.

Andarawis-Puri N, Flatow EL, Soslowsky LJ (2015) Tendon basic science: Development, repair, regeneration, and healing. *J Orthop Res* 33:780-784.

Bi Y, Ehirchiou D, Kilts TM, *et al.* (2007) Identification of tendon stem/progenitor cells and the role of the extracellular matrix in their niche. *Nat Med* 13:1219-1227.

Brandau O, Meindl A, Fässler R, Aszódi A (2001) A novel gene, tendin, is strongly expressed in tendons and ligaments and shows high homology with chondromodulin-I. *Dev Dyn* 221:72-80.

Brent AE, Braun T, Tabin CJ (2005) Genetic analysis of interactions between the somitic muscle, cartilage and tendon cell lineages during mouse development. *Development* 132:515-528.

Chazaud B (2014) Macrophages: supportive cells for tissue repair and regeneration. *Immunobiology* 219:172-178.

Che H, Li J, Li Y, *et al*. (2020) p16 deficiency attenuates intervertebral disc degeneration by adjusting oxidative stress and nucleus pulposus cell cycle. *Elife* 9. pii: e52570.

Chhabra A, Tsou D, Clark RT, Gaschen V, Hunziker EB, Mikic B (2003) GDF-5 deficiency in mice delays Achilles tendon healing. *J Orthop Res* 21:826-835.

Chong AK, Ang AD, Goh JC, Hui JH, Lim AY, Lee EH, Lim BH (2007) Bone marrow-derived mesenchymal stem cells influence early tendon-healing in a rabbit Achilles tendon model. *J Bone Joint Surg Am* 89:74-81.

Clarke AW, Alyas F, Morris T, Robertson CJ, Bell J, Connell DA (2011) Skin-derived tenocyte-like cells for the treatment of patellar tendinopathy. *Am J Sports Med* 39:614-623.

Delgado Caceres M, Pfeifer CG, Docheva D (2018) Understanding tendons: lessons from transgenic mouse models. *Stem Cells Dev* 27:1161-1174.

Deng D, Wang W, Wang B, Zhang P, Zhou G, Zhang WJ, Cao Y, Liu W (2014) Repair of Achilles tendon defect with autologous ASCs engineered tendon in a rabbit model. *Biomaterials* 35:8801-8809.

Dex S, Alberton P, Willkomm L, *et al.* (2017) Tenomodulin is required for tendon endurance running and collagen I fibril adaptation to mechanical load. *EBioMedicine* 20:240-254.

Dex S, Lin D, Shukunami C, Docheva D (2016) Tenogenic modulating insider factor: Systematic assessment on the functions of tenomodulin gene. *Gene* 587:1-17.

Disser NP, Sugg KB, Talarek JR, Sarver DC, Rourke BJ, Mendias CL (2019) Insulin-like growth factor1 signaling in tenocytes is required for adult tendon growth. *FASEB J* 33:12680-12695.

Docheva D, Hunziker EB, Fässler R, Brandau O (2005) Tenomodulin is necessary for tenocyte proliferation and tendon maturation. *Mol Cell Biol* 25:699-705.

Docheva D, Müller SA, Majewski M, Evans CH (2015) Biologics for tendon repair. *Adv Drug Deliv Rev* 84:222-239.

Dyment NA, Hagiwara Y, Matthews BG, Li Y, Kalajzic I, Rowe DW (2014) Lineage tracing of resident tendon progenitor cells during growth and natural healing. *PLoS One* 9: e96113.

Evrova O, Buschmann J (2017) In vitro and in vivo effects of PDGF-BB delivery strategies on tendon healing: a review.

Eur Cell Mater 34:15-39.

Fontana G, See E, Pandit A (2015) Current trends in biologics delivery to restore intervertebral disc anabolism. *Adv Drug Deliv Rev* 84:146-158.

Freemont AJ, Peacock TE, Goupille P, Hoyland JA, O'Brien J, Jayson MI (1997) Nerve ingrowth into diseased intervertebral disc in chronic back pain. *Lancet* 350:178-181.

Gaspar D, Spanoudes K, Holladay C, Pandit A, Zeugolis D (2015) Progress in cell-based therapies for tendon repair. *Adv Drug Deliv Rev* 84:240-256.

Glenn NO, Henry CA (2019) How muscle contraction strengthens tendons. *Elife* 8. pii: e44149.

González-Muniesa P, Marrades MP, Martínez JA, Moreno-Aliaga MJ (2013) Differential proinflammatory and oxidative stress response and vulnerability to metabolic syndrome in habitual high-fat young male consumers putatively predisposed by their genetic background. *Int J Mol Sci* 14:17238-17255.

Gorth DJ, Ottone OK, Shapiro IM, Risbud MV (2019) Differential effect of long-term systemic exposure of TNFα on health of the annulus fibrosus and nucleus pulposus of the intervertebral disc. *J Bone Miner Res*. doi: 10.1002/jbmr.3931.

Gorth DJ, Shapiro IM, Risbud MV (2019) A new understanding of the role of IL-1 in age-related intervertebral disc degeneration in a murine model. *J Bone Miner Res* 34:1531-1542.

Grinstein M, Dingwall HL, O'Connor LD, Zou K, Capellini TD, Galloway JL (2019) A distinct transition from cell growth to physiological homeostasis in the tendon. *Elife* 8. pii: e48689.

Guerquin MJ, Charvet B, Nourissat G, *et al*. (2013) Transcription factor EGR1 directs tendon differentiation and promotes tendon repair. *J Clin Invest* 123:3564-3576.

Harvey T, Flamenco S, Fan CM (2019) A Tppp3+Pdgfra+ tendon stem cell population contributes to regeneration and reveals a shared role for PDGF signalling in regeneration and fibrosis. *Nat Cell Biol* 21:1490-1503.

Hiraki Y, Tanaka H, Inoue H, Kondo J, Kamizono A, Suzuki F (1991) Molecular cloning of a new class of cartilage-specific matrix, chondromodulin-I, which stimulates growth of cultured chondrocytes. *Biochem Biophys Res Commun* 175:971-977.

Huang YC, Urban JP, Luk KD (2014) Intervertebral disc regeneration: do nutrients lead the ways? *Nat Rev Rheumatol* 10:561-566.

Ito Y, Toriuchi N, Yoshitaka T, *et al*. (2010) The Mohawk homeobox gene is a critical regulator of tendon differentiation. *Proc Natl Acad Sci U S A* 107:10538-10542.

Jiang Y, Shi Y, He J, Zhang Z, Zhou G, Zhang W, Cao Y, Liu W (2017) Enhanced tenogenic differentiation and tendon-like tissue formation by tenomodulin overexpression in murine mesenchymal stem cells. *J Tissue Eng Regen Med* 11:2525-2536.

Jo CH, Lim HJ, Yoon KS (2019) Characterization of tendon-specific markers in various human tissues, tenocytes and mesenchymal stem cells. *Tissue Eng Regen Med* 16:151-159.

Kadow T, Sowa G, Vo N, Kang JD (2015) Molecular basis of intervertebral disc degeneration and herniations: what are the important translational questions? *Clin Orthop Relat Res* 473:1903-1912.

Katzel EB, Wolenski M, Loiselle AE, Basile P, Flick LM, Langstein HN, Hilton MJ, Awad HA, Hammert WC, O'Keefe RJ (2011) Impact of Smad3 loss of function on scarring and adhesion formation during tendon healing. *J Orthop Res* 29:684-693.

Kimura N, Shukunami C, Hakuno D, *et al*. (2008) Local tenomodulin absence, angiogenesis, and matrix metalloproteinase activation are associated with the rupture of the chordae tendineae cordis. *Circulation* 118:1737-

1747.

Kohler J, Popov C, Klotz B, *et al.* (2013) Uncovering the cellular and molecular changes in tendon stem/progenitor cells attributed to tendon aging and degeneration. *Aging Cell* 12:988-999.

Kraus TM, Imhoff FB, Wexel G, *et al*. (2014) Stem cells and basic fibroblast growth factor failed to improve tendon healing: an in vivo study using lentiviral gene transfer in a rat model. *J Bone Joint Surg Am* 96:761-769.

Lee CH, Lee FY, Tarafder S, Kao K, Jun Y, Yang G, Mao JJ (2015) Harnessing endogenous stem/progenitor cells for tendon regeneration. *J Clin Invest* 125:2690-2701.

Lee JM, Song JY, Baek M, Jung HY, Kang H, Han IB, Kwon YD, Shin DE (2011) Interleukin-1β induces angiogenesis and innervation in human intervertebral disc degeneration. *J Orthop Res* 29:265-269.

Leong NL, Kator JL, Clemens TL, James A, Enamoto-Iwamoto M, Jiang J (2020) Tendon and ligament healing and current approaches to tendon and ligament regeneration. *J Orthop Res* 38:7-12.

Li K, Deng G, Deng Y, Chen S, Wu H, Cheng C, Zhang X, Yu B, Zhang K (2019) High cholesterol inhibits tendon-related gene expressions in tendon-derived stem cells through reactive oxygen species-activated nuclear factor-κB signaling. *J Cell Physiol* 234:18017-18028.

Liu W, Chen B, Deng D, Xu F, Cui L, Cao Y (2006) Repair of tendon defect with dermal fibroblast engineered tendon in a porcine model. *Tissue Eng* 12:775-788.

Liu W, Watson SS, Lan Y, Keene DR, Ovitt CE, Liu H, Schweitzer R, Jiang R (2010) The atypical homeodomain transcription factor Mohawk controls tendon morphogenesis. *Mol Cell Biol* 30:4797-4807.

Lomas AJ, Ryan CN, Sorushanova A, *et al*. (2015) The past, present and future in scaffold-based tendon treatments. *Adv Drug Deliv Rev* 84:257-277.

Lyu FJ, Cheung KM, Zheng Z, Wang H, Sakai D, Leung VY (2019) IVD progenitor cells: a new horizon for understanding disc homeostasis and repair. *Nat Rev Rheumatol* 15:102-112.

Manning CN, Havlioglu N, Knutsen E, Sakiyama-Elbert SE, Silva MJ, Thomopoulos S, Gelberman RH (2014) The early inflammatory response after flexor tendon healing: a gene expression and histological analysis. *J Orthop Res* 32:645-652.

Minogue BM, Richardson SM, Zeef LA, Freemont AJ, Hoyland JA (2010) Transcriptional profiling of bovine intervertebral disc cells: implications for identification of normal and degenerate human intervertebral disc cell phenotypes. *Arthritis Res Ther* 12:R22.

Murchison ND, Price BA, Conner DA, Keene DR, Olson EN, Tabin CJ, Schweitzer R (2007) Regulation of tendon differentiation by scleraxis distinguishes force-transmitting tendons from muscle-anchoring tendons. *Development* 134:2697-2708.

Nakamichi R, Ito Y, Inui M, *et al*. (2016) Mohawk promotes the maintenance and regeneration of the outer annulus fibrosus of intervertebral discs. *Nat Commun* 7:12503.

Nguyen C, Poiraudeau S, Rannou F (2015) From Modic 1 vertebral-endplate subchondral bone signal changes detected by MRI to the concept of 'active discopathy'. *Ann Rheum Dis* 74:1488-1494.

No YJ, Castilho M, Ramaswamy Y, Zreiqat H (2019) Role of biomaterials and controlled architecture on tendon/ligament repair and regeneration. *Adv Mater*. doi: 10.1002/adma.201904511.

Nourissat G, Berenbaum F, Duprez D (2015) Tendon injury: from biology to tendon repair. *Nat Rev Rheumatol* 11:223-233.

Okamoto N, Kushida T, Oe K, Umeda M, Ikehara S, Iida H (2010) Treating Achilles tendon rupture in rats with bone-marrow-cell transplantation therapy. *J Bone Joint Surg Am* 92:2776-2784.

Oshima Y, Sato K, Tashiro F, Miyazaki J, Nishida K, Hiraki Y, Tano Y, Shukunami C (2004) Anti-angiogenic action of the C-terminal domain of tenomodulin that shares homology with chondromodulin-I. *J Cell Sci* 117:2731-2744.

Palmes D, Spiegel HU, Schneider TO, Langer M, Stratmann U, Budny T, Probst A (2002) Achilles tendon healing: long-term biomechanical effects of postoperative mobilization and immobilization in a new mouse model. *J Orthop Res* 20:939-946.

Patil P, Dong Q, Wang D, *et al.* (2019) Systemic clearance of $p16^{INK4a}$ -positive senescent cells mitigates age-associated intervertebral disc degeneration. *Aging Cell*. doi: 10.1111/acel.12927.

Pohl PH, Lozito TP, Cuperman T, *et al*. (2016) Catabolic effects of endothelial cell-derived microparticles on disc cells: Implications in intervertebral disc neovascularization and degeneration. *J Orthop Res* 34:1466-1474.

Pye SR, Reid DM, Adams JE, Silman AJ, O'Neill TW (2007) Influence of weight, body mass index and lifestyle factors on radiographic features of lumbar disc degeneration. *Ann Rheum Dis* 66:426-427.

Risbud MV, Shapiro IM (2014) Role of cytokines in intervertebral disc degeneration: pain and disc content. *Nat Rev Rheumatol* 10:44-56.

Ruiz-Ojeda FJ, Anguita-Ruiz A, Rupérez AI, *et al.* (2019) Effects of X-chromosome tenomodulin genetic variants on obesity in a children's cohort and implications of the gene in adipocyte metabolism. *Sci Rep* 9:3979.

Saiki A, Olsson M, Jernås M, *et al*. (2009) Tenomodulin is highly expressed in adipose tissue, increased in obesity, and down-regulated during diet-induced weight loss. *J Clin Endocrinol Metab* 94:3987-3994.

Sakai D, Andersson GB (2015) Stem cell therapy for intervertebral disc regeneration: obstacles and solutions. *Nat Rev Rheumatol* 11:243-256.

Sánchez-Pulido L, Devos D, Valencia A (2002) BRICHOS: a conserved domain in proteins associated with dementia, respiratory distress and cancer. *Trends Biochem Sci* 27:329-332.

Schneider M, Angele P, Järvinen TAH, Docheva D (2018) Rescue plan for Achilles: Therapeutics steering the fate and functions of stem cells in tendon wound healing. *Adv Drug Deliv Rev* 129:352-375.

Senol-Cosar O, Flach RJ, DiStefano M, *et al*. (2016) Tenomodulin promotes human adipocyte differentiation and beneficial visceral adipose tissue expansion. *Nat Commun* 7:10686.

Sharma A, Pilgram T, Wippold FJ 2nd (2009) Association between annular tears and disk degeneration: a longitudinal study. *AJNR Am J Neuroradiol* 30:500-506.

Shukunami C, Oshima Y, Hiraki Y (2001) Molecular cloning of tenomodulin, a novel chondromodulin-I related gene. *Biochem Biophys Res Commun* 280:1323-1327.

Shukunami C, Oshima Y, Hiraki Y (2005) Chondromodulin-I and tenomodulin: a new class of tissue-specific angiogenesis inhibitors found in hypovascular connective tissues. *Biochem Biophys Res Commun* 333:299-307.

Shukunami C, Takimoto A, Nishizaki Y, *et al*. (2018) Scleraxis is a transcriptional activator that regulates the expression of Tenomodulin, a marker of mature tenocytes and ligamentocytes. *Sci Rep* 8:3155.

Shukunami C, Takimoto A, Oro M, Hiraki Y (2006) Scleraxis positively regulates the expression of tenomodulin, a differentiation marker of tenocytes. *Dev Biol* 298:234-247.

Silagi ES, Novais EJ, Bisetto S, et al. (2019) Lactate efflux from intervertebral disc cells is required for maintenance of spine health. *J Bone Miner Res*. doi: 10.1002/jbmr.3908.

Song Y, Li S, Geng W, *et al.* (2018) Sirtuin 3-dependent mitochondrial redox homeostasis protects against AGEs-induced intervertebral disc degeneration. *Redox Biol* 19:339-353.

Stauber T, Blache U, Snedeker JG (2019) Tendon tissue microdamage and the limits of intrinsic repair. *Matrix Biol*. doi: 10.1016/j.matbio.2019.07.008.

Steinmann S, Pfeifer CG, Brochhausen C, Docheva D (2020) Spectrum of tendon pathologies: triggers, trails and end-state. *Int J Mol Sci*. doi: 10.3390/ijms21030844.

Su AI, Cooke MP, Ching KA, *et al*. (2002) Large-scale analysis of the human and mouse transcriptomes. *Proc Natl Acad Sci U S A* 99:4465-4470.

Suzuki H, Ito Y, Shinohara M, *et al.* (2016) Gene targeting of the transcription factor Mohawk in rats causes heterotopic ossification of Achilles tendon via failed tenogenesis. *Proc Natl Acad Sci U S A* 113:7840-7845.

Tessier S, Doolittle AC, Sao K, Rotty JD, Bear JE, Ulici V, Loeser RF, Shapiro IM, Diekman BO, Risbud MV (2020) Arp2/3 inactivation causes intervertebral disc and cartilage degeneration with dysregulated TonEBP-mediated osmoadaptation. *JCI Insight*. doi: 10.1172/jci.insight.131382.

Tessier S, Tran VA, Ottone OK, Novais EJ, Doolittle A, DiMuzio MJ, Shapiro IM, Risbud MV (2019) TonEBP-deficiency accelerates intervertebral disc degeneration underscored by matrix remodeling, cytoskeletal rearrangements, and changes in proinflammatory gene expression. *Matrix Biol*. doi: 10.1016/j.matbio. 2019.10.007.

Thomopoulos S, Parks WC, Rifkin DB, Derwin KA (2015) Mechanisms of tendon injury and repair. *J Orthop Res* 33:832-839.

Titan AL, Longaker MT (2019) A fine balance in tendon healing. *Nat Cell Biol* 21:1466-1467.

Tolppanen AM, Helisalmi S, Hiltunen M, Kolehmainen M, Schwab U, Pirttilä T, Pulkkinen L, Uusitupa M, Soininen H (2011) Tenomodulin variants, APOE and Alzheimer's disease in a Finnish case-control cohort. *Neurobiol Aging* 32:546.e7-9.

Tolppanen AM, Kolehmainen M, Pulkkinen L, Uusitupa M (2010) Tenomodulin gene and obesity-related phenotypes. *Ann Med* 42:265-275.

Tolppanen AM, Nevalainen T, Kolehmainen M, Seitsonen S, Immonen I, Uusitupa M, Kaarniranta K, Pulkkinen L (2009) Single nucleotide polymorphisms of the tenomodulin gene (TNMD) in age-related macular degeneration. *Mol Vis* 15:762-770.

Tolppanen AM, Pulkkinen L, Kolehmainen M, Schwab U, Lindström J, Tuomilehto J, Uusitupa M; Finnish Diabetes Prevention Study Group (2007) Tenomodulin is associated with obesity and diabetes risk: the Finnish diabetes prevention study. *Obesity (Silver Spring)* 15:1082-1088.

Tolppanen AM, Pulkkinen L, Kuulasmaa T, Kolehmainen M, Schwab U, Lindström J, Tuomilehto J, Uusitupa M, Kuusisto J (2008) The genetic variation in the tenomodulin gene is associated with serum total and LDL cholesterol in a body size-dependent manner. *Int J Obes (Lond)* 32:1868-1872.

Walker MH, Anderson DG (2004) Molecular basis of intervertebral disc degeneration. *Spine J* 4:158S-166S.

Wang B, Liu W, Zhang Y, Jiang Y, Zhang WJ, Zhou G, Cui L, Cao Y (2008) Engineering of extensor tendon complex by an ex vivo approach. *Biomaterials* 29:2954-2961.

Wang Z, Lee WJ, Koh BTH, Hong M, Wang W, Lim PN, Feng J, Park LS, Kim M, Thian ES (2018) Functional regeneration of tendons using scaffolds with physical anisotropy engineered viamicroarchitectural manipulation. *Sci Adv* 4:eaat4537.

Williams FM, Popham M, Sambrook PN, Jones AF, Spector TD, MacGregor AJ (2011) Progression of lumbar disc degeneration over a decade: a heritability study. *Ann Rheum Dis* 70:1203-1207.

Acknowledgements

Firstly, I would like to express my sincere gratitude to my advisor, Prof. Dr. Denitsa Docheva for her continuous support of my Ph.D. study and related research and for her patience, motivation, and immense knowledge. Her guidance helped me throughout my research and manuscript preparation. I could not imagine a better advisor and mentor for my Ph.D. study.

I would also like to thank Prof. Matthias Schieker and PD Attila Aszodi for welcoming me in their laboratory and supporting me during these last few years.

I also sincerely thank Dr. Paolo Alberton, Dr. Chi-Fen Hsieh, and Sarah Dex, who taught me the required methods and contributed to the welcoming atmosphere.

Last but not the least, I would like to thank my family. Words cannot express how grateful I am to my parents for all of the sacrifices that they've made on my behalf. I would also like to thank all of my friends who incentivized me to strive towards my goal. Finally, I would like to express my appreciation to my beloved wife and our son.